JRC Scientific and Technical Reports

Bio-optical Algorithms for European Seas

Performance and Applicability of Neural-Net Inversion Schemes

Davide D'Alimonte[1], Giuseppe Zibordi[2], Jean-François Berthon[2], Elisabetta Canuti[2] and Tamito Kajiyama[1]

[1] Universidade Nova de Lisboa, Departamento de Informática, Quinta da Torre – Caparica, Portugal
[2] Institute for Environment and Sustainability, Global Environment and Monitoring Unit, Ispra, Italy

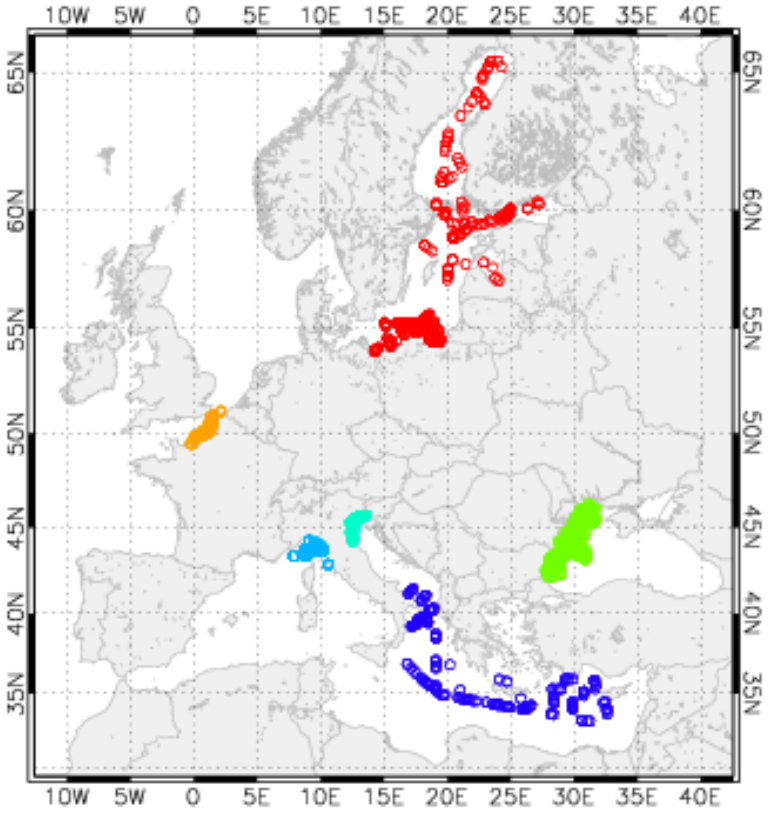

EUR 24920 EN - 2011

The mission of the JRC-IES is to provide scientific - technical support to the European Union's policies for the protection and sustainable development of the European and global environment.

European Commission
Joint Research Centre
Institute for Environment and Sustainability

Contact information

Davide D'Alimonte
davide.dalimonte@gmail.com
Tel.: +351 21 294 8536
Fax: +351 21 294 8541

Giuseppe Zibordi
giuseppe.zibordi@jrc.ec.europa.eu
Tel.: +39 0332 785902
Fax: +39 0332 789034

http://ies.jrc.ec.europa.eu/
http://www.jrc.ec.europa.eu/

Legal Notice
Neither the European Commission nor any person acting on behalf of the Commission is responsible for the use which might be made of this publication.

Europe Direct is a service to help you find answers to your questions about the European Union

Freephone number (*):

00 800 6 7 8 9 10 11

(*) Certain mobile telephone operators do not allow access to 00 800 numbers or these calls may be billed.

A great deal of additional information on the European Union is available on the Internet.
It can be accessed through the Europa server http://europa.eu/

JRC 66326

EUR 24920 EN
ISBN 978-92-79-21028-0
ISSN 1831-9424
doi:10.2788/56321

Luxembourg: Publications Office of the European Union

© European Union, 2011

Reproduction is authorised provided the source is acknowledged

Printed in Italy

Bio-optical Algorithms for European Seas: Performance and Applicability of Neural-Net Inversion Schemes

Davide D'Alimonte, Giuseppe Zibordi, Jean-François Berthon,
Elisabetta Canuti and Tamito Kajiyama

September 5, 2011

Abstract

This report presents and discusses the application of Multi Layer Perceptron (MLP) neural networks to derive Chlorophyll-a concentration (*Chl-a*), absorption of the yellow substance at 412 nm ($a_{ys}(412)$) and concentration of the total suspended matter (TSM) from remote sensing reflectance R_{RS} values. MLPs were developed on the basis of data collected within the framework of the Coastal Atmosphere and Sea Time Series (CoASTS) and Bio-Optical mapping of Marine Properties (BiOMaP) programs carried out by the Institute for Environment and Sustainability (IES) of the Joint Research Centre (Ispra, Italy). Investigated oceanographic regions include the Eastern Mediterranean Sea, the Ligurian Sea, the Northern Adriatic Sea, the Western Black Sea, the English Channel and the Baltic Sea. The study verifies the applicability of MLPs to retrieve ocean color data products in each basin. For instance, the highest accuracy in retrieving *Chl-a* has been found in the Easter Mediterranean Sea and the Ligurian Sea (14 and 25 %, respectively). In the case of $a_{ys}(412)$, the MLP is the most performing in the waters of the English Channel and the Baltic Sea (14 and 13%). Instead, the TSM retrieval is the most accurate in the Black Sea and at the Acqua Alta Oceanographic Tower (14 and 19%). To enhance mission specific ocean color resuls, MLP coefficients are also computed applying band-shift corrections to produce R_{RS} spectra at wavelengths matching those of SeaWiFS, MODIS and MERIS. Resulting tables of MLP parameters are reported to permit independent applications of neural networks presented in this study.

1 Overview

This report presents and discusses the application of Multi Layer Perceptron (MLP) neural networks to derive Chlorophyll-a concentration *Chl-a*, absorption of the yellow substance at 412 nm $a_{ys}(412)$ and concentration of the total suspended matter TSM from remote sensing reflectance R_{RS} spectral values. In agreement with methods developed in former investigations (D'Alimonte and Zibordi, 2003; D'Alimonte et al., 2004; Kajiyama et al., 2011) the MLPs applied in this study use R_{RS} at individual wavelengths as input for bio-optical non-linear models applicable to selected European seas. In-situ data for MLP development and performance assessment are those collected in the Coastal Atmosphere and Sea Time Series (CoASTS 1998–2009, Zibordi et al., 2004) and Bio-Optical mapping of Marine Properties (BiOMaP 2000–2010, Zibordi et al., 2011) programs carried out by the Joint Research Centre (JRC).

Investigated oceanographic regions include the Eastern Mediterranean Sea (EMED, comprising areas of the southern Adriatic Sea), the Ligurian Sea (LIGS), the Northern Adriatic Sea (VADR, with both samples from the Acqua Alta Oceanographic Tower AAOT and geographically distributed field measurements NADR), the Western Black Sea (BLKS), the English Channel (ECHN) and the Baltic Sea (BLTS). Complementary analyses are undertaken with the NASA Bio-Optical Marine Data Set, NOMAD (Werdell and Bailey, 2005).

Enhancing the MLP applications to remote sensing data for different ocean color missions is a major concern of the present study. For this purpose distinct MLP coefficients are computed applying band-shift corrections to produce R_{RS} spectra at wavelengths matching those of SeaWiFS, MODIS and MERIS (Zibordi et al., 2011).

Section 2 of this document reviews methods applied in MLP development and validation. The MLP performance to retrieve data products in the selected European seas is discussed in Section 3, together with MLP parameter tables. An analysis of cross-basin algorithm applicability is addressed in Section 4. Section 5 concludes the report with a result summary and remarks for improving the retrieval of ocean color products in optically complex coastal waters.

2 Methods

As explained in Section 2.1, MLP "may be viewed as a practical vehicle for performing a nonlinear input-output mapping of general nature" (Haykin, 1994). Data pre-processing schemes applied in the present study to improve MLP performances (e.g. Bishop, 1995) are discussed in Section 2.2. Methods for MLP architecture selection and performance assessment are presented in Section 2.3. The description of the band-shift correction to compute R_{RS} values at central wavelengths relevant to space-born sensors is given Section 2.4.

2.1 Multi Layer Perceptron Neural Network

The Multi Layer Perceptron neural network (Figure 1) consists of successive layers of units—with each unit in one layer connected to each unit of the next layer (Bishop, 1995; Nabney, 2001)—and can represent any continuous input-output mapping (Haykin, 1994). Let $y = f(\mathbf{x})$ denote the MLP mapping, where input vector $\mathbf{x}$ has entries x_i for $i = 1, \ldots, d$ (d is the dimension of the input space). In the present analysis, x_i quantifies the spectral remote sensing reflectance R_{RS} at $\lambda = 412$, 442, 491, 511, 555, and 665 nm (or corresponding central wavelengths for mission-specific applications). Distinct algorithms are developed to retrieve *Chl-a*, $a_{ys}(412)$ and TSM, so the MLP output y is a scalar.

The MLP hidden units a_j are linear combinations of the input values with the network *weights*:

$$a_j = \mathrm{b}_j^{(1)} + \sum_{i=1}^{d} \mathrm{w}_{ji}^{(1)} x_i, \tag{1}$$

where $\mathrm{w}_{ji}^{(1)}$ represent the weights linking the input unit i to the hidden unit j, and $\mathrm{b}_j^{(1)}$ is the bias adaptive parameter. The *activation* of the hidden unit j, identified with z_j and representing the input for the next layer, is obtained by applying the activation function g to the summation of (1):

$$z_j \;=\; g\left(a_j\right) = \frac{e^{a_j} - e^{-a_j}}{e^{a_j} + e^{-a_j}}. \tag{2}$$

The MLP output y is given by weighted combination of the activations of the hidden units z_j through the

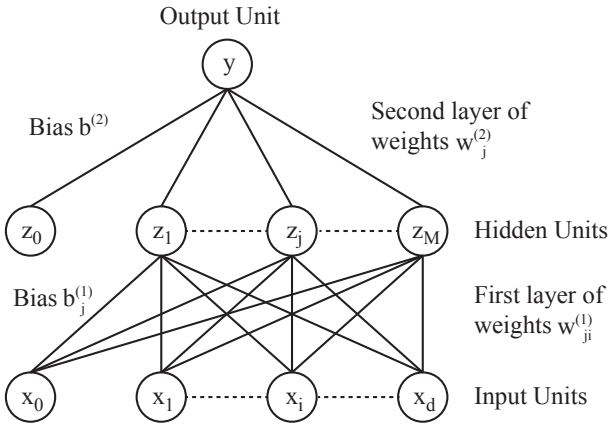

FIGURE 1: Schematic of MLP with two layers of adaptive parameters. The bias parameters $b_j^{(1)}$ in the first layer are shown as weights from an extra input having fixed value of $x_0 = 1$. Similarly, the bias coefficient $b^{(2)}$ in the second layer is shown as weight from an extra hidden unit $z_0 = 1$.

second layer of weights $w_j^{(2)}$:

$$y = b^{(2)} + \sum_{j=1}^{M} w_j^{(2)} z_j, \tag{3}$$

where M indicates the number of hidden units and $b^{(2)}$ is the bias coefficient.

In agreement with previous studies (D'Alimonte and Zibordi, 2003; D'Alimonte et al., 2004), the adopted MLP architecture has one layer of hidden neurons, a sigmoid activation function for the hidden layer and a linear activation function for the output layer. The weight decay coefficients was set to 0.01 in order to improve the MLP generalization performance (D'Alimonte and Zibordi, 2003). The Scaled Conjugate Gradient (SCG) was used to set the MLP weights (Bishop, 1995), while the number of training cycles was 100.

MLP algorithms presented in this report were implemented by means of the Netlab toolbox* for MATLAB (Nabney, 2001). Table 1 details numerical steps for the operational MLP application, whereas the MLP weight and bias values applied in this study are reported in the next sections. The appendix section of this document finally provides the complete C code for the MLP implementation.

2.2 Data pre- and post-processing

Data are pre-processed to enhance the MLP performance by applying the log-transformation and the z-score scaling described hereafter (see Kajiyama et al., 2011, for details).

2.2.1 Data log-transformation

The rationale for log-transforming bio-optical data relies on the log-normal distribution of seawater optical properties and concentration of optically significant constituents over several order of magnitude (Campbell, 1995). Their logarithm is hence close to be uniformly distributed. Besides, uncertainty budgets affecting measurements of optically active seawater compounds are percent values. After taking the logarithm, these multiplicative factors become additive components, which fits the maximum likelihood theory when the least-squares minimizaton is applied to set the MLP coefficients.

*Available at `http://www1.aston.ac.uk/eas/research/groups/ncrg/resources/netlab/`

2.2.2 Z-score scaling

Log-transformed R_{RS} data, henceforth denoted $\mathbf{l}$, are z-score scaled as

$$\mathbf{x} = (\mathbf{l} - \boldsymbol{\mu}_l)/\boldsymbol{\sigma}_l, \tag{4}$$

where $\boldsymbol{\mu}_l$ and $\boldsymbol{\sigma}_l$ are the mean and standard deviation of $\mathbf{l}$ training values. By the same token c indicates the log-transformed MLP target quantity (i.e., $\log_{10}(\textit{Chl-a})$, $\log_{10}(a_{ys}(412))$ or $\log_{10}(\text{TSM})$). The y value of Eq. 3 hence corresponds to

$$y = (c - \mu_c)/\sigma_c, \tag{5}$$

being μ_c and σ_c the mean and standard deviation of c training values.

Once the MLP output has been computed, data post-processing has to be applied to transform y into physical quantities t. Taking the chlorophyll-a case as an example:

$$\textit{Chl-a} = 10^{(y \cdot \sigma_c + \mu_c)}. \tag{6}$$

Tables of pre- and post processing parameters are in Section 3.

2.3 Performance assessment

The objective of the MLP training is to learn the general relationship between the input and output data. Thus, the MLP validation has to assess the model generalization performance and not its capability to fit training points. The scheme used here to select the number of MLP hidden units is the *cross-validation* (Cherkassky and Muller, 1998), whereas the MLP performance is assessed through the absolute and signed percent differences between measured and modeled values.

2.3.1 Cross-validation

Cross-validation requires to separate the data set into different segments: all except one are used for the MLP development, while that discarded is used for the validation. The procedure is then reiterated, each

TABLE 1: Listing of the code for the pre-processing, MLP mapping and post-processing steps to compute the ocean color data product `c` from the remote sensing reflectance `RRS`. The values of the mean and the standard deviation `mu_l`, `s_l`, `mu_c`, `s_c`, as well as the set of MLP weights and biases are reported for each European sea addressed in the present study. The code formalism is that applied in the Netlab toolbox for MATLAB (Nabney, 2001). A full set of functions coded in C and an application example are in Appendix A.

```
% Pre-processing
l = log10(RRS);
ndata = size(l, 1);
tmp = l-repmat(mu_l, ndata, 1);
x = tmp ./ repmat(s_l, ndata, 1);

% MLP mapping
z = tanh(x*net.w1 + ones(ndata, 1)*net.b1);
y = z*net.w2 + ones(ndata, 1)*net.b2;

% Post-processing
tmp = y.*repmat(s_c, ndata, 1);
c = 10^(tmp+repmat(mu_c, ndata, 1));
```

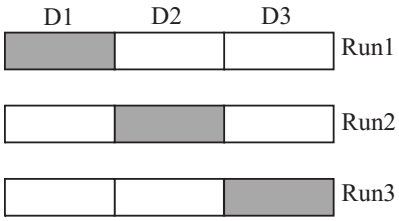

FIGURE 2: Dataset partitioning into 3 segments (D1, ..., D3) for the cross-validation. The MLP is trained (run) 3 times, each time omitting one of the segments (shown shadowed). Each network is then tested with the data of the segment that was omitted during its training (adapted from Bishop, 1995).

time using a different segment for the validation, until the MLP performance has been evaluated over the entire data set. Cross-validation was implemented dividing the data set in three segments (Figure 2). Data partition takes into account that one water sample may correspond to various successive R_{RS} measurements. All R_{RS} values associated to the same water sample were so included into a unique segment to ensure the highest independence of validation data. It is noted that the number of records reported in the scatter plots and summary tables of the result section refer to the number of independent R_{RS} measurements and not to the number of water samples.

Although the model performance is assessed through cross-validation, MLP coefficients for operational use are derived using all data for a single training because the larger is the training data set, the better the MLP learning performs. For completeness, this report provides both cross-validation and single training results.

2.3.2 Performance parameters

The scattering and the bias of the post-processed MLP results $\hat{t}$ with respect to corresponding measured values t are presented in this report in terms of absolute ε (Eq. 7a) and signed δ (Eq. 7b) percent differences:

$$\varepsilon = 100\frac{1}{\mathrm{N}}\sum_{i=1}^{\mathrm{N}}\frac{|\hat{t}_i - t_i|}{t_i} \tag{7a}$$

$$\delta = 100\frac{1}{\mathrm{N}}\sum_{i=1}^{\mathrm{N}}\frac{\hat{t}_i - t_i}{t_i}, \tag{7b}$$

where N is the total number of samples and i the sample subscription.

2.4 Band-shift Correction

In-situ data are corrected for differences in center-wavelength with respect to satellite sensors by applying a band-shift correction scheme (Mélin and Zibordi, 2007; Zibordi et al., 2006, 2011). Specifically, synthetic $R_{RS}(\lambda)$ values at the center-wavelength λ are determined from actual $R_{RS}(\lambda_0)$ at a near center-wavelength

TABLE 2: Center wavelengths (in units of nm) of in-situ and space-born sensors addressed in this study.

In-situ	412	442	490	510	555	665
SeaWiFS	412	443	490	510	555	670
MODIS	412	443	488	530	547	667
MERIS	413	443	490	510	560	665

λ_0 assuming ideal (square) 10 nm wide spectral band-pass, through

$$R_{RS}(\lambda) = R_{RS}(\lambda_0) \cdot \frac{b_b(\lambda)}{a(\lambda) + b_b(\lambda)} \cdot \frac{a(\lambda_0) + b_b(\lambda_0)}{b_b(\lambda_0)}, \tag{8}$$

where a indicates the seawater absorption coefficient resulting from the sum of phytoplankton a_{ph}, detritus a_{dt}, yellow substance a_{ys}, and pure seawater a_w (Pope and Fry, 1997); and b_b is the seawater backscattering coefficient (with $b_b \ll a$) given by the sum of particle b_{bp} and pure seawater b_{bw} (Buiteveld et al., 1994).

3 Regional algorithms

This section includes: 1) the assessment of the MLP performance as a function of the number of hidden units; 2) statistical figures quantifying the agreement between modeled and measured ocean color products; 3) tables of MLP weight and bias values for determining optically active seawater components from R_{RS} spectra (Eq. 1–3), as well as parameter sets for data pre- and post-processing (Eq. 4–6). Results at individual basins are complemented by an analysis of the MLP resulting from the BiOMaP data ensemble.

It is anticipated that in many of the cases addressed here, the MLP generalization capability displays a weak dependence on the network architecture: adding or removing one hidden unit does not change significantly validation results. This can be explained by two aspects: 1) the general relationship between R_{RS} and modeled ocean color data products is fairly linear, and 2) field measurements are highly consistent (i.e., low noise level with respect to the number of training samples and very few outliers). The general principle followed in this study is hence to select the largest MLP architecture that does not show over-training problems.

3.1 Northern Adriatic Sea (BiOMaP and CoASTS data)

MLPs training data are those collected within the CoASTS program and during a BiOMaP oceanographic cruise executed in 2000 (Figure 3(a)). In agreement with the MLP performance trends of Panels (b) to (d) of Figure 3, the selected number of hidden units is ten. Scatter plots of Figure 4 are derived through cross-validation. Table 3 quantifies differences between cross-validation and single training results.

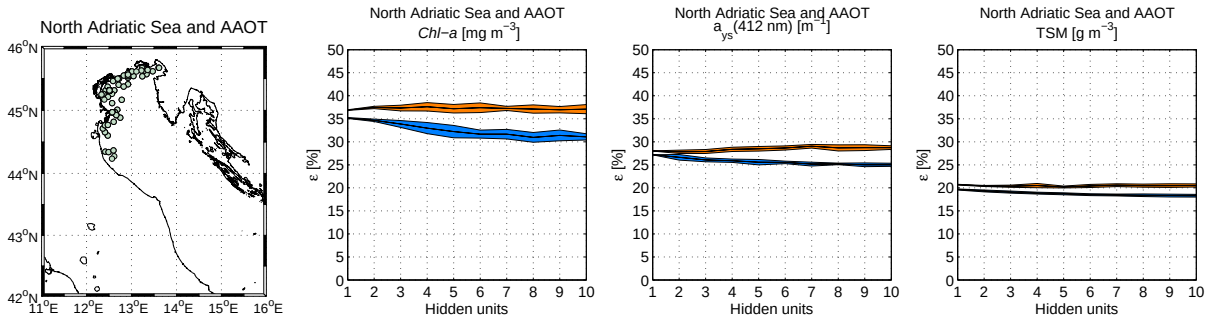

(a) (b) (c) (d)

FIGURE 3: BiOMaP and CoASTS stations in the Adriatic Sea (Panel 3(a)) and MLP performance (expressed through the percent error ε) as a function of the number of hidden units (Panels 3(b)–3(d) refer to *Chl-a*, $a_{ys}(412)$ and TSM, respectively). Results from cross-validation are in orange, those from single training in blue. The width of the trend bands indicate one standard deviation of ε when retraining 10 times each MLP architecture.

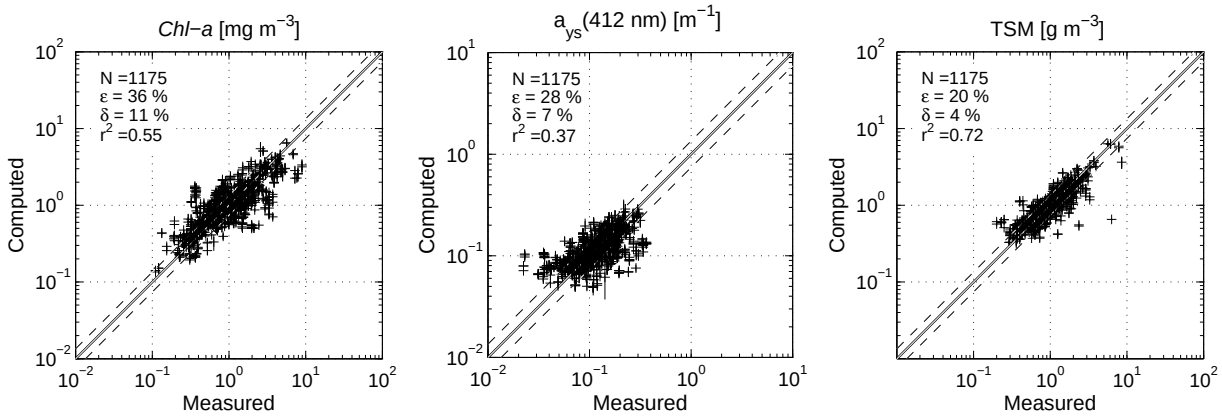

(a) (b) (c)

FIGURE 4: Scatter plot of modeled (cross-validation results based on the MLP with 10 hidden units) versus measured values of *Chl-a*, $a_{ys}(412)$ and TSM (Panel 4(a), Panel 4(b) and Panel 4(c), respectively.)

TABLE 3: Summary of cross-validation results (MLP with 10 hidden units) from the comparison between modeled and measured quantities in the Adriatic Sea (values within brackets are those obtained using all data for a single training).

	N	ϵ [%]	δ [%]	r^2
Chl-a	1175	36.3(30.9)	10.4(6.4)	55.9(67.0)
$a_{ys}(412)$	1175	28.8(24.9)	7.5(5.1)	35.8(47.7)
TSM	1175	20.7(18.2)	3.5(2.8)	70.0(76.5)

TABLE 4: Parameters for data pre- and post-processing, as well as MLP weights to derive *Chl-a* values in the Northern Adriatic Sea. Training data include samples from both BiOMaP and CoASTS programs. Input R_{RS} wavelengths are those of the in-situ measurements (see Table. 2). The notation $(\mathbf{w}^{(2)})^{\mathrm{T}}$ indicates the transpose of the weight vector $\mathbf{w}^{(2)}$.

$$\boldsymbol{\mu_l} = \begin{bmatrix} -2.4140 & -2.3562 & -2.2420 & -2.2459 & -2.3001 & -3.1077 \end{bmatrix}$$

$$\boldsymbol{\sigma_l} = \begin{bmatrix} 0.1266 & 0.1376 & 0.1410 & 0.1531 & 0.1913 & 0.2898 \end{bmatrix}$$

$$\mathbf{w}^{(1)} = \begin{bmatrix} 0.8171 & 0.1020 & 0.0055 & -0.7657 & 1.3000 & 0.9552 & -0.0389 & 0.2977 & -0.3111 & -1.3794 \\ 0.7788 & -0.8233 & -0.1462 & 1.0440 & -0.0541 & 0.5041 & 0.2709 & -0.2039 & -0.9394 & 0.2407 \\ -0.5943 & 0.2567 & 0.1180 & -0.0121 & -0.5634 & 0.0795 & 0.3766 & -0.0012 & -0.2342 & 0.5870 \\ 0.9183 & -0.2228 & -0.2723 & -0.3433 & 0.7181 & -0.3145 & -0.2038 & -0.8187 & -0.7295 & 0.2357 \\ 1.1696 & 0.0653 & -0.0641 & -0.4761 & 0.2034 & -0.4225 & 0.5823 & 0.5535 & -0.9467 & -1.6642 \\ -0.0250 & 0.4470 & 0.6222 & 0.3024 & -0.2759 & -0.4216 & 0.7834 & 0.2380 & -0.3021 & -0.2630 \end{bmatrix}$$

$$\mathbf{b}^{(1)} = \begin{bmatrix} 0.6897 & 0.4251 & -0.1718 & -0.5192 & 0.0070 & -0.0633 & -0.0405 & -0.7154 & -0.0193 & 0.0832 \end{bmatrix}$$

$$(\mathbf{w}^{(2)})^{\mathrm{T}} = \begin{bmatrix} -0.5005 & 1.0459 & 1.1365 & -1.5768 & -0.0562 & 0.5799 & 0.7121 & 1.1483 & -0.9814 & 1.2666 \end{bmatrix} \text{ and } b^{(2)} = \text{-0.0907}$$

$$\mu_c = \text{-0.0185 and } \sigma_c = 0.3270$$

TABLE 5: As in Table 4 but for $a_{ys}(412)$.

$$\boldsymbol{\mu_l} = \begin{bmatrix} -2.4140 & -2.3562 & -2.2420 & -2.2459 & -2.3001 & -3.1077 \end{bmatrix}$$

$$\boldsymbol{\sigma_l} = \begin{bmatrix} 0.1266 & 0.1376 & 0.1410 & 0.1531 & 0.1913 & 0.2898 \end{bmatrix}$$

$$\mathbf{w}^{(1)} = \begin{bmatrix} 0.2233 & -0.7578 & 0.8336 & 1.2510 & 0.0237 & 0.3461 & 0.1012 & -0.6802 & -1.4377 & 1.0023 \\ 0.5092 & -0.1101 & -0.5110 & -0.5836 & 0.1251 & 0.2449 & 0.9426 & 0.2566 & -0.0163 & -0.7003 \\ -0.0599 & -0.1872 & -0.2886 & -0.5372 & -0.5940 & -0.0861 & -0.4465 & 0.3972 & -0.2748 & 0.2281 \\ 1.0209 & -0.2877 & 0.2677 & 0.5260 & 0.0337 & -0.1808 & -0.9591 & 0.1795 & 0.3080 & 0.4769 \\ 0.9789 & -0.3166 & 0.2624 & -0.6010 & 0.3508 & 0.1359 & 0.3830 & 0.2778 & -0.9504 & -0.6414 \\ -0.1025 & 0.0274 & -0.0051 & -0.3997 & 0.8058 & 0.4734 & -0.3462 & 0.6451 & -0.7130 & 0.0771 \end{bmatrix}$$

$$\mathbf{b}^{(1)} = \begin{bmatrix} 0.3337 & 0.7471 & -0.5700 & -0.5316 & -1.2875 & 0.3377 & -0.6500 & 0.1255 & -0.0555 & -0.1734 \end{bmatrix}$$

$$(\mathbf{w}^{(2)})^{\mathrm{T}} = \begin{bmatrix} 0.4833 & -0.4766 & -0.3968 & -1.1132 & 0.8885 & 0.5687 & 1.4714 & 0.2887 & 0.8214 & -0.8127 \end{bmatrix} \text{ and } b^{(2)} = 0.6208$$

$$\mu_c = \text{-0.9377 and } \sigma_c = 0.2071$$

TABLE 6: As in Table 4 but for TSM.

$$\boldsymbol{\mu_l} = \begin{bmatrix} -2.4140 & -2.3562 & -2.2420 & -2.2459 & -2.3001 & -3.1077 \end{bmatrix}$$

$$\boldsymbol{\sigma_l} = \begin{bmatrix} 0.1266 & 0.1376 & 0.1410 & 0.1531 & 0.1913 & 0.2898 \end{bmatrix}$$

$$\mathbf{w}^{(1)} = \begin{bmatrix} 0.0696 & -0.1232 & 0.4410 & 0.9266 & -0.0497 & -0.4592 & 0.0932 & 0.4081 & 0.7782 & -0.2571 \\ 0.8133 & 0.2551 & -0.4458 & 0.5056 & 0.1368 & 0.0863 & -0.3154 & -0.1751 & -0.4217 & 0.1212 \\ 0.3940 & 0.3519 & -0.0743 & -0.7341 & -0.3401 & 0.1972 & -0.8497 & 0.0575 & 0.0101 & 0.6884 \\ -0.3274 & 0.2701 & -0.0709 & 0.0097 & 0.1551 & 0.4414 & 0.4083 & 0.4400 & -0.6401 & -0.3737 \\ 0.3092 & 0.6498 & 0.1621 & 0.3418 & 0.1426 & -0.5497 & 0.0834 & -0.3959 & 0.2311 & -0.5149 \\ -0.2709 & -0.4804 & -0.5203 & -0.3118 & 0.1224 & -0.3773 & 0.3685 & -0.1834 & -0.6568 & 0.7905 \end{bmatrix}$$

$$\mathbf{b}^{(1)} = \begin{bmatrix} -0.4473 & 0.1050 & 1.0700 & -0.6825 & 0.3422 & -0.5801 & 0.7436 & 0.5615 & 0.1653 & -0.8992 \end{bmatrix}$$

$$(\mathbf{w}^{(2)})^{\mathrm{T}} = \begin{bmatrix} -0.6843 & 0.6932 & -0.5843 & 0.9053 & 0.6901 & -0.5844 & 1.0146 & -0.9226 & 0.4147 & 1.2575 \end{bmatrix} \text{ and } b^{(2)} = 0.7820$$

$$\mu_c = 0.0031 \text{ and } \sigma_c = 0.2398$$

TABLE 7: As in Table 4 but for the center wavelengths of the SeaWiFS sensor (see Table. 2).

$$\boldsymbol{\mu_l} = \begin{bmatrix} -2.4140 & -2.3562 & -2.2420 & -2.2459 & -2.3001 & -3.1084 \end{bmatrix}$$

$$\boldsymbol{\sigma_l} = \begin{bmatrix} 0.1266 & 0.1376 & 0.1410 & 0.1531 & 0.1913 & 0.2895 \end{bmatrix}$$

$$\mathbf{w}^{(1)} = \begin{bmatrix} 1.1574 & -0.4736 & -0.3913 & -0.3796 & -0.0250 & 0.0876 & -0.0602 & -0.5365 & -0.6964 & -0.0833 \\ 0.2615 & -0.6343 & 0.0375 & 0.4644 & 0.2270 & -0.8365 & -0.2420 & 0.8841 & -0.9790 & 0.3070 \\ -0.4629 & -0.5799 & 0.1487 & -0.2449 & -0.7742 & 0.3346 & 0.4786 & -0.3160 & 0.1079 & 0.4982 \\ -0.4996 & -1.6587 & -0.3681 & 0.1843 & 0.0513 & -0.3579 & -0.2490 & 0.0062 & 0.8231 & -0.5325 \\ 1.5030 & -0.8271 & 0.3470 & -0.4017 & 0.3193 & 0.2147 & 0.2491 & -0.2505 & 0.4502 & 0.0671 \\ 0.2873 & -0.2364 & -0.0865 & -0.2927 & 0.6797 & 0.1686 & 0.5717 & 0.1641 & -0.2358 & -0.1935 \end{bmatrix}$$

$$\mathbf{b}^{(1)} = \begin{bmatrix} 0.1406 & 0.2013 & -0.1360 & -0.8786 & -1.1433 & 0.0973 & -0.0657 & 0.0029 & -0.3181 & 0.0963 \end{bmatrix}$$

$$(\mathbf{w}^{(2)})^{\mathrm{T}} = \begin{bmatrix} -1.1095 & -0.7562 & 0.2475 & -0.7966 & 0.9654 & 1.3824 & 0.9253 & -1.0149 & -0.8623 & -0.0527 \end{bmatrix} \text{ and } b^{(2)} = 0.0966$$

μ_c = -0.0185 and σ_c = 0.3270

TABLE 8: As in Table 7 but for $a_{ys}(412)$.

$$\boldsymbol{\mu_l} = \begin{bmatrix} -2.4140 & -2.3562 & -2.2420 & -2.2459 & -2.3001 & -3.1084 \end{bmatrix}$$

$$\boldsymbol{\sigma_l} = \begin{bmatrix} 0.1266 & 0.1376 & 0.1410 & 0.1531 & 0.1913 & 0.2895 \end{bmatrix}$$

$$\mathbf{w}^{(1)} = \begin{bmatrix} 1.0947 & 0.0076 & -0.1071 & 1.1454 & 0.2095 & -0.3682 & -0.5433 & 0.8960 & 0.2445 & 0.0358 \\ -0.4599 & 0.0566 & -0.7307 & -0.7750 & -0.4229 & 0.3772 & -0.4849 & -0.4438 & -0.0217 & -0.7261 \\ -0.5452 & 0.4066 & 0.4562 & 1.2090 & -0.6253 & 0.9199 & -0.6331 & -0.2480 & 0.0252 & -0.6818 \\ 0.8098 & 0.1700 & 0.7127 & -0.4661 & -0.1105 & 0.5875 & 1.1509 & -0.5149 & 0.4331 & -0.4271 \\ -1.0701 & -0.8316 & -0.4728 & -0.6257 & -0.6857 & -1.1963 & 0.6278 & -0.0254 & -0.1103 & -0.0017 \\ -0.0023 & -0.6611 & 0.5058 & -0.9945 & -0.3592 & -1.4968 & -0.1191 & -0.8009 & -0.2161 & 0.0181 \end{bmatrix}$$

$$\mathbf{b}^{(1)} = \begin{bmatrix} -0.8586 & 1.1185 & 0.8108 & 0.1387 & 1.1782 & 0.4898 & 0.7153 & 0.1004 & -0.7218 & 0.7689 \end{bmatrix}$$

$$(\mathbf{w}^{(2)})^{\mathrm{T}} = \begin{bmatrix} -1.4166 & -0.7695 & -1.0949 & -1.3152 & 0.0911 & 1.1395 & -0.7291 & -0.5776 & -0.6340 & -0.1441 \end{bmatrix} \text{ and } b^{(2)} = 0.1558$$

μ_c = -0.9377 and σ_c = 0.2071

TABLE 9: As in Table 7 but for TSM.

$$\boldsymbol{\mu_l} = \begin{bmatrix} -2.4140 & -2.3562 & -2.2420 & -2.2459 & -2.3001 & -3.1084 \end{bmatrix}$$

$$\boldsymbol{\sigma_l} = \begin{bmatrix} 0.1266 & 0.1376 & 0.1410 & 0.1531 & 0.1913 & 0.2895 \end{bmatrix}$$

$$\mathbf{w}^{(1)} = \begin{bmatrix} -0.6125 & -0.1054 & -1.7371 & -0.3999 & 0.5044 & 0.3613 & -0.0889 & 0.1955 & 0.0894 & -0.6389 \\ 0.3879 & 0.0744 & 0.4241 & 0.5024 & -0.1400 & -0.3187 & -0.0977 & -0.1134 & -0.0986 & 0.8111 \\ 0.6133 & 0.1749 & 0.2434 & -0.1872 & 0.7654 & 0.1430 & 0.3807 & 0.2057 & -0.7989 & 0.5546 \\ -0.6410 & -0.4488 & 0.3500 & 0.0361 & -0.1928 & 0.6066 & -0.1220 & -0.7177 & 0.2398 & 0.2682 \\ -0.6116 & -0.3522 & 0.0146 & 0.3741 & 0.1804 & 1.0043 & 0.0334 & -0.1666 & 0.3437 & 0.5368 \\ 1.0403 & -0.3653 & -0.1060 & 0.0379 & -0.3633 & -0.5823 & 0.2940 & -0.2148 & 0.3494 & 0.6619 \end{bmatrix}$$

$$\mathbf{b}^{(1)} = \begin{bmatrix} -1.1081 & 0.4766 & 0.5782 & -0.6580 & -0.3664 & 0.1056 & -0.3629 & -0.5297 & 0.8853 & -0.2408 \end{bmatrix}$$

$$(\mathbf{w}^{(2)})^{\mathrm{T}} = \begin{bmatrix} 1.4983 & -0.0855 & -0.8129 & 0.9143 & -0.8649 & 0.9602 & 0.3671 & 0.1361 & 1.2758 & -0.4713 \end{bmatrix} \text{ and } b^{(2)} = 0.9749$$

μ_c = 0.0031 and σ_c = 0.2398

TABLE 10: As in Table 4 but for the center wavelengths of the MODIS sensor (see Table. 2).

$$\boldsymbol{\mu_l} = \begin{bmatrix} -2.4140 & -2.3562 & -2.2553 & -2.1736 & -2.3204 & -3.1077 \end{bmatrix}$$

$$\boldsymbol{\sigma_l} = \begin{bmatrix} 0.1266 & 0.1376 & 0.1424 & 0.1540 & 0.1895 & 0.2898 \end{bmatrix}$$

$$\mathbf{w}^{(1)} = \begin{bmatrix} 0.2738 & 0.1364 & 0.8566 & -0.7260 & 0.0254 & -0.2636 & -0.6227 & 0.5869 & 0.5262 & -0.6805 \\ 0.6207 & -0.2331 & 0.4795 & 1.0676 & -0.6293 & 0.6482 & 0.4555 & -0.1337 & 0.7887 & 0.0890 \\ -0.1057 & -0.6363 & -0.9912 & 0.0176 & -0.2559 & 0.0984 & -0.7364 & -0.0058 & 0.8719 & 1.0792 \\ -0.4822 & -0.2883 & 0.7256 & -1.1016 & -0.2875 & -0.5707 & 0.1906 & -0.1323 & 1.0274 & -0.2134 \\ -0.0547 & 0.3877 & 0.9710 & 0.3959 & 0.4404 & 0.3638 & -0.3588 & -0.0592 & 0.7497 & -0.3280 \\ -0.4617 & 0.6842 & -0.0221 & -0.2732 & 0.2160 & -0.2454 & -0.3195 & 0.2780 & 0.4598 & -0.4779 \end{bmatrix}$$

$$\mathbf{b}^{(1)} = \begin{bmatrix} 1.2399 & 0.0627 & 0.3923 & -0.8821 & 0.7922 & -0.1400 & 0.3161 & -0.2442 & -0.1787 & 1.2646 \end{bmatrix}$$

$$(\mathbf{w}^{(2)})^{\mathrm{T}} = \begin{bmatrix} -0.8738 & -0.3987 & -0.9943 & -1.5753 & 0.7860 & -0.9891 & 0.3859 & 0.7251 & 0.8236 & -1.1111 \end{bmatrix} \text{ and } b^{(2)} = 0.3464$$

$$\mu_c = \text{-0.0185 and } \sigma_c = 0.3270$$

TABLE 11: As in Table 10 but for $a_{ys}(412)$.

$$\boldsymbol{\mu_l} = \begin{bmatrix} -2.4140 & -2.3562 & -2.2553 & -2.1736 & -2.3204 & -3.1077 \end{bmatrix}$$

$$\boldsymbol{\sigma_l} = \begin{bmatrix} 0.1266 & 0.1376 & 0.1424 & 0.1540 & 0.1895 & 0.2898 \end{bmatrix}$$

$$\mathbf{w}^{(1)} = \begin{bmatrix} 0.9593 & 0.7660 & -0.0598 & -0.4237 & -0.3971 & -0.0712 & -0.2054 & -0.3502 & 0.0368 & 1.4893 \\ -0.1396 & 0.9548 & 0.2143 & -0.7576 & -0.2386 & -0.0408 & -0.3020 & 0.1450 & -0.3709 & -0.3754 \\ 1.3578 & -1.2006 & 0.1576 & -0.5184 & -0.7252 & 0.1402 & 0.3477 & -0.0437 & -0.6474 & -0.2476 \\ -1.3948 & 0.9450 & -0.3134 & -1.1071 & 0.1833 & 0.2791 & 0.4677 & -0.2702 & 0.0259 & -0.8592 \\ -0.0170 & -0.0851 & 0.2726 & 0.0822 & -0.4924 & -0.1513 & -0.0320 & 0.1907 & -0.3175 & 0.2663 \\ -0.3813 & -0.7023 & -0.8375 & -0.0833 & 0.3687 & 0.0761 & -0.6130 & -0.3797 & 0.8345 & 0.5140 \end{bmatrix}$$

$$\mathbf{b}^{(1)} = \begin{bmatrix} 0.1615 & 0.0572 & 0.9788 & 0.8301 & -0.1032 & -0.2003 & 0.4550 & -0.3849 & -1.1954 & 0.1970 \end{bmatrix}$$

$$(\mathbf{w}^{(2)})^{\mathrm{T}} = \begin{bmatrix} -1.6518 & 1.7019 & -0.9927 & -0.0871 & 0.5679 & -0.0498 & -0.6205 & -0.2876 & -0.5947 & -0.9666 \end{bmatrix} \text{ and } b^{(2)} = 0.6044$$

$$\mu_c = \text{-0.9377 and } \sigma_c = 0.2071$$

TABLE 12: As in Table 10 but for TSM.

$$\boldsymbol{\mu_l} = \begin{bmatrix} -2.4140 & -2.3562 & -2.2553 & -2.1736 & -2.3204 & -3.1077 \end{bmatrix}$$

$$\boldsymbol{\sigma_l} = \begin{bmatrix} 0.1266 & 0.1376 & 0.1424 & 0.1540 & 0.1895 & 0.2898 \end{bmatrix}$$

$$\mathbf{w}^{(1)} = \begin{bmatrix} -0.0916 & 0.7159 & 0.1794 & 0.9317 & -0.2249 & 0.6139 & 0.7021 & 0.0775 & 0.2384 & -0.5554 \\ 0.5265 & 0.0905 & -0.3342 & 0.2126 & -0.4328 & -0.2235 & -0.3479 & -0.2129 & 0.0035 & -0.0604 \\ -0.0952 & 0.2480 & -0.8008 & -0.6551 & 0.0217 & -0.0645 & -0.7238 & -0.7198 & 0.1826 & 0.5054 \\ -0.8082 & 0.4152 & 0.5914 & 0.1588 & -0.3182 & -0.2741 & -0.0929 & -0.0795 & 0.6100 & -0.2306 \\ 0.3499 & -0.0185 & -0.1252 & 0.1396 & -0.2031 & -0.6565 & 0.3960 & 0.3984 & 0.7057 & -0.2283 \\ 0.6385 & -0.3065 & 0.4432 & -0.2033 & 0.1088 & 0.1043 & -0.3165 & 0.2062 & -0.4379 & 0.7074 \end{bmatrix}$$

$$\mathbf{b}^{(1)} = \begin{bmatrix} -0.8292 & -0.0152 & 0.8331 & -0.5626 & 0.3363 & -0.0332 & 1.0771 & 0.0507 & 0.5673 & -1.5780 \end{bmatrix}$$

$$(\mathbf{w}^{(2)})^{\mathrm{T}} = \begin{bmatrix} 0.7924 & -0.1903 & 1.7400 & 0.8826 & 0.1618 & -0.0439 & -0.7472 & 0.2786 & 0.5153 & 1.0540 \end{bmatrix} \text{ and } b^{(2)} = 1.0548$$

$$\mu_c = 0.0031 \text{ and } \sigma_c = 0.2398$$

TABLE 13: As in Table 4 but for the center wavelengths of the MERIS sensor (see Table. 2).

$$\boldsymbol{\mu_l} = \begin{bmatrix} -2.4140 & -2.3562 & -2.2420 & -2.2459 & -2.2907 & -3.1077 \end{bmatrix}$$

$$\boldsymbol{\sigma_l} = \begin{bmatrix} 0.1266 & 0.1376 & 0.1410 & 0.1531 & 0.1925 & 0.2898 \end{bmatrix}$$

$$\mathbf{w}^{(1)} = \begin{bmatrix} 0.4472 & 0.4965 & -0.0218 & -0.2342 & -0.4999 & -0.0308 & 1.0439 & -0.7708 & 0.3020 & -0.5067 \\ -0.7941 & -0.9030 & -0.4324 & -0.9466 & -0.5898 & 1.2785 & 0.6665 & 0.8822 & 0.0137 & -0.2682 \\ 0.4666 & 0.3532 & -0.9555 & -0.3573 & -0.5824 & 0.4523 & -0.8948 & -0.2752 & 0.0474 & 0.0931 \\ 1.2426 & -0.1470 & 0.0477 & -0.1504 & -0.2341 & 0.4691 & -0.3124 & 0.3772 & 0.5373 & 0.0623 \\ 0.0478 & 0.0436 & -0.0833 & -0.9168 & 0.5391 & 0.9507 & 1.6142 & -0.2850 & 0.1661 & 0.2961 \\ 0.0938 & 0.3660 & -0.2476 & 0.5359 & 0.0314 & 0.7076 & 0.0830 & -0.0920 & 0.4490 & 0.9353 \end{bmatrix}$$

$$\mathbf{b}^{(1)} = \begin{bmatrix} -0.1184 & 0.5219 & 0.9161 & 0.5621 & 0.4963 & -0.0785 & 0.2570 & -0.1336 & 0.8561 & -1.2557 \end{bmatrix}$$

$$(\mathbf{w}^{(2)})^{\mathrm{T}} = \begin{bmatrix} -0.8907 & 0.9246 & -0.0753 & -0.9120 & 0.6632 & 0.9768 & -1.2835 & -1.5729 & 0.7301 & 0.6917 \end{bmatrix} \text{ and } b^{(2)} = \text{-0.2500}$$

$$\mu_c = \text{-0.0185 and } \sigma_c = 0.3270$$

TABLE 14: As in Table 13 but for $a_{ys}(412)$.

$$\boldsymbol{\mu_l} = \begin{bmatrix} -2.4140 & -2.3562 & -2.2420 & -2.2459 & -2.2907 & -3.1077 \end{bmatrix}$$

$$\boldsymbol{\sigma_l} = \begin{bmatrix} 0.1266 & 0.1376 & 0.1410 & 0.1531 & 0.1925 & 0.2898 \end{bmatrix}$$

$$\mathbf{w}^{(1)} = \begin{bmatrix} -0.0710 & -1.2323 & -1.1892 & -0.3630 & 0.6280 & 0.0593 & -0.2459 & 0.0681 & -0.2300 & 0.1847 \\ -0.4407 & 0.7023 & -0.4797 & -0.5171 & -0.9762 & 1.0219 & -0.3911 & 0.6138 & -0.6305 & 0.0611 \\ -0.0566 & 0.5436 & -0.2195 & -0.9050 & 0.2886 & -0.2331 & -0.0846 & -0.1410 & 0.3102 & -0.4441 \\ 0.7560 & -0.6420 & 0.0723 & 0.4973 & 0.8810 & -0.0287 & 0.7204 & 0.4965 & -0.0720 & -0.3842 \\ -0.1416 & 0.7571 & -0.5754 & 0.3493 & -0.3024 & 0.1599 & -0.0653 & 0.9262 & -0.0166 & -0.1404 \\ 0.4517 & 0.2432 & -0.5094 & -0.0933 & -0.3135 & 0.2282 & 0.5314 & -0.7638 & -0.6338 & -0.0394 \end{bmatrix}$$

$$\mathbf{b}^{(1)} = \begin{bmatrix} -0.8497 & 0.4902 & -0.1555 & -0.3899 & -0.3724 & 0.0839 & 0.8164 & -0.0531 & -0.2481 & -0.5607 \end{bmatrix}$$

$$(\mathbf{w}^{(2)})^{\mathrm{T}} = \begin{bmatrix} 0.6800 & 1.3121 & 0.7692 & 0.5445 & -1.3808 & 0.8008 & -1.1028 & 0.7352 & -0.3284 & 0.1172 \end{bmatrix} \text{ and } b^{(2)} = 0.2072$$

$$\mu_c = \text{-0.9377 and } \sigma_c = 0.2071$$

TABLE 15: As in Table 13 but for TSM.

$$\boldsymbol{\mu_l} = \begin{bmatrix} -2.4140 & -2.3562 & -2.2420 & -2.2459 & -2.2907 & -3.1077 \end{bmatrix}$$

$$\boldsymbol{\sigma_l} = \begin{bmatrix} 0.1266 & 0.1376 & 0.1410 & 0.1531 & 0.1925 & 0.2898 \end{bmatrix}$$

$$\mathbf{w}^{(1)} = \begin{bmatrix} 0.0240 & -0.0678 & -0.0591 & 0.6236 & 0.0465 & 0.2560 & 0.1701 & 0.3188 & 0.1143 & -0.2238 \\ 0.2380 & 0.5468 & -1.0697 & 0.0758 & 0.2574 & -0.0842 & 0.6504 & -0.0790 & -0.1886 & 0.1803 \\ 0.0583 & 0.0644 & -0.2948 & -0.4824 & -0.2246 & 0.1087 & 0.5637 & -0.7766 & -0.1416 & 0.2609 \\ -0.3847 & -0.5464 & -0.1753 & 0.0993 & -0.3429 & 0.6057 & -0.6847 & 0.0932 & -0.2353 & 0.0748 \\ 0.3103 & -0.2308 & 0.2990 & 0.0957 & 0.4827 & 0.8865 & 0.3750 & -0.0883 & 0.5503 & -0.2357 \\ -0.0943 & 0.8111 & 0.3607 & -0.6349 & -0.0894 & -0.9566 & 0.0020 & 0.7461 & 0.0786 & -0.1989 \end{bmatrix}$$

$$\mathbf{b}^{(1)} = \begin{bmatrix} 0.5676 & -0.7439 & -0.4312 & 1.6443 & 0.1358 & 0.0014 & -0.6327 & 0.6780 & -0.7142 & -0.4190 \end{bmatrix}$$

$$(\mathbf{w}^{(2)})^{\mathrm{T}} = \begin{bmatrix} 0.6668 & 1.1786 & 0.3862 & -1.2578 & 0.5703 & 0.7872 & -0.4271 & 0.8905 & -0.3098 & -0.6920 \end{bmatrix} \text{ and } b^{(2)} = 0.3886$$

$$\mu_c = 0.0031 \text{ and } \sigma_c = 0.2398$$

3.2 Northern Adriatic Sea (CoASTS data)

Data discussed in this section are only those collected at the Acqua Alta Oceanographic Tower in the Northern Adriatic Sea (Panel 5(a)) within the CoASTS program (Zibordi et al., 2004). The selected MLP architecture has ten hidden units. Scatter plots between measured and modeled values are in Figure 6, whereas comparison between MLP performance assessed through cross-validation and single training are in Table 16.

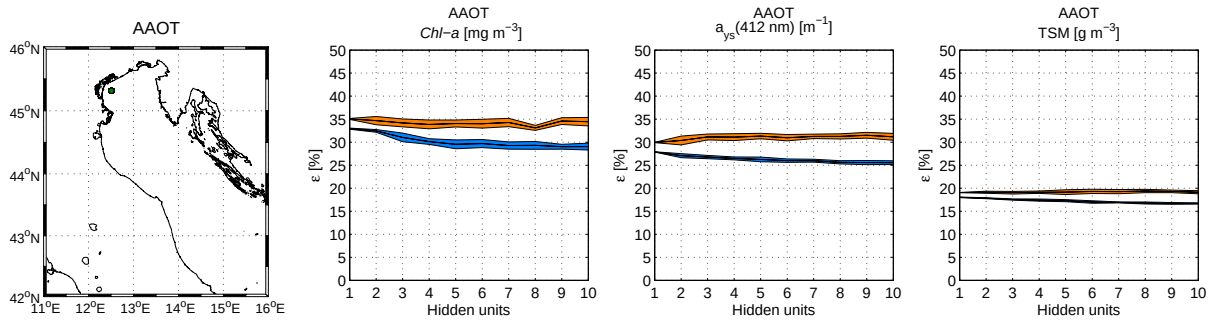

FIGURE 5: As in Figure 3, but only considering data collected at the Acqua Alta Oceanographic Tower in the Northern Adriatic Sea.

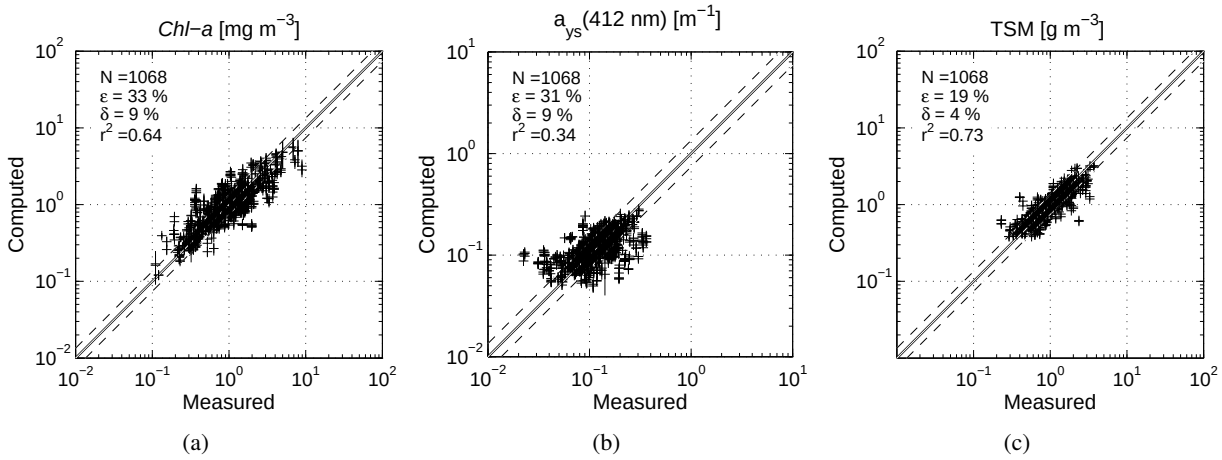

FIGURE 6: As in Figure 4, but only considering data collected at the Acqua Alta Oceanographic Tower in the Northern Adriatic Sea. Results based on the MLP with ten units in the hidden layer.

TABLE 16: As in Table 3, but only considering data collected at the Acqua Alta Oceanographic Tower in the Northern Adriatic Sea. Results based on the MLP with ten units in the hidden layer.

	N	ϵ [%]	δ [%]	r^2
Chl-a	1068	33.2(28.4)	7.4(6.6)	60.0(66.2)
$a_{ys}(412)$	1068	30.0(25.4)	8.0(6.2)	34.9(45.9)
TSM	1068	19.3(16.5)	4.0(2.6)	71.3(78.1)

TABLE 17: Data pre- and post-processing parameters, as well as MLP weights to derive *Chl-a* values in the Northern Adriatic Sea only considering data collected at the Acqua Alta Oceanographic Tower. Input R_{RS} wavelengths are those of the in-situ measurements (see Table. 2).

$$\boldsymbol{\mu_l} = \begin{bmatrix} -2.4092 & -2.3522 & -2.2408 & -2.2435 & -2.3018 & -3.1084 \end{bmatrix}$$

$$\boldsymbol{\sigma_l} = \begin{bmatrix} 0.1238 & 0.1364 & 0.1407 & 0.1513 & 0.1865 & 0.2795 \end{bmatrix}$$

$$\mathbf{w}^{(1)} = \begin{bmatrix} 0.0379 & -0.5039 & -0.6005 & -1.5511 & 0.4162 & 0.1784 & 0.1019 & -0.4420 & -1.0634 & 0.2948 \\ -0.1872 & 0.9970 & -0.7612 & 0.1627 & -0.0113 & -0.9650 & -0.4126 & 0.6455 & -0.0560 & -0.1065 \\ -0.2851 & -0.1683 & -0.6537 & 0.5639 & -0.7943 & 0.0608 & -0.8087 & -0.3083 & 0.2577 & 0.3517 \\ -0.6575 & -0.0921 & -0.7049 & 0.3693 & -0.6641 & -0.0398 & 0.4030 & -0.2542 & 0.1039 & 0.0139 \\ 0.1131 & -0.1923 & -1.3539 & -1.7808 & 0.7950 & 0.3048 & 0.7103 & 0.2893 & 0.2255 & -0.3241 \\ -0.1071 & -0.3986 & -0.1942 & -0.0053 & 0.4192 & 0.1801 & 0.0550 & -0.3441 & 0.2883 & -0.5446 \end{bmatrix}$$

$$\mathbf{b}^{(1)} = \begin{bmatrix} 0.1188 & -0.9491 & 0.2748 & 0.0015 & -1.5588 & 0.6430 & -0.0537 & 0.0587 & 0.1872 & 0.8609 \end{bmatrix}$$

$$(\mathbf{w}^{(2)})^{\mathrm{T}} = \begin{bmatrix} -0.0231 & -1.4689 & -0.8722 & 1.2077 & 1.4153 & 1.0108 & -0.3526 & -0.8610 & -0.5800 & -1.1364 \end{bmatrix} \text{ and } b^{(2)} = 0.6340$$

μ_c = -0.0400 and σ_c = 0.3180

TABLE 18: As in Table 17 but for $a_{ys}(412)$.

$$\boldsymbol{\mu_l} = \begin{bmatrix} -2.4092 & -2.3522 & -2.2408 & -2.2435 & -2.3018 & -3.1084 \end{bmatrix}$$

$$\boldsymbol{\sigma_l} = \begin{bmatrix} 0.1238 & 0.1364 & 0.1407 & 0.1513 & 0.1865 & 0.2795 \end{bmatrix}$$

$$\mathbf{w}^{(1)} = \begin{bmatrix} 0.0904 & 0.4687 & 0.2326 & 0.8425 & -0.9799 & 0.0269 & -0.2858 & -0.2296 & 1.2403 & 1.0611 \\ 0.3361 & 0.2411 & -0.3213 & -1.2881 & -0.4519 & -0.8888 & -0.1203 & 0.0708 & 0.0257 & -0.7976 \\ 0.9119 & -0.1797 & -0.0835 & -0.0380 & -0.1892 & 0.4038 & 0.2243 & -0.3337 & 0.4510 & -0.4647 \\ 0.2499 & -1.0883 & 0.2508 & 0.1268 & 0.0541 & 0.7787 & 0.0468 & 0.5740 & -0.3842 & 1.1748 \\ -0.0093 & -0.0675 & -0.1259 & -0.5071 & -0.3850 & -0.5461 & 0.0069 & -0.0668 & -0.3261 & -0.2773 \\ -0.5162 & -0.0573 & -0.2749 & 0.1021 & -0.6545 & 0.5448 & 0.4232 & -0.4654 & -0.9973 & -0.5530 \end{bmatrix}$$

$$\mathbf{b}^{(1)} = \begin{bmatrix} 0.9101 & 0.3181 & -0.6056 & -0.5119 & -0.4867 & 0.7186 & 0.5841 & 0.8566 & 0.2553 & -1.2223 \end{bmatrix}$$

$$(\mathbf{w}^{(2)})^{\mathrm{T}} = \begin{bmatrix} -0.5734 & -0.6310 & -0.4792 & -1.4171 & 0.3353 & -1.3084 & -0.4605 & -0.7941 & -0.4334 & -1.6282 \end{bmatrix} \text{ and } b^{(2)} = -0.1237$$

μ_c = -0.9425 and σ_c = 0.2086

TABLE 19: As in Table 17 but for TSM.

$$\boldsymbol{\mu_l} = \begin{bmatrix} -2.4092 & -2.3522 & -2.2408 & -2.2435 & -2.3018 & -3.1084 \end{bmatrix}$$

$$\boldsymbol{\sigma_l} = \begin{bmatrix} 0.1238 & 0.1364 & 0.1407 & 0.1513 & 0.1865 & 0.2795 \end{bmatrix}$$

$$\mathbf{w}^{(1)} = \begin{bmatrix} -0.0046 & 0.5941 & -0.7109 & 1.0085 & 0.2338 & 0.4210 & -0.3186 & -0.0236 & -0.0264 & -1.2637 \\ -0.0574 & 0.2090 & -0.6227 & -0.3688 & 0.7035 & 0.0632 & 0.2308 & -0.2596 & -0.0937 & 0.0471 \\ -0.4862 & -0.2544 & -0.2513 & -0.2562 & -0.0723 & -0.3341 & 1.0697 & -0.1600 & 0.2281 & -0.0078 \\ -0.3934 & -0.7492 & -0.7618 & -0.3351 & 0.3944 & -0.2824 & -0.4238 & 0.1338 & 0.1485 & -0.3901 \\ -1.1147 & -0.1988 & 0.3398 & 0.1236 & -0.3553 & -0.0812 & -0.1385 & 0.3906 & 0.3017 & -0.3611 \\ 0.8726 & 1.0039 & -0.2766 & -0.6723 & -0.3483 & -0.1444 & -0.6186 & 0.3559 & 0.2601 & 0.5668 \end{bmatrix}$$

$$\mathbf{b}^{(1)} = \begin{bmatrix} -0.2851 & -0.4832 & 0.0526 & 0.9940 & 0.2340 & 0.0956 & -1.1893 & 0.8652 & -0.1992 & 0.2003 \end{bmatrix}$$

$$(\mathbf{w}^{(2)})^{\mathrm{T}} = \begin{bmatrix} -0.7367 & 1.1620 & 0.5991 & -0.6390 & -0.6283 & 0.0294 & -1.1545 & 0.1509 & -0.3080 & -0.6798 \end{bmatrix} \text{ and } b^{(2)} = -0.1137$$

μ_c = 0.0002 and σ_c = 0.2206

TABLE 20: As in Table 17 but for the center wavelengths of the SeaWiFS sensor (see Table. 2).

$$\boldsymbol{\mu_l} = \begin{bmatrix} -2.4092 & -2.3522 & -2.2408 & -2.2435 & -2.3018 & -3.1091 \end{bmatrix}$$

$$\boldsymbol{\sigma_l} = \begin{bmatrix} 0.1238 & 0.1364 & 0.1407 & 0.1513 & 0.1865 & 0.2791 \end{bmatrix}$$

$$\mathbf{w}^{(1)} = \begin{bmatrix} -1.0796 & 0.1685 & 0.4228 & -0.0502 & 1.0982 & -0.2822 & -1.1182 & -0.6282 & -0.2225 & 0.5533 \\ -0.7064 & 0.8783 & 0.1208 & -0.2014 & -0.5827 & 0.1419 & -0.4472 & 1.3983 & 0.3082 & -0.2647 \\ 0.9203 & 1.0432 & 0.0528 & 0.1203 & 0.1476 & -0.1043 & 1.2676 & 0.2546 & 0.3107 & 0.4343 \\ 0.3022 & 0.3024 & 0.3754 & 0.0524 & 0.2374 & 0.2908 & 0.1803 & -0.3290 & 0.1884 & 0.8822 \\ 0.3653 & 1.2908 & -0.4753 & 0.5294 & -0.2619 & 0.6676 & -1.3494 & -0.6045 & -0.0348 & -0.2475 \\ 0.0040 & -0.1884 & -0.9823 & -0.0716 & 0.6650 & 0.0467 & -0.1273 & -0.0673 & -0.1595 & 0.1691 \end{bmatrix}$$

$$\mathbf{b}^{(1)} = \begin{bmatrix} -0.3457 & -0.3160 & 1.2340 & 0.3590 & 0.7151 & 0.1346 & -0.2807 & -0.9945 & 0.5826 & -0.1260 \end{bmatrix}$$

$$(\mathbf{w}^{(2)})^{\mathrm{T}} = \begin{bmatrix} -0.7103 & 0.8422 & -1.0349 & 0.5446 & 1.0749 & 0.6078 & 1.4129 & -1.3005 & -1.0369 & -0.4583 \end{bmatrix} \text{ and } b^{(2)} = \text{-0.2230}$$

μ_c = -0.0400 and σ_c = 0.3180

TABLE 21: As in Table 20 but for $a_{ys}(412)$.

$$\boldsymbol{\mu_l} = \begin{bmatrix} -2.4092 & -2.3522 & -2.2408 & -2.2435 & -2.3018 & -3.1091 \end{bmatrix}$$

$$\boldsymbol{\sigma_l} = \begin{bmatrix} 0.1238 & 0.1364 & 0.1407 & 0.1513 & 0.1865 & 0.2791 \end{bmatrix}$$

$$\mathbf{w}^{(1)} = \begin{bmatrix} -1.3362 & -0.3878 & -0.2826 & -0.0704 & 0.1553 & 0.3137 & -0.3926 & 0.6905 & 0.1549 & -0.0979 \\ 0.6455 & -0.6661 & 1.1318 & 0.4492 & 0.3011 & 0.6312 & 0.2376 & -0.5718 & -0.0021 & 0.2671 \\ 0.5934 & -0.6321 & -0.3939 & 0.0716 & 0.0036 & 0.0144 & 0.5226 & 0.9199 & 0.3146 & 0.0953 \\ -0.3444 & -0.3776 & 0.4499 & -0.5641 & -0.7266 & -1.0717 & -1.1365 & 0.2559 & 0.0687 & -0.0058 \\ 0.4253 & -0.1857 & 0.7266 & 0.3062 & 0.2601 & 0.2757 & 0.2956 & -0.2261 & -0.0719 & -0.3101 \\ 0.3529 & -0.5216 & -0.5634 & -0.1003 & -0.4878 & -0.4559 & 0.3795 & -0.2660 & -0.4888 & -0.1773 \end{bmatrix}$$

$$\mathbf{b}^{(1)} = \begin{bmatrix} 0.4850 & -0.0153 & -0.0078 & -0.2171 & 0.7416 & -0.8786 & 0.7386 & 0.0825 & -0.2630 & -0.1546 \end{bmatrix}$$

$$(\mathbf{w}^{(2)})^{\mathrm{T}} = \begin{bmatrix} 1.0835 & 0.3678 & 1.3277 & 0.2471 & -1.0407 & 1.2120 & 1.1102 & -1.0788 & -0.2180 & 0.2684 \end{bmatrix} \text{ and } b^{(2)} = 0.2934$$

μ_c = -0.9425 and σ_c = 0.2086

TABLE 22: As in Table 20 but for TSM.

$$\boldsymbol{\mu_l} = \begin{bmatrix} -2.4092 & -2.3522 & -2.2408 & -2.2435 & -2.3018 & -3.1091 \end{bmatrix}$$

$$\boldsymbol{\sigma_l} = \begin{bmatrix} 0.1238 & 0.1364 & 0.1407 & 0.1513 & 0.1865 & 0.2791 \end{bmatrix}$$

$$\mathbf{w}^{(1)} = \begin{bmatrix} -0.4152 & 0.7830 & 0.7331 & 0.0434 & -0.2798 & -0.1422 & 0.0434 & 0.6225 & -0.2821 & 0.9275 \\ -0.3920 & 0.6333 & -0.3487 & 0.0079 & -1.1312 & -0.4706 & -0.5005 & 0.0121 & -0.0908 & -0.3756 \\ -0.3436 & -0.5487 & 0.1974 & 1.2007 & -0.1022 & -0.0642 & -0.1325 & 0.0602 & -0.1583 & -0.7000 \\ -0.0897 & -0.1993 & -0.6512 & -0.4627 & 0.2429 & -0.6941 & -0.6464 & 0.5683 & -0.2853 & 0.1429 \\ 0.0302 & -0.0155 & -0.1770 & -0.1734 & 0.0933 & 0.7814 & -0.2223 & 0.8238 & -0.3551 & 0.1787 \\ -0.6979 & 0.0142 & 0.7859 & -0.5209 & 0.7195 & -0.0376 & 0.2168 & -0.7392 & -0.2388 & -0.5171 \end{bmatrix}$$

$$\mathbf{b}^{(1)} = \begin{bmatrix} 0.1506 & -0.4613 & -0.4210 & -1.3344 & -0.0330 & -0.1546 & 0.3440 & -0.1219 & -1.0486 & 0.7670 \end{bmatrix}$$

$$(\mathbf{w}^{(2)})^{\mathrm{T}} = \begin{bmatrix} 0.4980 & 0.8906 & 0.9220 & -1.3211 & 0.3838 & 0.8045 & -0.1132 & 0.6185 & -0.4249 & -0.8623 \end{bmatrix} \text{ and } b^{(2)} = \text{-0.0415}$$

μ_c = 0.0002 and σ_c = 0.2206

TABLE 23: As in Table 17 but for the center wavelengths of the MODIS sensor (see Table. 2).

$$\boldsymbol{\mu_l} = \begin{bmatrix} -2.4092 & -2.3522 & -2.2542 & -2.1715 & -2.3218 & -3.1084 \end{bmatrix}$$

$$\boldsymbol{\sigma_l} = \begin{bmatrix} 0.1238 & 0.1364 & 0.1420 & 0.1523 & 0.1846 & 0.2795 \end{bmatrix}$$

$$\mathbf{w}^{(1)} = \begin{bmatrix} -0.3993 & 0.1271 & -0.2764 & 0.3246 & -0.8585 & -0.9343 & 1.0226 & -0.4754 & 0.1341 & 0.7277 \\ 0.4436 & -1.0444 & 0.3738 & -0.9515 & -0.3127 & -0.0588 & -0.0544 & -0.3332 & -0.4932 & -0.4304 \\ -0.1047 & -1.3869 & -0.1785 & 0.0032 & -0.0497 & 0.4316 & -1.8955 & -0.5923 & -0.0632 & -0.0376 \\ -0.5272 & -0.8368 & 0.0820 & 0.5677 & 0.5204 & 0.0140 & 0.4084 & 0.0599 & 0.9681 & -0.0613 \\ 0.5672 & -0.2472 & 1.0192 & 0.1447 & 0.2102 & -1.1125 & 0.2215 & 0.5395 & 0.1371 & 0.4591 \\ -0.2179 & -0.3107 & -1.2322 & -0.0862 & 0.9110 & -0.0664 & 0.5161 & -0.7365 & -0.3934 & -0.3710 \end{bmatrix}$$

$$\mathbf{b}^{(1)} = \begin{bmatrix} -0.0099 & 0.4234 & -0.5205 & 0.7738 & -1.6636 & -0.2763 & -1.4656 & 0.7893 & 0.8048 & -0.4959 \end{bmatrix}$$

$$(\mathbf{w}^{(2)})^{\mathrm{T}} = \begin{bmatrix} -0.7700 & -0.8177 & -1.0673 & 1.2114 & 0.6530 & 0.8224 & 1.6350 & 0.5561 & 0.9985 & 0.3602 \end{bmatrix} \text{ and } b^{(2)} = 0.2386$$

μ_c = -0.0400 and σ_c = 0.3180

TABLE 24: As in Table 23 but for $a_{ys}(412)$.

$$\boldsymbol{\mu_l} = \begin{bmatrix} -2.4092 & -2.3522 & -2.2542 & -2.1715 & -2.3218 & -3.1084 \end{bmatrix}$$

$$\boldsymbol{\sigma_l} = \begin{bmatrix} 0.1238 & 0.1364 & 0.1420 & 0.1523 & 0.1846 & 0.2795 \end{bmatrix}$$

$$\mathbf{w}^{(1)} = \begin{bmatrix} -0.5721 & 0.3315 & -0.3158 & 0.4948 & 0.0855 & -0.1232 & -0.2655 & -0.6873 & 0.3934 & 0.0849 \\ 0.1191 & -0.2131 & -0.1214 & -0.7847 & -0.9093 & 0.0886 & 0.3038 & 0.1452 & -0.7531 & 0.2156 \\ -0.0242 & 0.2352 & -0.8737 & 1.6852 & 0.1784 & 0.0145 & 0.0553 & 0.0872 & 0.1411 & 0.4934 \\ -0.2870 & 0.1716 & 0.4711 & -1.3955 & 0.4823 & 1.1642 & 0.4415 & -0.4019 & -0.1655 & -0.7848 \\ -0.2893 & 0.0092 & -0.0873 & 0.0454 & 0.0960 & -1.5341 & 0.0981 & -0.0169 & -0.2617 & -0.5315 \\ 0.6049 & -0.0538 & -0.0581 & -0.7832 & 0.2825 & -1.1987 & 0.4856 & -0.0146 & 0.2580 & 0.0125 \end{bmatrix}$$

$$\mathbf{b}^{(1)} = \begin{bmatrix} 1.3218 & -0.1128 & -0.3927 & -0.2802 & 0.9685 & -0.4126 & 0.3136 & -0.3165 & -0.0603 & 0.2118 \end{bmatrix}$$

$$(\mathbf{w}^{(2)})^{\mathrm{T}} = \begin{bmatrix} 0.9566 & -0.1066 & 0.7019 & -2.0497 & -1.0352 & 1.6626 & 0.4586 & -0.2794 & -0.6404 & -0.9496 \end{bmatrix} \text{ and } b^{(2)} = -0.0448$$

μ_c = -0.9425 and σ_c = 0.2086

TABLE 25: As in Table 23 but for TSM.

$$\boldsymbol{\mu_l} = \begin{bmatrix} -2.4092 & -2.3522 & -2.2542 & -2.1715 & -2.3218 & -3.1084 \end{bmatrix}$$

$$\boldsymbol{\sigma_l} = \begin{bmatrix} 0.1238 & 0.1364 & 0.1420 & 0.1523 & 0.1846 & 0.2795 \end{bmatrix}$$

$$\mathbf{w}^{(1)} = \begin{bmatrix} -0.7403 & -0.1801 & 0.4189 & 0.8534 & 0.4923 & -0.1324 & -0.1224 & 0.0662 & 0.1194 & 0.2637 \\ -0.2202 & 0.2026 & -0.4998 & 0.2151 & -0.0872 & -0.3218 & 0.1722 & 0.4529 & -0.1139 & -0.0083 \\ 0.5621 & 0.0999 & 0.5451 & -0.2389 & -0.1909 & -0.0201 & 0.6865 & 0.2159 & -0.6896 & -0.1505 \\ 0.2629 & 0.9165 & 0.3535 & -0.4866 & -0.1039 & -1.0969 & -0.1381 & 0.0601 & 0.3303 & 0.9330 \\ 0.3080 & 0.1325 & 0.1620 & -0.5748 & -0.3781 & -0.2259 & 0.0859 & -0.3855 & 0.3094 & 0.2674 \\ -0.6499 & -0.5273 & -0.1486 & 0.0938 & -0.4302 & -0.3240 & -0.3574 & 0.3406 & 0.2895 & -0.1345 \end{bmatrix}$$

$$\mathbf{b}^{(1)} = \begin{bmatrix} 0.3044 & -0.0716 & -0.0326 & 0.0158 & 0.9904 & 0.1600 & -0.4954 & 0.5202 & 0.8955 & 0.6169 \end{bmatrix}$$

$$(\mathbf{w}^{(2)})^{\mathrm{T}} = \begin{bmatrix} -1.1438 & 0.2186 & 0.3268 & -0.3287 & -0.6953 & 0.3155 & -0.7469 & -0.5215 & 0.9892 & 0.5303 \end{bmatrix} \text{ and } b^{(2)} = -0.2105$$

μ_c = 0.0002 and σ_c = 0.2206

TABLE 26: As in Table 17 but for the center wavelengths of the MERIS sensor (see Table. 2).

$$\boldsymbol{\mu_l} = \begin{bmatrix} -2.4092 & -2.3522 & -2.2408 & -2.2435 & -2.2924 & -3.1084 \end{bmatrix}$$

$$\boldsymbol{\sigma_l} = \begin{bmatrix} 0.1238 & 0.1364 & 0.1407 & 0.1513 & 0.1877 & 0.2795 \end{bmatrix}$$

$$\mathbf{w}^{(1)} = \begin{bmatrix} -0.1966 & -1.4616 & -0.6065 & -0.7693 & -0.3104 & 0.4282 & -0.5591 & -1.0897 & -0.3669 & -0.7147 \\ 0.2711 & -0.0099 & -0.0711 & -0.0549 & -0.0693 & -0.7666 & 0.0940 & 1.4991 & 0.3807 & -0.4755 \\ 1.2877 & 1.0552 & -0.0774 & -0.2487 & 1.0122 & 0.2969 & -0.7500 & 0.2322 & -0.2436 & -0.7901 \\ 0.1452 & 0.1708 & 0.0273 & -0.5869 & 0.6399 & -0.0094 & 0.1272 & -0.1920 & -0.0665 & -0.4632 \\ 0.1108 & -1.5764 & 0.3815 & 0.2972 & -0.8039 & 0.7291 & 0.0939 & -0.0566 & -0.0614 & -1.3891 \\ -0.4580 & -0.0052 & -0.8190 & -0.1680 & -0.7935 & -0.5263 & -0.1414 & -0.5038 & 0.6245 & -0.0735 \end{bmatrix}$$

$$\mathbf{b}^{(1)} = \begin{bmatrix} -0.3103 & -0.0240 & -0.1616 & 0.0853 & 1.7432 & 0.3148 & 0.2970 & -0.9904 & -0.3328 & 0.3654 \end{bmatrix}$$

$$(\mathbf{w}^{(2)})^{\mathrm{T}} = \begin{bmatrix} 0.5420 & 1.4015 & -0.9836 & 0.3984 & -1.6315 & 0.8891 & 0.3410 & -1.7970 & 0.5072 & -0.7644 \end{bmatrix} \text{ and } b^{(2)} = 0.0933$$

$$\mu_c = \text{-0.0400 and } \sigma_c = 0.3180$$

TABLE 27: As in Table 26 but for $a_{ys}(412)$.

$$\boldsymbol{\mu_l} = \begin{bmatrix} -2.4092 & -2.3522 & -2.2408 & -2.2435 & -2.2924 & -3.1084 \end{bmatrix}$$

$$\boldsymbol{\sigma_l} = \begin{bmatrix} 0.1238 & 0.1364 & 0.1407 & 0.1513 & 0.1877 & 0.2795 \end{bmatrix}$$

$$\mathbf{w}^{(1)} = \begin{bmatrix} -1.3693 & 1.7368 & 0.2004 & 0.4001 & 0.5334 & 0.3072 & -0.1804 & 1.2737 & -0.4155 & -0.2196 \\ -0.3791 & -0.5830 & -0.2115 & -1.2028 & 1.0502 & -0.3336 & -0.0724 & -0.0311 & -0.7559 & -0.5316 \\ -0.3444 & -1.3683 & -1.2133 & 0.2557 & -0.5957 & -0.4176 & 0.2337 & 0.5310 & 0.1178 & 0.2408 \\ -0.1824 & 0.8138 & 0.2915 & -0.4539 & -1.4790 & -0.0418 & 0.2531 & 0.1104 & -0.0876 & -0.3561 \\ -0.4323 & -0.6382 & -0.5612 & -0.9340 & 0.5160 & 1.1362 & -0.0877 & -1.0356 & 0.0857 & -0.4541 \\ -0.2341 & -0.1157 & -0.2749 & 0.2991 & -0.1414 & 0.5230 & 0.7922 & -0.7086 & 0.2033 & 0.0817 \end{bmatrix}$$

$$\mathbf{b}^{(1)} = \begin{bmatrix} -0.4816 & -0.6651 & 0.4828 & -0.0818 & -0.6941 & -0.1212 & -0.5391 & 0.2954 & -0.0784 & -0.0354 \end{bmatrix}$$

$$(\mathbf{w}^{(2)})^{\mathrm{T}} = \begin{bmatrix} 0.7304 & -1.6400 & 0.7835 & -1.0897 & 1.7414 & -0.6150 & 1.2557 & -0.7196 & -0.2626 & -0.3039 \end{bmatrix} \text{ and } b^{(2)} = 0.4452$$

$$\mu_c = \text{-0.9425 and } \sigma_c = 0.2086$$

TABLE 28: As in Table 26 but for TSM.

$$\boldsymbol{\mu_l} = \begin{bmatrix} -2.4092 & -2.3522 & -2.2408 & -2.2435 & -2.2924 & -3.1084 \end{bmatrix}$$

$$\boldsymbol{\sigma_l} = \begin{bmatrix} 0.1238 & 0.1364 & 0.1407 & 0.1513 & 0.1877 & 0.2795 \end{bmatrix}$$

$$\mathbf{w}^{(1)} = \begin{bmatrix} -0.3557 & 0.5999 & 0.8575 & 0.3279 & -1.6375 & -0.2784 & -0.4640 & 0.1633 & 0.3140 & 1.0921 \\ 0.0023 & 0.1851 & -0.3376 & 0.0162 & 0.0866 & -0.6724 & -0.0105 & 0.4786 & -0.3664 & -0.2688 \\ 0.7468 & -0.7161 & -0.7056 & 0.1975 & 1.0516 & 0.2732 & -0.1239 & 0.2200 & 0.6265 & 0.0998 \\ -0.4314 & -0.1882 & 0.2479 & 0.1620 & -0.3636 & -0.3229 & 0.0832 & 0.0101 & 0.1453 & -0.0075 \\ -0.2347 & 0.1874 & -0.1978 & 0.3512 & -0.3676 & 0.1106 & 0.0921 & 0.2486 & -0.7208 & 0.3776 \\ 0.8186 & 0.4786 & 0.0177 & 0.1230 & 0.5199 & -1.0796 & 0.0672 & -0.6777 & -0.2444 & 0.2053 \end{bmatrix}$$

$$\mathbf{b}^{(1)} = \begin{bmatrix} -0.8708 & -0.1678 & 0.0661 & 0.1827 & 0.7175 & 0.1338 & 0.3722 & -0.4386 & -1.1578 & 0.5317 \end{bmatrix}$$

$$(\mathbf{w}^{(2)})^{\mathrm{T}} = \begin{bmatrix} 0.9674 & 0.8620 & -0.5868 & 0.4601 & -1.0228 & 0.5598 & 0.6562 & -0.9595 & -0.8493 & 0.2613 \end{bmatrix} \text{ and } b^{(2)} = \text{-0.1068}$$

$$\mu_c = 0.0002 \text{ and } \sigma_c = 0.2206$$

3.3 Northern Adriatic Sea (BiOMaP data)

BiOMaP data from the Northern Adriatic Sea (Figure 3(a)) were collected during a single cruise executed in 2000 (55 stations). Panels 7(b) to 7(d) show that the MLP performance reduces when increasing the number of hidden units. This trend, quite different from that observed for the CoASTS data (Panels 5(b) to 5(d)), is likely due to the reduced number of BiOMaP data in the Norther Adriatic Sea and possibly to the presence of a few outliers which hamper the training of complex MLP architectures. Results shown in Figure 8 and Table 29 are derived from the MLP with two hidden units.

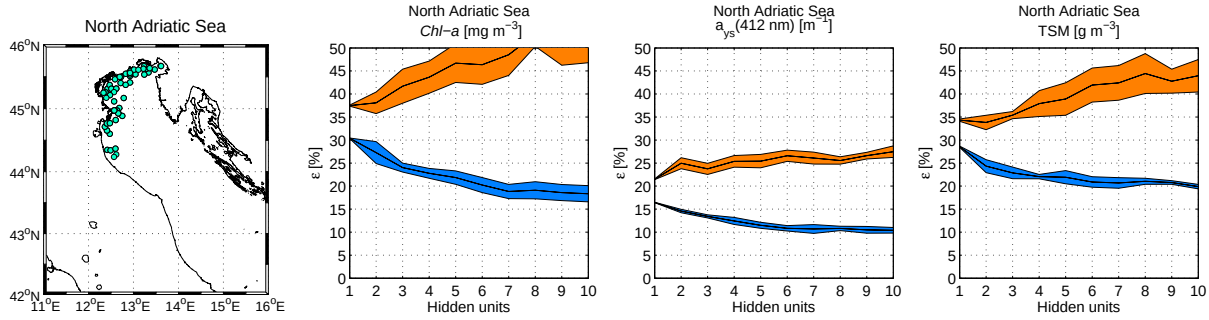

FIGURE 7: As in Figure 3, but only considering BiOMaP data.

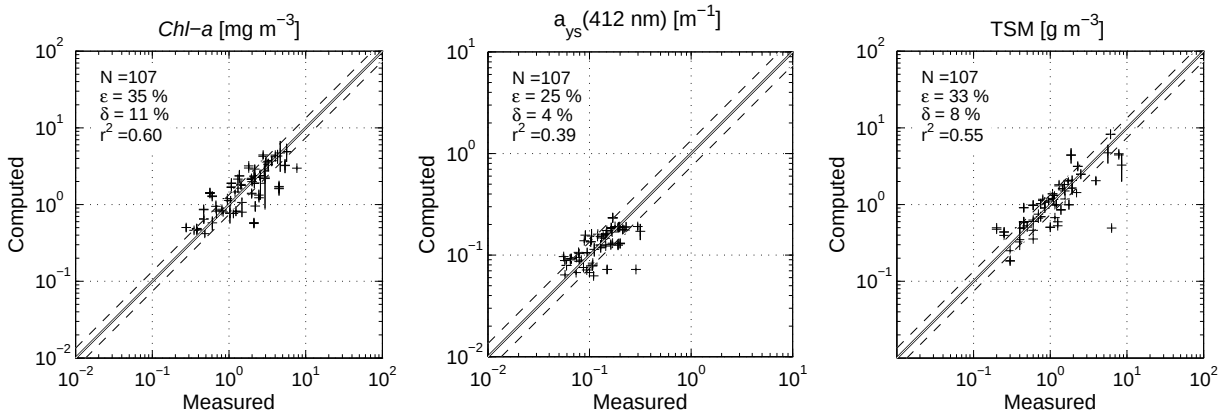

FIGURE 8: As in Figure 4, but only considering BiOMaP data. Results based on the MLP with two units in the hidden layer.

TABLE 29: As in Table 3, but only considering BiOMaP data. Results based on the MLP with two units in the hidden layer.

	N	ϵ [%]	δ [%]	r^2
Chl-a	107	37.8(24.6)	10.1(3.9)	49.2(78.2)
$a_{ys}(412)$	107	26.3(14.5)	4.9(2.0)	39.1(78.3)
TSM	107	32.7(23.5)	6.6(5.4)	53.8(85.2)

TABLE 30: Parameter sets to compute data pre- and post-processing, as well as MLP weights to derive *Chl-a* values in the Northern Adriatic Sea when considering BiOMaP data only). Input R_{RS} wavelengths are those of the in-situ measurements (see Table. 2).

$$\boldsymbol{\mu_l} = \begin{bmatrix} -2.4617 & -2.3965 & -2.2536 & -2.2705 & -2.2836 & -3.1011 \end{bmatrix}$$

$$\boldsymbol{\sigma_l} = \begin{bmatrix} 0.1442 & 0.1434 & 0.1447 & 0.1693 & 0.2344 & 0.3797 \end{bmatrix}$$

$$\mathbf{w}^{(1)} = \begin{bmatrix} 1.7004 & -1.3115 \\ -2.2328 & 0.0791 \\ 0.0749 & 0.6367 \\ 0.1321 & 0.9367 \\ 0.2947 & 0.9192 \\ 0.2485 & -0.4675 \end{bmatrix}$$

$$\mathbf{b}^{(1)} = \begin{bmatrix} 0.4979 & -1.9559 \end{bmatrix}$$

$$(\mathbf{w}^{(2)})^{\mathrm{T}} = \begin{bmatrix} 2.8077 & 1.1122 \end{bmatrix} \text{ and } b^{(2)} = \text{-0.3636}$$

$$\mu_c = \text{0.1956 and } \sigma_c = \text{0.3401}$$

TABLE 31: As in Table 30 but for $a_{ys}(412)$.

$$\boldsymbol{\mu_l} = \begin{bmatrix} -2.4617 & -2.3965 & -2.2536 & -2.2705 & -2.2836 & -3.1011 \end{bmatrix}$$

$$\boldsymbol{\sigma_l} = \begin{bmatrix} 0.1442 & 0.1434 & 0.1447 & 0.1693 & 0.2344 & 0.3797 \end{bmatrix}$$

$$\mathbf{w}^{(1)} = \begin{bmatrix} 1.0103 & 0.9078 \\ -1.3160 & 0.0502 \\ -1.8945 & -1.3035 \\ 0.4459 & -0.9071 \\ 1.0321 & 1.4545 \\ 0.6729 & -0.3905 \end{bmatrix}$$

$$\mathbf{b}^{(1)} = \begin{bmatrix} -0.0325 & 1.3651 \end{bmatrix}$$

$$(\mathbf{w}^{(2)})^{\mathrm{T}} = \begin{bmatrix} 1.0589 & -1.7302 \end{bmatrix} \text{ and } b^{(2)} = \text{1.3685}$$

$$\mu_c = \text{-0.8897 and } \sigma_c = \text{0.1852}$$

TABLE 32: As in Table 30 but for TSM.

$$\boldsymbol{\mu_l} = \begin{bmatrix} -2.4617 & -2.3965 & -2.2536 & -2.2705 & -2.2836 & -3.1011 \end{bmatrix}$$

$$\boldsymbol{\sigma_l} = \begin{bmatrix} 0.1442 & 0.1434 & 0.1447 & 0.1693 & 0.2344 & 0.3797 \end{bmatrix}$$

$$\mathbf{w}^{(1)} = \begin{bmatrix} 1.1207 & -0.4233 \\ -0.5835 & 0.2598 \\ -1.0231 & 1.4553 \\ -0.4274 & -0.8275 \\ 0.6505 & -0.3246 \\ -0.1580 & -0.0793 \end{bmatrix}$$

$$\mathbf{b}^{(1)} = \begin{bmatrix} 1.1892 & -0.2036 \end{bmatrix}$$

$$(\mathbf{w}^{(2)})^{\mathrm{T}} = \begin{bmatrix} -2.2343 & -2.0183 \end{bmatrix} \text{ and } b^{(2)} = \text{1.1924}$$

$$\mu_c = \text{0.0317 and } \sigma_c = \text{0.3827}$$

TABLE 33: As in Table 30 but for the center wavelengths of the SeaWiFS sensor (see Table. 2).

$$\boldsymbol{\mu_l} = \begin{bmatrix} -2.4617 & -2.3965 & -2.2536 & -2.2705 & -2.2836 & -3.1021 \end{bmatrix}$$

$$\boldsymbol{\sigma_l} = \begin{bmatrix} 0.1442 & 0.1434 & 0.1447 & 0.1693 & 0.2344 & 0.3794 \end{bmatrix}$$

$$\mathbf{w}^{(1)} = \begin{bmatrix} 0.8488 & 1.8246 \\ 0.2755 & -2.4727 \\ -0.3176 & 0.3339 \\ -0.7687 & -0.0925 \\ -1.1634 & 0.4105 \\ 0.1691 & 0.2771 \end{bmatrix}$$

$$\mathbf{b}^{(1)} = \begin{bmatrix} 2.0493 & 0.6446 \end{bmatrix}$$

$$(\mathbf{w}^{(2)})^{\mathrm{T}} = \begin{bmatrix} -0.9094 & 2.6995 \end{bmatrix} \text{ and } b^{(2)} = \text{-0.7193}$$

$$\mu_c = \text{0.1956 and } \sigma_c = \text{0.3401}$$

TABLE 34: As in Table 33 but for $a_{ys}(412)$.

$$\boldsymbol{\mu_l} = \begin{bmatrix} -2.4617 & -2.3965 & -2.2536 & -2.2705 & -2.2836 & -3.1021 \end{bmatrix}$$

$$\boldsymbol{\sigma_l} = \begin{bmatrix} 0.1442 & 0.1434 & 0.1447 & 0.1693 & 0.2344 & 0.3794 \end{bmatrix}$$

$$\mathbf{w}^{(1)} = \begin{bmatrix} 0.8333 & 0.9408 \\ 0.0756 & -1.2318 \\ -1.2218 & -1.7857 \\ -0.8812 & 0.1446 \\ 1.4332 & 1.1431 \\ -0.4428 & 0.7494 \end{bmatrix}$$

$$\mathbf{b}^{(1)} = \begin{bmatrix} 1.3518 & -0.0133 \end{bmatrix}$$

$$(\mathbf{w}^{(2)})^{\mathrm{T}} = \begin{bmatrix} -1.7391 & 1.0242 \end{bmatrix} \text{ and } b^{(2)} = \text{1.3626}$$

$$\mu_c = \text{-0.8897 and } \sigma_c = \text{0.1852}$$

TABLE 35: As in Table 33 but for TSM.

$$\boldsymbol{\mu_l} = \begin{bmatrix} -2.4617 & -2.3965 & -2.2536 & -2.2705 & -2.2836 & -3.1021 \end{bmatrix}$$

$$\boldsymbol{\sigma_l} = \begin{bmatrix} 0.1442 & 0.1434 & 0.1447 & 0.1693 & 0.2344 & 0.3794 \end{bmatrix}$$

$$\mathbf{w}^{(1)} = \begin{bmatrix} 0.8065 & 0.8949 \\ -0.9684 & -0.4539 \\ -1.0172 & -0.7097 \\ 0.4230 & -0.5411 \\ 0.6324 & 0.8117 \\ -0.0296 & -0.4023 \end{bmatrix}$$

$$\mathbf{b}^{(1)} = \begin{bmatrix} 0.1246 & 1.0695 \end{bmatrix}$$

$$(\mathbf{w}^{(2)})^{\mathrm{T}} = \begin{bmatrix} 1.4417 & -2.4037 \end{bmatrix} \text{ and } b^{(2)} = \text{1.4657}$$

$$\mu_c = \text{0.0317 and } \sigma_c = \text{0.3827}$$

TABLE 36: As in Table 30 but for the center wavelengths of the MODIS sensor (see Table. 2).

$$\boldsymbol{\mu_l} = \begin{bmatrix} -2.4617 & -2.3965 & -2.2668 & -2.1940 & -2.3059 & -3.1011 \end{bmatrix}$$

$$\boldsymbol{\sigma_l} = \begin{bmatrix} 0.1442 & 0.1434 & 0.1468 & 0.1685 & 0.2332 & 0.3797 \end{bmatrix}$$

$$\mathbf{w}^{(1)} = \begin{bmatrix} 1.6490 & -1.1553 \\ -0.5738 & 1.5687 \\ -0.6939 & 0.5723 \\ -0.6281 & -1.5248 \\ -0.8041 & 0.6214 \\ 0.2653 & -0.1436 \end{bmatrix}$$

$$\mathbf{b}^{(1)} = \begin{bmatrix} 2.1460 & -0.1896 \end{bmatrix}$$

$$(\mathbf{w}^{(2)})^{\mathrm{T}} = \begin{bmatrix} -1.2900 & -2.7952 \end{bmatrix} \text{ and } b^{(2)} = 0.4791$$

$$\mu_c = 0.1956 \text{ and } \sigma_c = 0.3401$$

TABLE 37: As in Table 36 but for $a_{ys}(412)$.

$$\boldsymbol{\mu_l} = \begin{bmatrix} -2.4617 & -2.3965 & -2.2668 & -2.1940 & -2.3059 & -3.1011 \end{bmatrix}$$

$$\boldsymbol{\sigma_l} = \begin{bmatrix} 0.1442 & 0.1434 & 0.1468 & 0.1685 & 0.2332 & 0.3797 \end{bmatrix}$$

$$\mathbf{w}^{(1)} = \begin{bmatrix} -0.9053 & 0.6845 \\ 0.0459 & -1.0617 \\ 1.5575 & -1.2664 \\ 0.6029 & 1.5419 \\ -1.8401 & -0.2296 \\ 0.5614 & 0.2690 \end{bmatrix}$$

$$\mathbf{b}^{(1)} = \begin{bmatrix} -1.0377 & 0.0806 \end{bmatrix}$$

$$(\mathbf{w}^{(2)})^{\mathrm{T}} = \begin{bmatrix} 2.1691 & 1.4578 \end{bmatrix} \text{ and } b^{(2)} = 1.4669$$

$$\mu_c = \text{-}0.8897 \text{ and } \sigma_c = 0.1852$$

TABLE 38: As in Table 36 but for TSM.

$$\boldsymbol{\mu_l} = \begin{bmatrix} -2.4617 & -2.3965 & -2.2668 & -2.1940 & -2.3059 & -3.1011 \end{bmatrix}$$

$$\boldsymbol{\sigma_l} = \begin{bmatrix} 0.1442 & 0.1434 & 0.1468 & 0.1685 & 0.2332 & 0.3797 \end{bmatrix}$$

$$\mathbf{w}^{(1)} = \begin{bmatrix} -0.1820 & -0.9702 \\ 0.4316 & 0.5712 \\ 0.8063 & 0.7913 \\ -1.1245 & 0.3152 \\ 0.2924 & -0.4985 \\ -0.1101 & 0.3558 \end{bmatrix}$$

$$\mathbf{b}^{(1)} = \begin{bmatrix} -0.3725 & -1.3998 \end{bmatrix}$$

$$(\mathbf{w}^{(2)})^{\mathrm{T}} = \begin{bmatrix} -1.8086 & 1.9415 \end{bmatrix} \text{ and } b^{(2)} = 0.8728$$

$$\mu_c = 0.0317 \text{ and } \sigma_c = 0.3827$$

TABLE 39: As in Table 30 but for the center wavelengths of the MERIS sensor (see Table. 2).

$$\boldsymbol{\mu_l} = \begin{bmatrix} -2.4617 & -2.3965 & -2.2536 & -2.2705 & -2.2732 & -3.1011 \end{bmatrix}$$

$$\boldsymbol{\sigma_l} = \begin{bmatrix} 0.1442 & 0.1434 & 0.1447 & 0.1693 & 0.2357 & 0.3797 \end{bmatrix}$$

$$\mathbf{w}^{(1)} = \begin{bmatrix} -0.8233 & 1.7997 \\ -0.1910 & -2.3956 \\ 0.1148 & 0.2992 \\ 0.8210 & -0.1782 \\ 1.1367 & 0.5104 \\ -0.0318 & 0.2546 \end{bmatrix}$$

$$\mathbf{b}^{(1)} = \begin{bmatrix} -2.0505 & 0.6554 \end{bmatrix}$$

$$(\mathbf{w}^{(2)})^{\mathrm{T}} = \begin{bmatrix} 0.8967 & 2.6835 \end{bmatrix} \text{ and } b^{(2)} = \text{-0.7401}$$

$$\mu_c = 0.1956 \text{ and } \sigma_c = 0.3401$$

TABLE 40: As in Table 39 but for $a_{ys}(412)$.

$$\boldsymbol{\mu_l} = \begin{bmatrix} -2.4617 & -2.3965 & -2.2536 & -2.2705 & -2.2732 & -3.1011 \end{bmatrix}$$

$$\boldsymbol{\sigma_l} = \begin{bmatrix} 0.1442 & 0.1434 & 0.1447 & 0.1693 & 0.2357 & 0.3797 \end{bmatrix}$$

$$\mathbf{w}^{(1)} = \begin{bmatrix} -0.8243 & -0.8503 \\ 1.2073 & 0.0749 \\ 1.6311 & 1.1220 \\ -0.2327 & 0.6116 \\ -0.9555 & -1.0352 \\ -0.7533 & 0.3828 \end{bmatrix}$$

$$\mathbf{b}^{(1)} = \begin{bmatrix} 0.0100 & -1.4117 \end{bmatrix}$$

$$(\mathbf{w}^{(2)})^{\mathrm{T}} = \begin{bmatrix} -1.0429 & 1.6213 \end{bmatrix} \text{ and } b^{(2)} = 1.2737$$

$$\mu_c = \text{-0.8897 and } \sigma_c = 0.1852$$

TABLE 41: As in Table 39 but for TSM.

$$\boldsymbol{\mu_l} = \begin{bmatrix} -2.4617 & -2.3965 & -2.2536 & -2.2705 & -2.2732 & -3.1011 \end{bmatrix}$$

$$\boldsymbol{\sigma_l} = \begin{bmatrix} 0.1442 & 0.1434 & 0.1447 & 0.1693 & 0.2357 & 0.3797 \end{bmatrix}$$

$$\mathbf{w}^{(1)} = \begin{bmatrix} 1.1323 & 0.8897 \\ -0.7827 & -0.8593 \\ -0.7489 & -1.3024 \\ -0.3585 & 0.5263 \\ 0.8325 & 0.7384 \\ -0.4299 & -0.1343 \end{bmatrix}$$

$$\mathbf{b}^{(1)} = \begin{bmatrix} 0.9292 & -0.0004 \end{bmatrix}$$

$$(\mathbf{w}^{(2)})^{\mathrm{T}} = \begin{bmatrix} -2.5060 & 1.6713 \end{bmatrix} \text{ and } b^{(2)} = 1.5438$$

$$\mu_c = 0.0317 \text{ and } \sigma_c = 0.3827$$

3.4 Eastern Mediterranean Sea

BiOMaP data from the Eastern Mediterranean Sea (Figure 9) were collected during two cruises executed in 2006 and 2007 (62 and 69 stations, respectively). Trends of Panels 9(b)–9(d) support the selection of a simple MLP architecture since the Eastern Mediterranean Sea mostly include oligotrophic waters, with optical properties dominated by the phytoplankton component and co-varying constituents. Validation results produced by the MLP with two hidden units are reported in Figure 10 and Table 42.

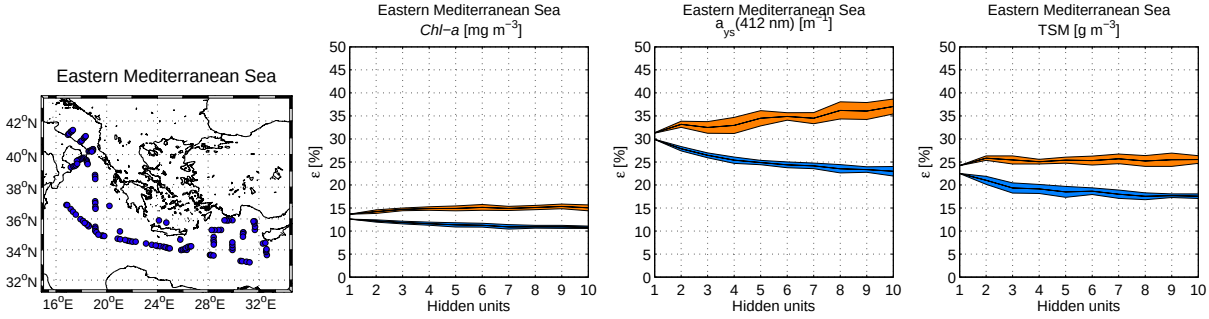

(a) (b) (c) (d)

FIGURE 9: As in Figure 3, but for the Eastern Mediterranean Sea.

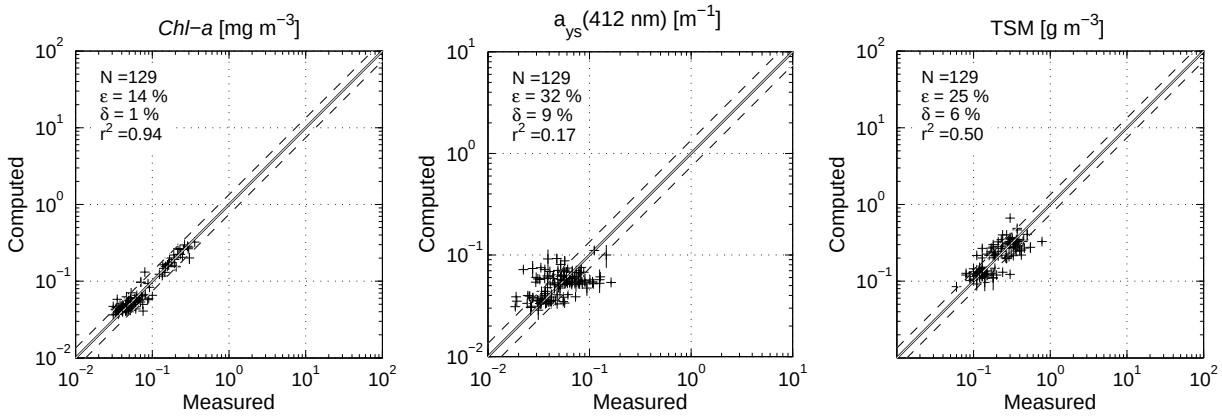

(a) (b) (c)

FIGURE 10: As in Figure 4, but for the Eastern Mediterranean Sea. Results based on the MLP with two units in the hidden layer.

TABLE 42: As in Table 3, but for the Eastern Mediterranean Sea. Results based on the MLP with two units in the hidden layer.

	N	ϵ [%]	δ [%]	r^2
Chl-a	129	14.2(12.3)	1.4(1.1)	93.8(96.7)
$a_{ys}(412)$	129	34.3(28.1)	9.8(5.9)	16.3(40.5)
TSM	129	25.5(20.5)	6.1(3.4)	51.6(68.0)

TABLE 43: Parameter sets to compute data pre- and post-processing, as well as MLP weights to derive *Chl-a* values in the Eastern Mediterranean Sea. Input R_{RS} wavelengths are those of the in-situ measurements (see Table 2).

$$\boldsymbol{\mu_l} = \begin{bmatrix} -2.0506 & -2.0796 & -2.2152 & -2.4125 & -2.7451 & -3.7660 \end{bmatrix}$$

$$\boldsymbol{\sigma_l} = \begin{bmatrix} 0.1170 & 0.0964 & 0.0475 & 0.0342 & 0.0675 & 0.1119 \end{bmatrix}$$

$$\mathbf{w}^{(1)} = \begin{bmatrix} 0.6336 & -0.1132 \\ 0.1188 & -0.4467 \\ -0.6629 & 0.2267 \\ -0.8861 & -0.0478 \\ 0.2049 & 0.3267 \\ -0.3425 & 0.0060 \end{bmatrix}$$

$$\mathbf{b}^{(1)} = \begin{bmatrix} 0.5712 & -0.5250 \end{bmatrix}$$

$$(\mathbf{w}^{(2)})^{\mathrm{T}} = \begin{bmatrix} 0.4118 & 2.2033 \end{bmatrix} \text{ and } b^{(2)} = 0.7481$$

$$\mu_c = \text{-1.1710 and } \sigma_c = 0.2746$$

TABLE 44: As in Table 43 but for $a_{ys}(412)$.

$$\boldsymbol{\mu_l} = \begin{bmatrix} -2.0506 & -2.0796 & -2.2152 & -2.4125 & -2.7451 & -3.7660 \end{bmatrix}$$

$$\boldsymbol{\sigma_l} = \begin{bmatrix} 0.1170 & 0.0964 & 0.0475 & 0.0342 & 0.0675 & 0.1119 \end{bmatrix}$$

$$\mathbf{w}^{(1)} = \begin{bmatrix} 0.0380 & 0.4125 \\ -1.7768 & 0.0380 \\ -0.7535 & -1.1030 \\ -0.2257 & 0.4502 \\ -0.5655 & -0.3477 \\ 0.1247 & 0.1944 \end{bmatrix}$$

$$\mathbf{b}^{(1)} = \begin{bmatrix} -0.0817 & -0.2492 \end{bmatrix}$$

$$(\mathbf{w}^{(2)})^{\mathrm{T}} = \begin{bmatrix} -0.9437 & 2.6849 \end{bmatrix} \text{ and } b^{(2)} = 0.3612$$

$$\mu_c = \text{-1.2949 and } \sigma_c = 0.1941$$

TABLE 45: As in Table 43 but for TSM.

$$\boldsymbol{\mu_l} = \begin{bmatrix} -2.0506 & -2.0796 & -2.2152 & -2.4125 & -2.7451 & -3.7660 \end{bmatrix}$$

$$\boldsymbol{\sigma_l} = \begin{bmatrix} 0.1170 & 0.0964 & 0.0475 & 0.0342 & 0.0675 & 0.1119 \end{bmatrix}$$

$$\mathbf{w}^{(1)} = \begin{bmatrix} 0.0350 & -0.4441 \\ 0.3708 & 0.0614 \\ -0.9827 & 0.4307 \\ 2.2556 & 0.0631 \\ -0.4562 & 0.9817 \\ 1.1051 & 0.2817 \end{bmatrix}$$

$$\mathbf{b}^{(1)} = \begin{bmatrix} -0.2676 & -0.1724 \end{bmatrix}$$

$$(\mathbf{w}^{(2)})^{\mathrm{T}} = \begin{bmatrix} -1.8266 & 2.8471 \end{bmatrix} \text{ and } b^{(2)} = 0.0861$$

$$\mu_c = \text{-0.7235 and } \sigma_c = 0.2264$$

TABLE 46: As in Table 43 but for the center wavelengths of the SeaWiFS sensor (see Table. 2).

$$\boldsymbol{\mu_l} = \begin{bmatrix} -2.0506 & -2.0796 & -2.2152 & -2.4125 & -2.7451 & -3.7661 \end{bmatrix}$$

$$\boldsymbol{\sigma_l} = \begin{bmatrix} 0.1170 & 0.0964 & 0.0475 & 0.0342 & 0.0675 & 0.1116 \end{bmatrix}$$

$$\mathbf{w}^{(1)} = \begin{bmatrix} -0.2789 & 0.1817 \\ 0.4256 & 0.3699 \\ 0.1567 & -0.3346 \\ -0.1120 & 0.3806 \\ -0.0983 & -0.4918 \\ 0.1495 & -0.2861 \end{bmatrix}$$

$$\mathbf{b}^{(1)} = \begin{bmatrix} -0.1819 & 0.7303 \end{bmatrix}$$

$$(\mathbf{w}^{(2)})^{\mathrm{T}} = \begin{bmatrix} -1.2656 & -1.2767 \end{bmatrix} \text{ and } b^{(2)} = 0.3868$$

μ_c = -1.1710 and σ_c = 0.2746

TABLE 47: As in Table 46 but for $a_{ys}(412)$.

$$\boldsymbol{\mu_l} = \begin{bmatrix} -2.0506 & -2.0796 & -2.2152 & -2.4125 & -2.7451 & -3.7661 \end{bmatrix}$$

$$\boldsymbol{\sigma_l} = \begin{bmatrix} 0.1170 & 0.0964 & 0.0475 & 0.0342 & 0.0675 & 0.1116 \end{bmatrix}$$

$$\mathbf{w}^{(1)} = \begin{bmatrix} 0.1634 & -2.6975 \\ 2.0369 & 0.0969 \\ -1.1451 & 2.0880 \\ -1.8018 & 0.8650 \\ -0.6444 & -0.3668 \\ 0.0635 & -0.4423 \end{bmatrix}$$

$$\mathbf{b}^{(1)} = \begin{bmatrix} 0.5819 & -0.4555 \end{bmatrix}$$

$$(\mathbf{w}^{(2)})^{\mathrm{T}} = \begin{bmatrix} -1.1692 & -1.7623 \end{bmatrix} \text{ and } b^{(2)} = -0.2123$$

μ_c = -1.2949 and σ_c = 0.1941

TABLE 48: As in Table 46 but for TSM.

$$\boldsymbol{\mu_l} = \begin{bmatrix} -2.0506 & -2.0796 & -2.2152 & -2.4125 & -2.7451 & -3.7661 \end{bmatrix}$$

$$\boldsymbol{\sigma_l} = \begin{bmatrix} 0.1170 & 0.0964 & 0.0475 & 0.0342 & 0.0675 & 0.1116 \end{bmatrix}$$

$$\mathbf{w}^{(1)} = \begin{bmatrix} -0.7270 & -0.5754 \\ -0.1094 & 0.2599 \\ 1.5178 & -0.2535 \\ -1.5664 & -0.1602 \\ 1.3895 & 1.8478 \\ -0.2674 & 1.3710 \end{bmatrix}$$

$$\mathbf{b}^{(1)} = \begin{bmatrix} 0.3546 & -0.7910 \end{bmatrix}$$

$$(\mathbf{w}^{(2)})^{\mathrm{T}} = \begin{bmatrix} 1.2143 & 0.4815 \end{bmatrix} \text{ and } b^{(2)} = -0.2090$$

μ_c = -0.7235 and σ_c = 0.2264

TABLE 49: As in Table 43 but for the center wavelengths of the MODIS sensor (see Table. 2).

$$\boldsymbol{\mu_l} = \begin{bmatrix} -2.0506 & -2.0796 & -2.2269 & -2.3758 & -2.7546 & -3.7660 \end{bmatrix}$$

$$\boldsymbol{\sigma_l} = \begin{bmatrix} 0.1170 & 0.0964 & 0.0488 & 0.0329 & 0.0679 & 0.1119 \end{bmatrix}$$

$$\mathbf{w}^{(1)} = \begin{bmatrix} 0.4599 & 0.3344 \\ -0.7559 & 0.1905 \\ -0.1845 & -0.0819 \\ 0.1198 & -0.0503 \\ 0.2632 & 0.0463 \\ -0.3716 & -0.2806 \end{bmatrix}$$

$$\mathbf{b}^{(1)} = \begin{bmatrix} 0.7220 & 0.6194 \end{bmatrix}$$

$$(\mathbf{w}^{(2)})^{\mathrm{T}} = \begin{bmatrix} 0.8757 & -1.6533 \end{bmatrix} \text{ and } b^{(2)} = 0.2433$$

$\mu_c =$ -1.1710 and $\sigma_c = 0.2746$

TABLE 50: As in Table 49 but for $a_{ys}(412)$.

$$\boldsymbol{\mu_l} = \begin{bmatrix} -2.0506 & -2.0796 & -2.2269 & -2.3758 & -2.7546 & -3.7660 \end{bmatrix}$$

$$\boldsymbol{\sigma_l} = \begin{bmatrix} 0.1170 & 0.0964 & 0.0488 & 0.0329 & 0.0679 & 0.1119 \end{bmatrix}$$

$$\mathbf{w}^{(1)} = \begin{bmatrix} 0.6800 & -0.1002 \\ -0.8120 & -0.1332 \\ 0.6407 & 0.8589 \\ -0.8146 & -0.8777 \\ 1.3018 & 0.4027 \\ -0.4915 & 0.1843 \end{bmatrix}$$

$$\mathbf{b}^{(1)} = \begin{bmatrix} -0.6799 & 0.9245 \end{bmatrix}$$

$$(\mathbf{w}^{(2)})^{\mathrm{T}} = \begin{bmatrix} -1.8216 & -1.6858 \end{bmatrix} \text{ and } b^{(2)} = 0.1512$$

$\mu_c =$ -1.2949 and $\sigma_c = 0.1941$

TABLE 51: As in Table 49 but for TSM.

$$\boldsymbol{\mu_l} = \begin{bmatrix} -2.0506 & -2.0796 & -2.2269 & -2.3758 & -2.7546 & -3.7660 \end{bmatrix}$$

$$\boldsymbol{\sigma_l} = \begin{bmatrix} 0.1170 & 0.0964 & 0.0488 & 0.0329 & 0.0679 & 0.1119 \end{bmatrix}$$

$$\mathbf{w}^{(1)} = \begin{bmatrix} 2.9454 & 0.3610 \\ 0.5722 & 0.5942 \\ -3.1243 & 0.8489 \\ 0.7962 & -0.9672 \\ -0.7928 & 0.8266 \\ -1.3689 & 0.2311 \end{bmatrix}$$

$$\mathbf{b}^{(1)} = \begin{bmatrix} -0.0958 & 1.6210 \end{bmatrix}$$

$$(\mathbf{w}^{(2)})^{\mathrm{T}} = \begin{bmatrix} -0.7379 & -0.4912 \end{bmatrix} \text{ and } b^{(2)} = 0.3297$$

$\mu_c =$ -0.7235 and $\sigma_c = 0.2264$

TABLE 52: As in Table 43 but for the center wavelengths of the MERIS sensor (see Table. 2).

$$\boldsymbol{\mu_l} = \begin{bmatrix} -2.0506 & -2.0796 & -2.2152 & -2.4125 & -2.7411 & -3.7660 \end{bmatrix}$$

$$\boldsymbol{\sigma_l} = \begin{bmatrix} 0.1170 & 0.0964 & 0.0475 & 0.0342 & 0.0673 & 0.1119 \end{bmatrix}$$

$$\mathbf{w}^{(1)} = \begin{bmatrix} -0.2795 & 0.4056 \\ -0.4718 & -0.4079 \\ 0.5581 & -0.5631 \\ -0.4298 & 0.3107 \\ 0.4199 & 0.2640 \\ 0.1347 & -0.3411 \end{bmatrix}$$

$$\mathbf{b}^{(1)} = \begin{bmatrix} -0.6791 & 0.8202 \end{bmatrix}$$

$$(\mathbf{w}^{(2)})^{\mathrm{T}} = \begin{bmatrix} 1.5832 & 1.0930 \end{bmatrix} \text{ and } b^{(2)} = 0.0566$$

$$\mu_c = \text{-1.1710 and } \sigma_c = 0.2746$$

TABLE 53: As in Table 52 but for $a_{ys}(412)$.

$$\boldsymbol{\mu_l} = \begin{bmatrix} -2.0506 & -2.0796 & -2.2152 & -2.4125 & -2.7411 & -3.7660 \end{bmatrix}$$

$$\boldsymbol{\sigma_l} = \begin{bmatrix} 0.1170 & 0.0964 & 0.0475 & 0.0342 & 0.0673 & 0.1119 \end{bmatrix}$$

$$\mathbf{w}^{(1)} = \begin{bmatrix} 2.4654 & 0.5511 \\ 0.4073 & 1.0146 \\ -1.9337 & -0.7626 \\ -1.3871 & -1.5864 \\ 1.6358 & -1.4425 \\ -0.1391 & -0.0924 \end{bmatrix}$$

$$\mathbf{b}^{(1)} = \begin{bmatrix} 0.5038 & 0.6078 \end{bmatrix}$$

$$(\mathbf{w}^{(2)})^{\mathrm{T}} = \begin{bmatrix} 1.6242 & -1.0039 \end{bmatrix} \text{ and } b^{(2)} = \text{-0.2288}$$

$$\mu_c = \text{-1.2949 and } \sigma_c = 0.1941$$

TABLE 54: As in Table 52 but for TSM.

$$\boldsymbol{\mu_l} = \begin{bmatrix} -2.0506 & -2.0796 & -2.2152 & -2.4125 & -2.7411 & -3.7660 \end{bmatrix}$$

$$\boldsymbol{\sigma_l} = \begin{bmatrix} 0.1170 & 0.0964 & 0.0475 & 0.0342 & 0.0673 & 0.1119 \end{bmatrix}$$

$$\mathbf{w}^{(1)} = \begin{bmatrix} -0.5469 & -0.4739 \\ -0.9644 & 0.5318 \\ -0.0523 & 0.9408 \\ 0.4826 & -1.3045 \\ -0.5346 & 1.5147 \\ -2.1312 & 0.5406 \end{bmatrix}$$

$$\mathbf{b}^{(1)} = \begin{bmatrix} -0.1870 & 0.0453 \end{bmatrix}$$

$$(\mathbf{w}^{(2)})^{\mathrm{T}} = \begin{bmatrix} 1.1453 & 2.2795 \end{bmatrix} \text{ and } b^{(2)} = 0.0683$$

$$\mu_c = \text{-0.7235 and } \sigma_c = 0.2264$$

3.5 Ligurian Sea

The MLP for the Ligurian Sea (Figure 11) has been developed on the basis of BiOMaP data collected in 2008 and 2009 (41 and 57 stations, respectively). Performance trends of Panels 11(b)–11(d) support the use of a MLP with two hidden neurons. The resulting comparison between modeled and measured values is in Figure 12 and Table 55. It is highlighted that both Ligurian Sea and Eastern Mediterranean Sea mostly include Case-1 waters (Morel and Prieur, 1977; Gordon and Morel, 1983) and this conforms with the agreement between MLP architectures selected for these basins.

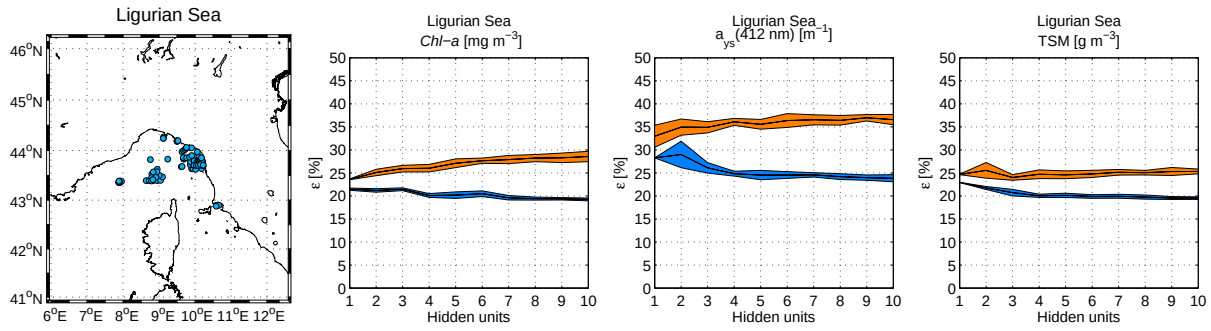

FIGURE 11: As in Figure 3, but for the Ligurian Sea.

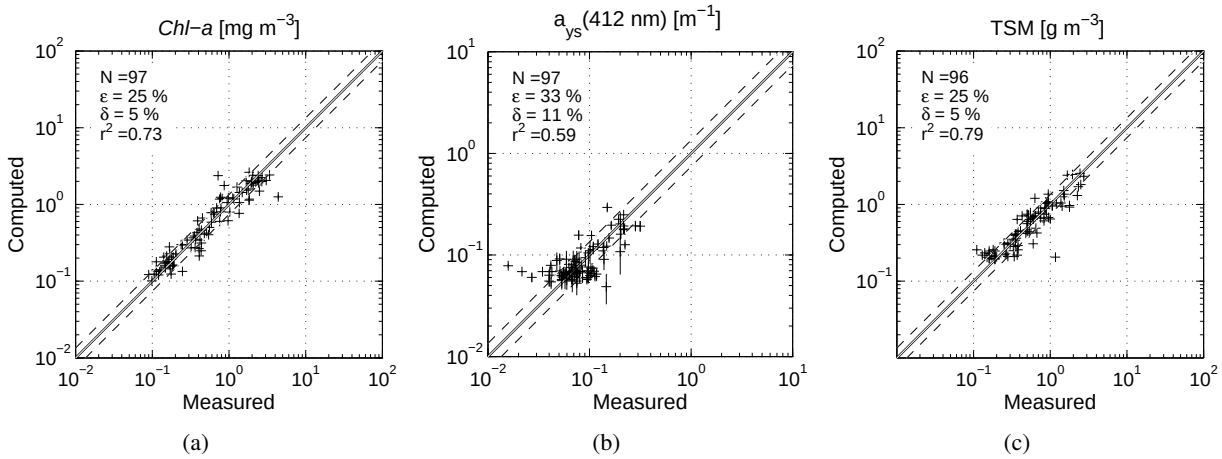

FIGURE 12: As in Figure 4, but for the Ligurian Sea. Results based on the MLP with two units in the hidden layer.

TABLE 55: As in Table 3, but for the Ligurian Sea. Results based on the MLP with two units in the hidden layer.

	N	ϵ [%]	δ [%]	r^2
Chl-a	97	25.2(21.3)	4.7(4.2)	72.2(79.2)
$a_{ys}(412)$	97	36.0(29.5)	8.2(7.6)	44.7(71.4)
TSM	96	27.2(22.4)	7.0(6.1)	77.2(87.9)

TABLE 56: Parameter sets to compute data pre- and post-processing, as well as MLP weights to derive *Chl-a* values in the Ligurian Sea. Input R_{RS} wavelengths are those of the in-situ measurements (see Table. 2).

$$\boldsymbol{\mu_I} = \begin{bmatrix} -2.3311 & -2.3078 & -2.2831 & -2.3418 & -2.4843 & -3.3656 \end{bmatrix}$$

$$\boldsymbol{\sigma_I} = \begin{bmatrix} 0.1515 & 0.1890 & 0.1997 & 0.2137 & 0.2760 & 0.3571 \end{bmatrix}$$

$$\mathbf{w}^{(1)} = \begin{bmatrix} -0.6262 & 0.7899 \\ 1.3541 & 0.7360 \\ 0.3363 & 0.4772 \\ -1.0015 & 0.4417 \\ 0.5957 & 0.1678 \\ -0.6019 & -0.0897 \end{bmatrix}$$

$$\mathbf{b}^{(1)} = \begin{bmatrix} -0.1340 & 0.5803 \end{bmatrix}$$

$$(\mathbf{w}^{(2)})^{\mathrm{T}} = \begin{bmatrix} -2.1604 & 0.2813 \end{bmatrix} \text{ and } b^{(2)} = \text{-0.2308}$$

$$\mu_c = \text{-0.2709 and } \sigma_c = 0.4592$$

TABLE 57: As in Table 56 but for $a_{ys}(412)$.

$$\boldsymbol{\mu_I} = \begin{bmatrix} -2.3311 & -2.3078 & -2.2831 & -2.3418 & -2.4843 & -3.3656 \end{bmatrix}$$

$$\boldsymbol{\sigma_I} = \begin{bmatrix} 0.1515 & 0.1890 & 0.1997 & 0.2137 & 0.2760 & 0.3571 \end{bmatrix}$$

$$\mathbf{w}^{(1)} = \begin{bmatrix} 0.1646 & 0.7733 \\ -0.4771 & -0.8843 \\ 0.3377 & -0.3755 \\ 1.3875 & -0.4270 \\ -0.5810 & 0.5732 \\ -0.2832 & -1.5098 \end{bmatrix}$$

$$\mathbf{b}^{(1)} = \begin{bmatrix} -0.9810 & 0.5959 \end{bmatrix}$$

$$(\mathbf{w}^{(2)})^{\mathrm{T}} = \begin{bmatrix} -1.9225 & -1.1881 \end{bmatrix} \text{ and } b^{(2)} = \text{-0.8682}$$

$$\mu_c = \text{-1.0796 and } \sigma_c = 0.2382$$

TABLE 58: As in Table 56 but for TSM.

$$\boldsymbol{\mu_I} = \begin{bmatrix} -2.3311 & -2.3076 & -2.2822 & -2.3400 & -2.4814 & -3.3611 \end{bmatrix}$$

$$\boldsymbol{\sigma_I} = \begin{bmatrix} 0.1523 & 0.1900 & 0.2006 & 0.2142 & 0.2760 & 0.3562 \end{bmatrix}$$

$$\mathbf{w}^{(1)} = \begin{bmatrix} -0.4102 & 0.9167 \\ 0.3314 & -0.5591 \\ -0.0917 & -0.8866 \\ -0.1788 & 0.6019 \\ -0.2623 & 0.8185 \\ 1.2398 & 0.1093 \end{bmatrix}$$

$$\mathbf{b}^{(1)} = \begin{bmatrix} -0.7426 & 0.7878 \end{bmatrix}$$

$$(\mathbf{w}^{(2)})^{\mathrm{T}} = \begin{bmatrix} 1.1066 & 0.9654 \end{bmatrix} \text{ and } b^{(2)} = 0.0328$$

$$\mu_c = \text{-0.2821 and } \sigma_c = 0.3446$$

TABLE 59: As in Table 56 but for the center wavelengths of the SeaWiFS sensor (see Table. 2).

$$\boldsymbol{\mu_l} = \begin{bmatrix} -2.3311 & -2.3078 & -2.2831 & -2.3418 & -2.4843 & -3.3661 \end{bmatrix}$$

$$\boldsymbol{\sigma_l} = \begin{bmatrix} 0.1515 & 0.1890 & 0.1997 & 0.2137 & 0.2760 & 0.3568 \end{bmatrix}$$

$$\mathbf{w}^{(1)} = \begin{bmatrix} 0.8343 & -0.8509 \\ 0.4980 & 1.6029 \\ 0.1484 & -0.2559 \\ -0.1906 & -0.8183 \\ -0.2002 & 0.8484 \\ -0.5557 & -0.6578 \end{bmatrix}$$

$$\mathbf{b}^{(1)} = \begin{bmatrix} -0.1852 & -0.1160 \end{bmatrix}$$

$$(\mathbf{w}^{(2)})^{\mathrm{T}} = \begin{bmatrix} -0.5624 & -1.6697 \end{bmatrix} \text{ and } b^{(2)} = \text{-0.1837}$$

$$\mu_c = \text{-0.2709 and } \sigma_c = 0.4592$$

TABLE 60: As in Table 59 but for $a_{ys}(412)$.

$$\boldsymbol{\mu_l} = \begin{bmatrix} -2.3311 & -2.3078 & -2.2831 & -2.3418 & -2.4843 & -3.3661 \end{bmatrix}$$

$$\boldsymbol{\sigma_l} = \begin{bmatrix} 0.1515 & 0.1890 & 0.1997 & 0.2137 & 0.2760 & 0.3568 \end{bmatrix}$$

$$\mathbf{w}^{(1)} = \begin{bmatrix} 0.8250 & -0.0730 \\ -0.8756 & 0.2599 \\ -0.3898 & -0.0287 \\ -0.6328 & -1.6055 \\ 0.4977 & 0.5248 \\ -1.3179 & 0.4131 \end{bmatrix}$$

$$\mathbf{b}^{(1)} = \begin{bmatrix} 0.6241 & 0.9373 \end{bmatrix}$$

$$(\mathbf{w}^{(2)})^{\mathrm{T}} = \begin{bmatrix} -1.1764 & 1.9260 \end{bmatrix} \text{ and } b^{(2)} = \text{-0.8426}$$

$$\mu_c = \text{-1.0796 and } \sigma_c = 0.2382$$

TABLE 61: As in Table 59 but for TSM.

$$\boldsymbol{\mu_l} = \begin{bmatrix} -2.3311 & -2.3076 & -2.2822 & -2.3400 & -2.4814 & -3.3616 \end{bmatrix}$$

$$\boldsymbol{\sigma_l} = \begin{bmatrix} 0.1523 & 0.1900 & 0.2006 & 0.2142 & 0.2760 & 0.3560 \end{bmatrix}$$

$$\mathbf{w}^{(1)} = \begin{bmatrix} -0.7896 & -0.4061 \\ 0.3871 & 0.3605 \\ 1.0948 & -0.1368 \\ -0.8543 & -0.1694 \\ -0.6824 & -0.2298 \\ -0.0587 & 1.2110 \end{bmatrix}$$

$$\mathbf{b}^{(1)} = \begin{bmatrix} -0.8490 & -0.7436 \end{bmatrix}$$

$$(\mathbf{w}^{(2)})^{\mathrm{T}} = \begin{bmatrix} -1.0431 & 1.1589 \end{bmatrix} \text{ and } b^{(2)} = \text{-0.0324}$$

$$\mu_c = \text{-0.2821 and } \sigma_c = 0.3446$$

TABLE 62: As in Table 56 but for the center wavelengths of the MODIS sensor (see Table. 2).

$$\boldsymbol{\mu_l} = \begin{bmatrix} -2.3311 & -2.3078 & -2.2971 & -2.2778 & -2.5017 & -3.3656 \end{bmatrix}$$

$$\boldsymbol{\sigma_l} = \begin{bmatrix} 0.1515 & 0.1890 & 0.2021 & 0.2121 & 0.2747 & 0.3571 \end{bmatrix}$$

$$\mathbf{w}^{(1)} = \begin{bmatrix} 0.4452 & 0.5384 \\ 0.3861 & -1.1099 \\ 0.6659 & -0.1293 \\ -0.0775 & 1.1734 \\ -0.4215 & -0.7878 \\ -0.5343 & 0.3763 \end{bmatrix}$$

$$\mathbf{b}^{(1)} = \begin{bmatrix} -0.4611 & -0.2104 \end{bmatrix}$$

$$(\mathbf{w}^{(2)})^{\mathrm{T}} = \begin{bmatrix} -0.3638 & 2.1286 \end{bmatrix} \text{ and } b^{(2)} = 0.3247$$

$$\mu_c = \text{-0.2709 and } \sigma_c = 0.4592$$

TABLE 63: As in Table 62 but for $a_{ys}(412)$.

$$\boldsymbol{\mu_l} = \begin{bmatrix} -2.3311 & -2.3078 & -2.2971 & -2.2778 & -2.5017 & -3.3656 \end{bmatrix}$$

$$\boldsymbol{\sigma_l} = \begin{bmatrix} 0.1515 & 0.1890 & 0.2021 & 0.2121 & 0.2747 & 0.3571 \end{bmatrix}$$

$$\mathbf{w}^{(1)} = \begin{bmatrix} -1.6575 & -2.1292 \\ 0.8850 & -0.1862 \\ -0.8340 & 0.9411 \\ 2.8563 & -0.3127 \\ -2.5255 & 1.0892 \\ 1.1729 & 0.4459 \end{bmatrix}$$

$$\mathbf{b}^{(1)} = \begin{bmatrix} -0.6619 & 0.8669 \end{bmatrix}$$

$$(\mathbf{w}^{(2)})^{\mathrm{T}} = \begin{bmatrix} 1.9388 & -0.7674 \end{bmatrix} \text{ and } b^{(2)} = 0.8842$$

$$\mu_c = \text{-1.0796 and } \sigma_c = 0.2382$$

TABLE 64: As in Table 62 but for TSM.

$$\boldsymbol{\mu_l} = \begin{bmatrix} -2.3311 & -2.3076 & -2.2963 & -2.2756 & -2.4990 & -3.3611 \end{bmatrix}$$

$$\boldsymbol{\sigma_l} = \begin{bmatrix} 0.1523 & 0.1900 & 0.2030 & 0.2120 & 0.2748 & 0.3562 \end{bmatrix}$$

$$\mathbf{w}^{(1)} = \begin{bmatrix} 0.0388 & -0.1159 \\ -0.3234 & 0.0719 \\ 0.0695 & 0.5912 \\ 0.7423 & -0.5732 \\ 0.5275 & 0.4121 \\ 0.4898 & -0.8469 \end{bmatrix}$$

$$\mathbf{b}^{(1)} = \begin{bmatrix} 0.4336 & 0.6134 \end{bmatrix}$$

$$(\mathbf{w}^{(2)})^{\mathrm{T}} = \begin{bmatrix} 0.4810 & -1.4248 \end{bmatrix} \text{ and } b^{(2)} = 0.5789$$

$$\mu_c = \text{-0.2821 and } \sigma_c = 0.3446$$

TABLE 65: As in Table 56 but for the center wavelengths of the MERIS sensor (see Table. 2).

$$\boldsymbol{\mu_l} = \begin{bmatrix} -2.3311 & -2.3078 & -2.2831 & -2.3418 & -2.4764 & -3.3656 \end{bmatrix}$$

$$\boldsymbol{\sigma_l} = \begin{bmatrix} 0.1515 & 0.1890 & 0.1997 & 0.2137 & 0.2769 & 0.3571 \end{bmatrix}$$

$$\mathbf{w}^{(1)} = \begin{bmatrix} -0.5940 & -0.9059 \\ 1.2282 & -0.9204 \\ 0.4819 & -1.0295 \\ -0.9676 & -0.2475 \\ 0.4226 & 0.1028 \\ -0.5189 & -0.2309 \end{bmatrix}$$

$$\mathbf{b}^{(1)} = \begin{bmatrix} -0.1532 & -0.6706 \end{bmatrix}$$

$$(\mathbf{w}^{(2)})^{\mathrm{T}} = \begin{bmatrix} -2.1415 & -0.2591 \end{bmatrix} \text{ and } b^{(2)} = \text{-0.2526}$$

$\mu_c =$ -0.2709 and $\sigma_c =$ 0.4592

TABLE 66: As in Table 65 but for $a_{ys}(412)$.

$$\boldsymbol{\mu_l} = \begin{bmatrix} -2.3311 & -2.3078 & -2.2831 & -2.3418 & -2.4764 & -3.3656 \end{bmatrix}$$

$$\boldsymbol{\sigma_l} = \begin{bmatrix} 0.1515 & 0.1890 & 0.1997 & 0.2137 & 0.2769 & 0.3571 \end{bmatrix}$$

$$\mathbf{w}^{(1)} = \begin{bmatrix} 1.4785 & -3.1268 \\ -0.4708 & 1.0910 \\ -1.0937 & 1.6056 \\ -0.0916 & 0.7643 \\ 0.1225 & -1.5073 \\ 0.3012 & 0.7417 \end{bmatrix}$$

$$\mathbf{b}^{(1)} = \begin{bmatrix} 0.3540 & -1.0803 \end{bmatrix}$$

$$(\mathbf{w}^{(2)})^{\mathrm{T}} = \begin{bmatrix} 1.6465 & 2.0800 \end{bmatrix} \text{ and } b^{(2)} = 0.5542$$

$\mu_c =$ -1.0796 and $\sigma_c =$ 0.2382

TABLE 67: As in Table 65 but for TSM.

$$\boldsymbol{\mu_l} = \begin{bmatrix} -2.3311 & -2.3076 & -2.2822 & -2.3400 & -2.4734 & -3.3611 \end{bmatrix}$$

$$\boldsymbol{\sigma_l} = \begin{bmatrix} 0.1523 & 0.1900 & 0.2006 & 0.2142 & 0.2768 & 0.3562 \end{bmatrix}$$

$$\mathbf{w}^{(1)} = \begin{bmatrix} 0.3609 & -0.2167 \\ -0.3991 & 0.3616 \\ -0.4264 & -0.4055 \\ 0.5342 & -0.2155 \\ 1.0863 & -0.0575 \\ 0.1285 & 1.2330 \end{bmatrix}$$

$$\mathbf{b}^{(1)} = \begin{bmatrix} 0.6044 & -0.8013 \end{bmatrix}$$

$$(\mathbf{w}^{(2)})^{\mathrm{T}} = \begin{bmatrix} 0.6210 & 1.0795 \end{bmatrix} \text{ and } b^{(2)} = 0.3733$$

$\mu_c =$ -0.2821 and $\sigma_c =$ 0.3446

3.6 Black Sea

BiOMaP stations in the Black Sea are shown in Figure 13(a). Field measurements were collected during 3 campaigns, the first in 2006 (93 stations) and the last two in 2009 (for a total of 113 stations). Analyzing the trends shown in Panels 13(b) to Panels 13(d), the MLP with ten hidden units has been selected to derive validation results reported in Figure 14 and Table 68.

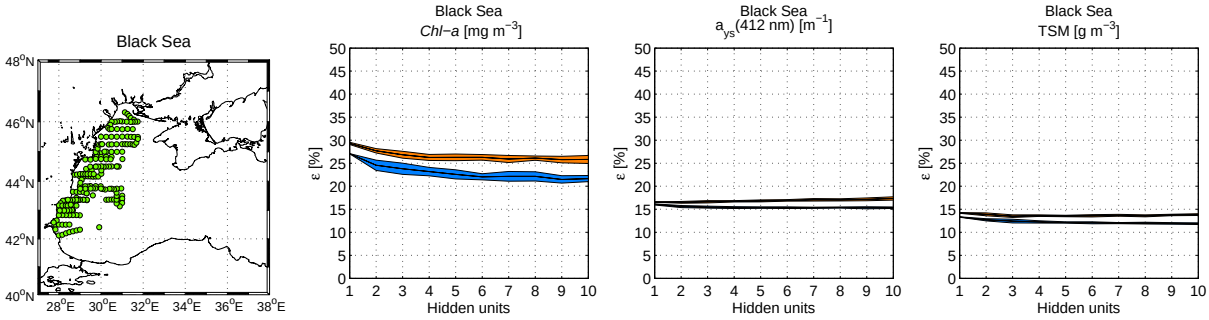

(a) (b) (c) (d)

FIGURE 13: As in Figure 3, but for the Black Sea.

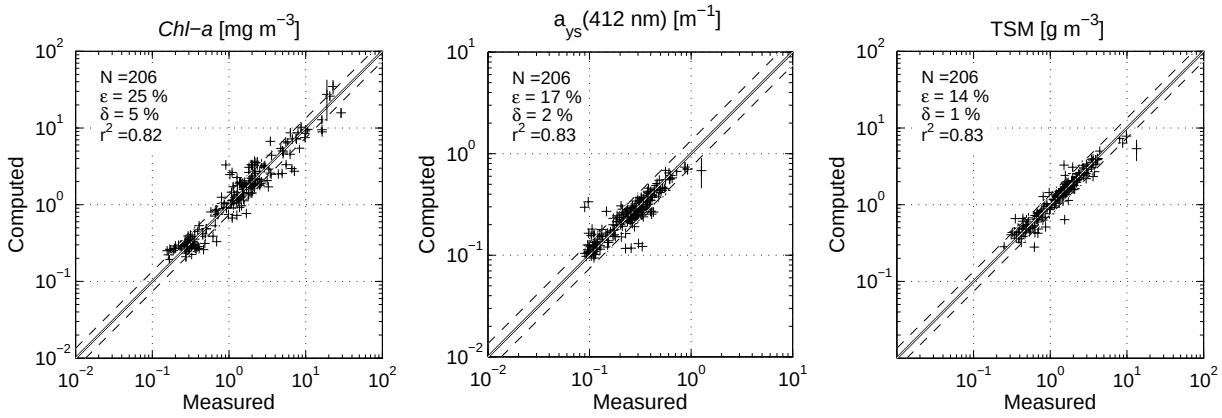

(a) (b) (c)

FIGURE 14: As in Figure 4, but for the Black Sea. Results based on the MLP with ten units in the hidden layer.

TABLE 68: As in Table 3, but for the Black Sea. Results based on the MLP with ten units in the hidden layer.

	N	ϵ [%]	δ [%]	r^2
Chl-a	206	25.7(21.5)	4.8(4.0)	85.2(91.0)
$a_{ys}(412)$	206	17.2(15.5)	1.6(2.9)	78.1(89.8)
TSM	206	13.9(11.7)	1.2(1.3)	78.3(96.6)

TABLE 69: Parameter sets to compute data pre- and post-processing, as well as MLP weights to derive *Chl-a* values in the Black Sea. Input R_{RS} wavelengths are those of the in-situ measurements (see Table. 2).

$$\boldsymbol{\mu_I} = \begin{bmatrix} -2.5084 & -2.4287 & -2.3087 & -2.2983 & -2.2867 & -3.0035 \end{bmatrix}$$

$$\boldsymbol{\sigma_I} = \begin{bmatrix} 0.2693 & 0.2715 & 0.2464 & 0.2144 & 0.1892 & 0.2593 \end{bmatrix}$$

$$\mathbf{w}^{(1)} = \begin{bmatrix} -0.0580 & -0.0353 & 0.0705 & 0.0195 & 0.5063 & -0.2952 & 0.3357 & 0.7249 & 0.4375 & 0.4944 \\ -0.1037 & -0.4448 & 0.2810 & 0.3198 & -0.2104 & -0.1684 & -0.4433 & -0.0395 & 0.3772 & 0.3109 \\ -0.0724 & -0.1457 & -0.2887 & 0.9340 & -0.0349 & -0.0112 & -0.0731 & -0.7481 & -0.2865 & 0.0435 \\ 0.4647 & 0.2963 & -0.0885 & 0.1949 & 0.1710 & -0.2967 & -0.3010 & -0.5438 & 0.1634 & 0.1840 \\ -0.2755 & 0.3785 & -0.6894 & -0.8707 & 0.1153 & 0.2532 & -0.2719 & 0.4324 & 0.2841 & -0.0657 \\ 0.5408 & 0.1159 & -0.3023 & -0.0929 & 0.2652 & -0.3609 & 0.9977 & 0.5891 & -0.0159 & -0.1243 \end{bmatrix}$$

$$\mathbf{b}^{(1)} = \begin{bmatrix} -0.2992 & -0.0297 & -0.0699 & 0.7682 & -0.0123 & 1.0473 & -1.4528 & 0.6412 & 0.5757 & 0.8181 \end{bmatrix}$$

$$(\mathbf{w}^{(2)})^{\mathrm{T}} = \begin{bmatrix} 0.6446 & 0.2844 & 0.2061 & 0.5890 & -0.2749 & 0.6909 & 1.5695 & 1.1214 & -0.1201 & 0.1044 \end{bmatrix} \text{ and } b^{(2)} = 0.2157$$

$$\mu_c = 0.0801 \text{ and } \sigma_c = 0.5139$$

TABLE 70: As in Table 69 but for $a_{ys}(412)$.

$$\boldsymbol{\mu_I} = \begin{bmatrix} -2.5084 & -2.4287 & -2.3087 & -2.2983 & -2.2867 & -3.0035 \end{bmatrix}$$

$$\boldsymbol{\sigma_I} = \begin{bmatrix} 0.2693 & 0.2715 & 0.2464 & 0.2144 & 0.1892 & 0.2593 \end{bmatrix}$$

$$\mathbf{w}^{(1)} = \begin{bmatrix} 0.3577 & 0.6357 & 0.1553 & 0.0926 & -0.4069 & 0.8631 & 0.4240 & 0.0241 & -0.0098 & -0.0836 \\ 0.7091 & 0.8508 & -0.1627 & 0.1411 & 0.2441 & -0.0738 & -0.0914 & -0.0579 & -0.1113 & -0.2187 \\ 0.1160 & 0.2760 & 0.6059 & -0.3491 & 0.5011 & -0.4626 & -0.7303 & 0.2009 & -0.0527 & 0.2106 \\ -0.1424 & 0.1883 & 0.3070 & -0.0639 & -0.4114 & 0.2716 & 0.7870 & -0.4103 & -0.2751 & 0.1577 \\ -0.0693 & 0.0097 & 0.0366 & -0.1602 & 0.0427 & 0.0565 & -0.3215 & 0.2218 & 0.2147 & -0.4924 \\ 0.0696 & 0.6101 & -0.4940 & 0.1357 & 0.1309 & -0.2948 & -0.0247 & 0.0633 & 0.0800 & -0.4882 \end{bmatrix}$$

$$\mathbf{b}^{(1)} = \begin{bmatrix} -0.5509 & 0.0510 & -0.1068 & -0.2054 & 0.1212 & 0.7150 & 0.1225 & 0.0120 & 0.4453 & 1.1350 \end{bmatrix}$$

$$(\mathbf{w}^{(2)})^{\mathrm{T}} = \begin{bmatrix} 0.2964 & 0.2072 & -0.2346 & -0.0884 & 0.4178 & -1.1487 & -1.2330 & 0.6607 & 0.5443 & -0.3158 \end{bmatrix} \text{ and } b^{(2)} = 0.7241$$

$$\mu_c = \text{-}0.6127 \text{ and } \sigma_c = 0.2427$$

TABLE 71: As in Table 69 but for TSM.

$$\boldsymbol{\mu_I} = \begin{bmatrix} -2.5084 & -2.4287 & -2.3087 & -2.2983 & -2.2867 & -3.0035 \end{bmatrix}$$

$$\boldsymbol{\sigma_I} = \begin{bmatrix} 0.2693 & 0.2715 & 0.2464 & 0.2144 & 0.1892 & 0.2593 \end{bmatrix}$$

$$\mathbf{w}^{(1)} = \begin{bmatrix} 0.4139 & -0.0729 & -0.3721 & -0.4482 & 0.4714 & 0.1679 & -0.3793 & 0.1778 & -0.2780 & -1.0390 \\ -0.0909 & 0.1567 & 0.3668 & 0.0868 & 0.2123 & -0.1510 & -0.2310 & -0.0661 & 0.1835 & -0.3402 \\ -1.0157 & 0.2717 & 0.2028 & -0.4287 & -0.1479 & 0.0791 & 0.0835 & 0.7434 & -0.2931 & 0.3255 \\ -0.2425 & -0.0862 & -0.1339 & -0.2250 & -0.1973 & 0.4628 & -0.1491 & -0.6574 & 0.1156 & 0.2269 \\ -0.1156 & -0.1113 & -0.2066 & 0.0157 & -0.1887 & 0.2544 & -0.5121 & 0.2031 & 0.1124 & -0.0661 \\ 0.2319 & -0.2551 & -0.0055 & -0.0429 & 0.0524 & 0.3045 & -0.0939 & -0.3973 & -0.4246 & -0.0053 \end{bmatrix}$$

$$\mathbf{b}^{(1)} = \begin{bmatrix} -0.5192 & 0.7060 & -0.2727 & 0.1851 & -0.2147 & 0.0760 & -0.8926 & 0.7700 & 0.6613 & 0.7016 \end{bmatrix}$$

$$(\mathbf{w}^{(2)})^{\mathrm{T}} = \begin{bmatrix} 0.9653 & -0.6044 & -0.8436 & -0.7539 & -0.3660 & -0.0957 & -0.5058 & -0.8309 & -0.6470 & 0.8127 \end{bmatrix} \text{ and } b^{(2)} = 0.6595$$

$$\mu_c = 0.0989 \text{ and } \sigma_c = 0.3176$$

TABLE 72: As in Table 69 but for the center wavelengths of the SeaWiFS sensor (see Table. 2).

$$\boldsymbol{\mu_l} = \begin{bmatrix} -2.5084 & -2.4287 & -2.3087 & -2.2983 & -2.2867 & -3.0045 \end{bmatrix}$$

$$\boldsymbol{\sigma_l} = \begin{bmatrix} 0.2693 & 0.2715 & 0.2464 & 0.2144 & 0.1892 & 0.2588 \end{bmatrix}$$

$$\mathbf{w}^{(1)} = \begin{bmatrix} -0.3438 & 0.4146 & 0.2547 & -0.2761 & -0.5395 & 0.4069 & -0.0756 & -0.1228 & -0.8282 & -0.1933 \\ 0.3976 & 0.6458 & -0.3751 & -0.0721 & 0.0678 & 0.1012 & 0.1735 & -0.0193 & 0.1129 & 0.1341 \\ 0.2772 & 0.0331 & -0.0124 & 0.0098 & 0.2194 & 0.3187 & -0.4293 & -0.0753 & 0.4298 & -0.0469 \\ 0.0017 & -0.7031 & 0.0389 & -0.3229 & 0.0999 & -0.0802 & -0.1517 & 0.2818 & 0.6092 & 0.2873 \\ -0.4523 & 0.3530 & 0.1061 & -0.0269 & 0.4154 & -0.0204 & -0.2107 & 1.0513 & -0.0709 & -0.2143 \\ -0.0352 & -0.1921 & 0.2200 & -0.4260 & 0.5352 & -0.5167 & -0.2627 & -1.1223 & -0.5281 & 0.0212 \end{bmatrix}$$

$$\mathbf{b}^{(1)} = \begin{bmatrix} -0.1873 & -0.8862 & 0.2199 & 0.5596 & -0.9306 & 0.1575 & -0.3612 & 1.3283 & -0.7445 & 0.2098 \end{bmatrix}$$

$$(\mathbf{w}^{(2)})^{\mathrm{T}} = \begin{bmatrix} -0.2294 & -1.0150 & 0.2597 & 0.2988 & 0.5846 & 0.3767 & -0.2309 & -1.4311 & -1.1065 & -0.0513 \end{bmatrix} \text{ and } b^{(2)} = \text{-0.0509}$$

$$\mu_c = \text{0.0801 and } \sigma_c = 0.5139$$

TABLE 73: As in Table 72 but for $a_{ys}(412)$.

$$\boldsymbol{\mu_l} = \begin{bmatrix} -2.5084 & -2.4287 & -2.3087 & -2.2983 & -2.2867 & -3.0045 \end{bmatrix}$$

$$\boldsymbol{\sigma_l} = \begin{bmatrix} 0.2693 & 0.2715 & 0.2464 & 0.2144 & 0.1892 & 0.2588 \end{bmatrix}$$

$$\mathbf{w}^{(1)} = \begin{bmatrix} -0.5233 & 0.2414 & -0.5892 & 0.7579 & -0.0611 & -0.1075 & -0.0291 & 0.0098 & -0.4961 & -0.1953 \\ -0.0580 & 0.4041 & 0.2500 & -0.3029 & -0.2685 & 0.5065 & 0.1144 & -0.4856 & -0.2930 & 0.1842 \\ 0.5833 & 0.1868 & 0.6976 & -0.1367 & 0.1164 & 0.3585 & -0.3371 & -0.1014 & -0.4250 & 0.2779 \\ 0.5107 & -0.0467 & -0.9063 & 0.1968 & -0.2777 & 0.4497 & 0.3024 & 0.4877 & -0.1972 & -1.1184 \\ 0.1828 & -0.1484 & 0.5839 & 0.1605 & 0.2444 & 0.0682 & 0.1891 & 0.0747 & -0.8367 & -0.1257 \\ 0.0749 & 0.0973 & -0.0875 & -0.3591 & 0.1852 & 0.0356 & -0.2388 & -0.6873 & 0.2304 & 0.0873 \end{bmatrix}$$

$$\mathbf{b}^{(1)} = \begin{bmatrix} 0.7554 & -0.0458 & -0.0983 & 0.5709 & 0.1867 & 0.6055 & -0.1770 & 0.9850 & 0.0234 & -0.3251 \end{bmatrix}$$

$$(\mathbf{w}^{(2)})^{\mathrm{T}} = \begin{bmatrix} 0.7192 & 0.2281 & 1.5347 & -0.7989 & 0.3273 & -0.1549 & -0.3156 & -0.7705 & -0.4437 & 0.8577 \end{bmatrix} \text{ and } b^{(2)} = 0.7570$$

$$\mu_c = \text{-0.6127 and } \sigma_c = 0.2427$$

TABLE 74: As in Table 72 but for TSM.

$$\boldsymbol{\mu_l} = \begin{bmatrix} -2.5084 & -2.4287 & -2.3087 & -2.2983 & -2.2867 & -3.0045 \end{bmatrix}$$

$$\boldsymbol{\sigma_l} = \begin{bmatrix} 0.2693 & 0.2715 & 0.2464 & 0.2144 & 0.1892 & 0.2588 \end{bmatrix}$$

$$\mathbf{w}^{(1)} = \begin{bmatrix} 0.0911 & 0.2357 & -0.3031 & 0.3482 & 0.4945 & -0.0689 & 0.4676 & -0.4519 & -0.5366 & 0.0935 \\ 0.0316 & -0.2914 & -0.1973 & 0.4839 & -0.5250 & 0.0488 & 0.5027 & 0.5947 & -0.5654 & -0.1589 \\ -0.1630 & 0.0602 & -0.3506 & 0.3533 & -0.4179 & 0.1098 & -0.1340 & 0.5342 & -0.2727 & -0.2792 \\ -0.1168 & 0.1887 & -0.3185 & 0.3445 & 0.2829 & -0.1184 & -0.1447 & 0.4997 & -0.3403 & 0.2050 \\ 0.0569 & -0.1718 & 0.0823 & 0.3738 & 0.6443 & 0.4894 & -0.0144 & 0.0389 & -0.0118 & 0.0979 \\ -0.1819 & -0.3187 & -0.0115 & 0.6908 & -0.0618 & -0.8544 & -0.0014 & -0.1039 & -0.4248 & 0.1478 \end{bmatrix}$$

$$\mathbf{b}^{(1)} = \begin{bmatrix} 0.2740 & 0.8777 & 0.2570 & 0.1963 & 0.5868 & 1.1353 & -0.5517 & 0.5196 & -0.5109 & -0.4514 \end{bmatrix}$$

$$(\mathbf{w}^{(2)})^{\mathrm{T}} = \begin{bmatrix} -0.1587 & -0.5398 & -0.2934 & -0.2935 & 0.9539 & -0.9120 & -0.7458 & -0.8240 & -0.5780 & 0.7337 \end{bmatrix} \text{ and } b^{(2)} = 0.7997$$

$$\mu_c = \text{0.0989 and } \sigma_c = 0.3176$$

TABLE 75: As in Table 69 but for the center wavelengths of the MODIS sensor (see Table. 2).

$$\boldsymbol{\mu_l} = \begin{bmatrix} -2.5084 & -2.4287 & -2.3222 & -2.2149 & -2.3104 & -3.0035 \end{bmatrix}$$

$$\boldsymbol{\sigma_l} = \begin{bmatrix} 0.2693 & 0.2715 & 0.2489 & 0.2028 & 0.1880 & 0.2593 \end{bmatrix}$$

$$\mathbf{w}^{(1)} = \begin{bmatrix} -0.6275 & -0.1540 & 0.4018 & 0.7828 & -0.3527 & -0.3398 & -0.4025 & -0.0318 & 0.2041 & -0.3274 \\ 0.2468 & 0.1821 & 0.7865 & -0.4450 & -0.3144 & 0.4567 & -0.0184 & 0.1598 & 0.0908 & 0.0960 \\ 0.4523 & -0.6513 & -0.1097 & -0.4494 & 0.2058 & 0.4459 & 0.8946 & 0.4201 & -0.1286 & -0.2860 \\ -0.1759 & -0.2794 & -0.5261 & 0.4748 & -0.2508 & -0.7378 & 0.6981 & 0.0892 & 0.2334 & -0.4394 \\ 0.8550 & -0.4358 & -0.0555 & -0.3294 & -0.1794 & 0.4001 & 0.2969 & -0.4909 & 0.2457 & 0.0396 \\ -0.4761 & 0.0240 & 0.5615 & 0.2414 & -0.3875 & -0.6367 & 0.0341 & -0.3171 & -0.3739 & 0.0304 \end{bmatrix}$$

$$\mathbf{b}^{(1)} = \begin{bmatrix} 0.5418 & 0.8660 & -0.3257 & 0.4289 & 0.1799 & 0.6591 & 0.2829 & -0.6403 & -0.7725 & -0.3100 \end{bmatrix}$$

$$(\mathbf{w}^{(2)})^{\mathrm{T}} = \begin{bmatrix} -1.2158 & -0.2448 & -0.7330 & 1.1446 & 0.3403 & -1.6787 & 0.4237 & -0.6157 & -0.3953 & -0.1484 \end{bmatrix} \text{ and } b^{(2)} = 0.2395$$

$\mu_c = 0.0801$ and $\sigma_c = 0.5139$

TABLE 76: As in Table 75 but for $a_{ys}(412)$.

$$\boldsymbol{\mu_l} = \begin{bmatrix} -2.5084 & -2.4287 & -2.3222 & -2.2149 & -2.3104 & -3.0035 \end{bmatrix}$$

$$\boldsymbol{\sigma_l} = \begin{bmatrix} 0.2693 & 0.2715 & 0.2489 & 0.2028 & 0.1880 & 0.2593 \end{bmatrix}$$

$$\mathbf{w}^{(1)} = \begin{bmatrix} 0.3518 & -0.1235 & 0.0717 & 0.2882 & -0.0102 & 0.1669 & 0.1943 & 0.2269 & 0.7019 & -0.0067 \\ -0.5874 & 0.2039 & 0.0544 & 0.1102 & -0.1355 & 0.2462 & -0.1107 & 0.1490 & -0.0893 & 0.6295 \\ -1.0907 & -0.6755 & -0.2951 & 0.2211 & -0.2844 & 1.0603 & 0.1668 & -0.5394 & -0.6311 & 0.2760 \\ 1.4000 & 0.6403 & 1.0724 & -0.2741 & 0.2469 & -1.4170 & 0.7470 & 0.3752 & 0.6120 & -0.3437 \\ -0.9415 & -0.2935 & -0.3337 & 0.2118 & 0.3929 & 0.2041 & 0.1665 & 0.0184 & 0.2852 & 0.0394 \\ 0.2707 & 0.1823 & -0.6454 & -0.3331 & -0.2234 & -0.0598 & -0.3260 & 0.1464 & -0.0939 & -0.2949 \end{bmatrix}$$

$$\mathbf{b}^{(1)} = \begin{bmatrix} 0.3921 & 0.5179 & -0.8321 & 0.4592 & 0.2067 & -0.3229 & -0.2272 & -0.3162 & -0.4622 & 0.5154 \end{bmatrix}$$

$$(\mathbf{w}^{(2)})^{\mathrm{T}} = \begin{bmatrix} 1.7303 & 0.8121 & 1.0820 & -0.5655 & 0.2779 & -1.6438 & 0.2740 & 0.6702 & 0.9701 & -0.6362 \end{bmatrix} \text{ and } b^{(2)} = 0.0954$$

$\mu_c =$ -0.6127 and $\sigma_c = 0.2427$

TABLE 77: As in Table 75 but for TSM.

$$\boldsymbol{\mu_l} = \begin{bmatrix} -2.5084 & -2.4287 & -2.3222 & -2.2149 & -2.3104 & -3.0035 \end{bmatrix}$$

$$\boldsymbol{\sigma_l} = \begin{bmatrix} 0.2693 & 0.2715 & 0.2489 & 0.2028 & 0.1880 & 0.2593 \end{bmatrix}$$

$$\mathbf{w}^{(1)} = \begin{bmatrix} -0.0082 & -0.1309 & 0.5719 & -0.3461 & -0.2711 & 0.0494 & -0.3469 & -0.1163 & 0.0626 & 0.2113 \\ -0.2783 & 0.2228 & 0.1762 & -0.5118 & 0.3633 & -0.1307 & -0.4524 & 0.2472 & -0.4325 & 0.4774 \\ 0.3008 & 0.6674 & -0.4794 & 0.0653 & 0.1295 & 0.1427 & 0.1859 & -0.0390 & 0.1223 & 0.2180 \\ -0.2918 & 0.0135 & 0.0871 & -0.3847 & 0.4898 & -0.2486 & -0.0651 & -0.0863 & -0.1987 & -0.3990 \\ -0.1132 & 0.2836 & -0.0512 & -0.1721 & 0.0011 & -0.0595 & -0.3402 & 0.1254 & 0.8903 & 0.0848 \\ -0.6264 & -0.4479 & 0.1111 & 0.2264 & 0.3374 & 0.5511 & -0.2261 & -0.4251 & -0.1073 & -0.1339 \end{bmatrix}$$

$$\mathbf{b}^{(1)} = \begin{bmatrix} 0.2852 & 0.4212 & 0.6116 & 0.0905 & 0.3358 & -0.9550 & 0.2074 & 0.8004 & 0.3330 & -0.5578 \end{bmatrix}$$

$$(\mathbf{w}^{(2)})^{\mathrm{T}} = \begin{bmatrix} 0.2290 & -0.7914 & 0.7003 & -0.3613 & 0.1181 & 0.9538 & 0.1713 & -0.9134 & 0.7930 & -0.6242 \end{bmatrix} \text{ and } b^{(2)} = 0.5027$$

$\mu_c = 0.0989$ and $\sigma_c = 0.3176$

TABLE 78: As in Table 69 but for the center wavelengths of the MERIS sensor (see Table. 2).

$$\boldsymbol{\mu_l} = \begin{bmatrix} -2.5084 & -2.4287 & -2.3087 & -2.2983 & -2.2747 & -3.0035 \end{bmatrix}$$

$$\boldsymbol{\sigma_l} = \begin{bmatrix} 0.2693 & 0.2715 & 0.2464 & 0.2144 & 0.1903 & 0.2593 \end{bmatrix}$$

$$\mathbf{w}^{(1)} = \begin{bmatrix} 0.0031 & -0.1414 & -0.4437 & 0.0051 & 0.6411 & 0.4145 & 0.1154 & -0.2248 & -0.2448 & -0.4254 \\ -0.3120 & 0.7051 & 0.5148 & 0.5039 & -0.3300 & 0.5296 & -0.2998 & 0.2776 & -0.3091 & 0.1723 \\ -0.3815 & -0.0660 & 0.1865 & 0.2143 & -0.2373 & -0.1512 & 0.1501 & 0.3572 & 0.0275 & -0.0611 \\ 0.5759 & 0.4968 & -0.1848 & -0.2649 & 0.4368 & 0.0697 & 0.0443 & 0.0947 & 0.1697 & 0.6446 \\ 0.5077 & -0.0726 & -0.0228 & -0.0186 & -0.2858 & 0.0307 & -0.0435 & -0.4408 & 0.0797 & 0.4874 \\ -0.6553 & -0.3820 & -0.3270 & -0.0801 & -0.7517 & 0.2278 & 0.2850 & -0.3211 & 0.8110 & -0.4554 \end{bmatrix}$$

$$\mathbf{b}^{(1)} = \begin{bmatrix} 0.3555 & 0.2759 & -0.2226 & -1.0403 & 1.2963 & -1.0110 & 0.0232 & -0.4631 & -0.0513 & 0.9438 \end{bmatrix}$$

$$(\mathbf{w}^{(2)})^{\mathrm{T}} = \begin{bmatrix} -0.5077 & 0.5634 & -0.8483 & -0.6299 & -0.9733 & -0.5010 & 0.3012 & -0.7991 & -0.2649 & -1.0549 \end{bmatrix} \text{ and } b^{(2)} = 0.2817$$

$$\mu_c = 0.0801 \text{ and } \sigma_c = 0.5139$$

TABLE 79: As in Table 78 but for $a_{ys}(412)$.

$$\boldsymbol{\mu_l} = \begin{bmatrix} -2.5084 & -2.4287 & -2.3087 & -2.2983 & -2.2747 & -3.0035 \end{bmatrix}$$

$$\boldsymbol{\sigma_l} = \begin{bmatrix} 0.2693 & 0.2715 & 0.2464 & 0.2144 & 0.1903 & 0.2593 \end{bmatrix}$$

$$\mathbf{w}^{(1)} = \begin{bmatrix} 0.8764 & -0.1651 & 0.5253 & 0.0347 & 0.2584 & -0.0004 & -0.6981 & 1.1353 & -0.7801 & 0.0445 \\ -0.3681 & 0.0031 & -0.3060 & 0.5477 & -0.1890 & 0.6955 & 0.1822 & 0.0214 & -0.2207 & 0.1835 \\ -0.7420 & -0.4628 & 0.0798 & 0.5275 & -0.5148 & 0.5729 & -0.1809 & -0.5033 & 0.9463 & -0.0815 \\ 0.6134 & 0.0900 & 0.2763 & -1.2438 & 0.7633 & -0.5459 & 0.7809 & -0.1606 & -0.1701 & 0.4570 \\ 0.1258 & -0.3319 & -0.4318 & 0.6973 & -0.3308 & -0.3480 & -0.5018 & 0.3120 & -0.8232 & -0.4055 \\ -0.2952 & -0.2271 & 0.1715 & -0.0765 & 0.0733 & 0.0713 & -0.1797 & -0.4880 & -0.5637 & 0.0856 \end{bmatrix}$$

$$\mathbf{b}^{(1)} = \begin{bmatrix} 0.3548 & -0.2051 & -0.2376 & -0.1375 & -0.0877 & -0.1077 & 0.4534 & 0.9537 & 0.0180 & -0.5573 \end{bmatrix}$$

$$(\mathbf{w}^{(2)})^{\mathrm{T}} = \begin{bmatrix} -1.0796 & -0.3908 & -0.9579 & 1.4493 & -0.8772 & 0.2307 & -0.8675 & -0.9590 & 0.4841 & -0.8115 \end{bmatrix} \text{ and } b^{(2)} = 0.7033$$

$$\mu_c = \text{-}0.6127 \text{ and } \sigma_c = 0.2427$$

TABLE 80: As in Table 78 but for TSM.

$$\boldsymbol{\mu_l} = \begin{bmatrix} -2.5084 & -2.4287 & -2.3087 & -2.2983 & -2.2747 & -3.0035 \end{bmatrix}$$

$$\boldsymbol{\sigma_l} = \begin{bmatrix} 0.2693 & 0.2715 & 0.2464 & 0.2144 & 0.1903 & 0.2593 \end{bmatrix}$$

$$\mathbf{w}^{(1)} = \begin{bmatrix} 0.0018 & 0.0647 & -0.1370 & 0.1340 & -0.1531 & 0.1561 & -0.6268 & 0.7985 & -0.1281 & 0.1236 \\ 0.2213 & -0.5452 & 0.3698 & -0.0690 & 0.2331 & 0.1687 & 0.0025 & 0.3949 & 0.4649 & 0.1567 \\ -0.1170 & 0.1724 & -0.1200 & -0.5577 & 0.5407 & -0.1966 & 0.3097 & -0.1215 & 0.0147 & -0.1158 \\ -0.5120 & 0.0723 & 0.2033 & -0.3507 & -0.0706 & 0.3802 & -0.0316 & -0.0341 & 0.5033 & 0.2303 \\ 0.0397 & -0.3181 & 0.0776 & -0.1325 & -0.4057 & -0.1043 & -0.3285 & 0.0243 & -0.7073 & 0.1244 \\ -0.0326 & -0.0723 & -0.7674 & 0.4804 & -0.0958 & -0.2150 & -0.3522 & -0.0655 & 0.0791 & -0.2906 \end{bmatrix}$$

$$\mathbf{b}^{(1)} = \begin{bmatrix} 0.3702 & 0.1526 & 1.4933 & -0.3468 & -0.2088 & -0.0035 & -0.9803 & 0.1792 & -0.6161 & 0.0818 \end{bmatrix}$$

$$(\mathbf{w}^{(2)})^{\mathrm{T}} = \begin{bmatrix} -0.4282 & 0.0895 & -1.2537 & 0.5182 & -0.6562 & 0.0536 & -0.4092 & 0.0881 & -0.4589 & -0.0743 \end{bmatrix} \text{ and } b^{(2)} = 0.6815$$

$$\mu_c = 0.0989 \text{ and } \sigma_c = 0.3176$$

3.7 English Channel

BiOMaP data for developing the MLP neural network for the English Channel (Figure 15(a)) were collected during a cruise executed in 2004 (55 stations). The MLP architecture selected on the basis of trends of Panels 15(b)–15(d) has ten hidden units. The resulting comparison between modeled and measured values is shown in Figure 16 and Table 81.

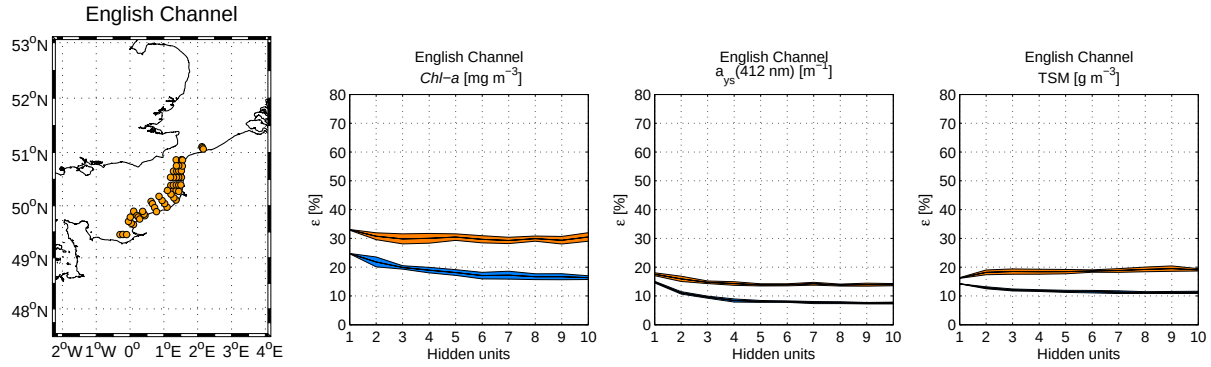

(a) (b) (c) (d)

FIGURE 15: As in Figure 3, but for the English Channel.

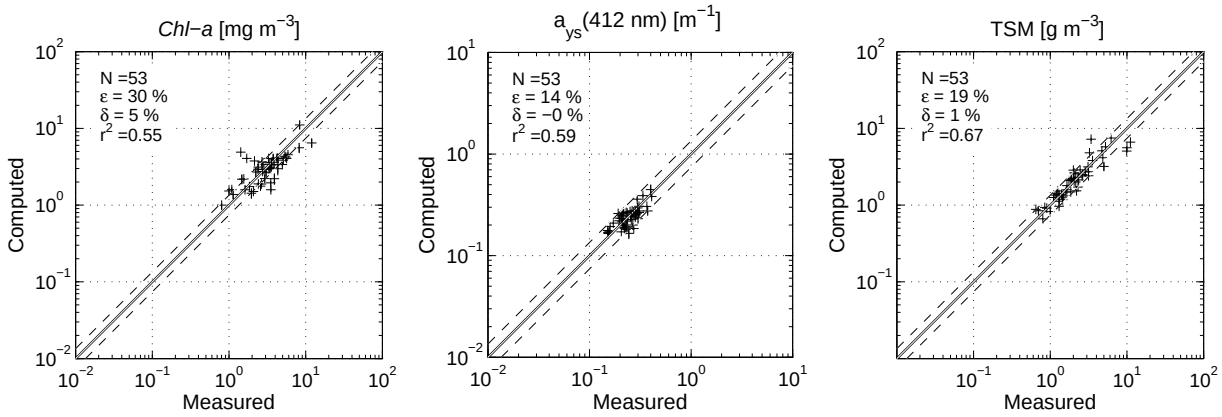

(a) (b) (c)

FIGURE 16: As in Figure 4, but for the English Channel. Results based on the MLP with ten units in the hidden layer.

TABLE 81: As in Table 3, but for the English Channel. Results based on the MLP with ten units in the hidden layer.

	N	ϵ [%]	δ [%]	r^2
Chl-a	53	28.9(16.2)	2.9(2.2)	58.1(90.6)
$a_{ys}(412)$	53	13.9(7.7)	-0.4(0.2)	53.6(86.0)
TSM	53	19.4(11.4)	1.5(0.9)	66.9(93.0)

TABLE 82: Parameter sets to compute data pre- and post-processing, as well as MLP weights to derive *Chl-a* values in the English Channel. Input R_{RS} wavelengths are those of the in-situ measurements (see Table. 2).

$$\boldsymbol{\mu_I} = \begin{bmatrix} -2.7696 & -2.7052 & -2.5144 & -2.4664 & -2.3741 & -2.9269 \end{bmatrix}$$

$$\boldsymbol{\sigma_I} = \begin{bmatrix} 0.1984 & 0.2304 & 0.2540 & 0.2602 & 0.2592 & 0.2878 \end{bmatrix}$$

$$\mathbf{w}^{(1)} = \begin{bmatrix} 1.2365 & -0.4293 & 0.2854 & -0.6478 & -0.4451 & -0.6407 & -0.2505 & -0.2951 & -0.3091 & -0.1801 \\ -0.2366 & 0.2882 & 1.3654 & 0.0007 & -0.7416 & -0.2919 & -0.6049 & -0.3955 & -0.4581 & -0.6319 \\ -0.8514 & 0.8192 & 0.3453 & 0.0894 & -0.7521 & -0.0517 & -0.4665 & 0.4349 & -0.0955 & 0.4180 \\ -0.1946 & 0.6564 & -0.9452 & -0.0345 & -0.9410 & -0.3913 & -0.7859 & 0.7324 & -0.3276 & -0.1636 \\ 0.7129 & -0.7573 & -0.5621 & -0.4527 & -0.6037 & 0.1213 & -0.4438 & 0.3658 & -0.7900 & 0.1577 \\ 0.6285 & -0.1127 & 0.4548 & -0.3701 & -0.4242 & -0.3698 & -0.5220 & -0.2975 & -0.1049 & 0.1492 \end{bmatrix}$$

$$\mathbf{b}^{(1)} = \begin{bmatrix} -0.8621 & -0.7910 & 1.0780 & 0.2720 & 0.5402 & -0.2697 & 0.4737 & -0.4200 & -0.4815 & 0.2288 \end{bmatrix}$$

$$(\mathbf{w}^{(2)})^{\mathrm{T}} = \begin{bmatrix} 1.4568 & -1.9201 & -2.0190 & -0.6973 & 0.7937 & -0.5201 & 0.4494 & -0.5502 & -0.8702 & 0.3270 \end{bmatrix} \text{ and } b^{(2)} = 0.3631$$

$$\mu_c = 0.4749 \text{ and } \sigma_c = 0.2342$$

TABLE 83: As in Table 82 but for $a_{ys}(412)$.

$$\boldsymbol{\mu_I} = \begin{bmatrix} -2.7696 & -2.7052 & -2.5144 & -2.4664 & -2.3741 & -2.9269 \end{bmatrix}$$

$$\boldsymbol{\sigma_I} = \begin{bmatrix} 0.1984 & 0.2304 & 0.2540 & 0.2602 & 0.2592 & 0.2878 \end{bmatrix}$$

$$\mathbf{w}^{(1)} = \begin{bmatrix} -0.0735 & -0.0543 & 0.3161 & 0.7222 & -0.7303 & 0.6907 & -0.9345 & -0.5565 & 0.1898 & 0.6544 \\ -0.0909 & -0.3189 & -0.1104 & -0.8698 & 0.4137 & -0.4311 & -0.2853 & -0.6790 & 1.4626 & 0.8511 \\ 0.4779 & 0.0205 & 0.3234 & -0.0490 & -0.5077 & -0.0356 & -0.2989 & -0.2649 & 0.6600 & 1.0094 \\ 0.0517 & -0.3482 & 1.3025 & -0.1356 & -0.2765 & -0.8212 & 0.1585 & -0.4454 & -0.1950 & 0.7828 \\ -0.2048 & -1.0267 & 0.9593 & -0.2757 & 0.6784 & -0.8104 & 0.1570 & 0.2924 & 0.2737 & 0.0893 \\ -0.2286 & -2.0453 & -0.3734 & 0.1249 & 0.7099 & 0.4959 & -0.3948 & 0.2752 & -1.8744 & -0.8170 \end{bmatrix}$$

$$\mathbf{b}^{(1)} = \begin{bmatrix} -0.7014 & -1.3823 & 1.2990 & -0.3118 & -0.6811 & 0.0557 & 0.1490 & -0.1403 & -0.4748 & 0.9588 \end{bmatrix}$$

$$(\mathbf{w}^{(2)})^{\mathrm{T}} = \begin{bmatrix} -0.4247 & -1.3110 & -0.9811 & -1.1123 & 1.6270 & -1.3347 & 0.7467 & 0.3640 & 1.4316 & -1.5867 \end{bmatrix} \text{ and } b^{(2)} = 0.9976$$

$$\mu_c = \text{-}0.6159 \text{ and } \sigma_c = 0.1041$$

TABLE 84: As in Table 82 but for TSM.

$$\boldsymbol{\mu_I} = \begin{bmatrix} -2.7696 & -2.7052 & -2.5144 & -2.4664 & -2.3741 & -2.9269 \end{bmatrix}$$

$$\boldsymbol{\sigma_I} = \begin{bmatrix} 0.1984 & 0.2304 & 0.2540 & 0.2602 & 0.2592 & 0.2878 \end{bmatrix}$$

$$\mathbf{w}^{(1)} = \begin{bmatrix} -0.1052 & 0.5546 & -0.1941 & -0.3895 & -0.1081 & -0.3296 & -0.1413 & -0.4669 & 0.2619 & -0.7692 \\ 0.3241 & -0.4135 & -0.1255 & -0.6909 & 0.0433 & -0.0281 & 0.1678 & -1.2198 & 0.1671 & 0.1165 \\ 0.0541 & 0.4339 & -0.3370 & -0.6460 & 0.1287 & 0.0165 & 0.2289 & -0.3921 & -0.1401 & 0.3579 \\ 0.1165 & 0.3379 & 0.2286 & -0.1735 & 0.2905 & -0.3660 & 0.2098 & 0.1373 & 0.3592 & 0.2056 \\ -0.4390 & 0.2053 & 0.1490 & 0.5786 & -0.0525 & 0.1215 & -0.0052 & 1.0132 & 0.6609 & 0.0432 \\ -0.4824 & -0.3642 & 0.0820 & 0.8237 & 0.1652 & -0.0077 & 0.0355 & 1.0272 & 0.0788 & -0.5383 \end{bmatrix}$$

$$\mathbf{b}^{(1)} = \begin{bmatrix} 0.3840 & -0.5250 & 0.3999 & -0.0397 & 0.1777 & 0.0097 & 0.2294 & 0.1505 & -0.3343 & 0.1074 \end{bmatrix}$$

$$(\mathbf{w}^{(2)})^{\mathrm{T}} = \begin{bmatrix} -0.5411 & 0.8879 & 0.2565 & -0.9260 & -0.3279 & -0.0963 & -0.3912 & 1.4320 & -0.5549 & -0.8524 \end{bmatrix} \text{ and } b^{(2)} = 0.2719$$

$$\mu_c = 0.3249 \text{ and } \sigma_c = 0.2816$$

TABLE 85: As in Table 82 but for the center wavelengths of the SeaWiFS sensor (see Table. 2).

$$\boldsymbol{\mu_l} = \begin{bmatrix} -2.7696 & -2.7052 & -2.5144 & -2.4664 & -2.3741 & -2.9288 \end{bmatrix}$$

$$\boldsymbol{\sigma_l} = \begin{bmatrix} 0.1984 & 0.2304 & 0.2540 & 0.2602 & 0.2592 & 0.2880 \end{bmatrix}$$

$$\mathbf{w}^{(1)} = \begin{bmatrix} 0.4403 & -0.0167 & -0.3953 & -0.4368 & -1.4310 & -0.1199 & 0.5981 & -0.5241 & -0.8046 & -0.4153 \\ 0.0867 & -0.0445 & -1.1752 & 0.1503 & 0.2021 & -0.9519 & -0.1347 & 0.0209 & -0.2782 & -0.0153 \\ 0.4661 & 0.4828 & -0.2337 & 0.8385 & 0.7935 & -0.7144 & 0.3102 & 0.2083 & -0.1733 & -0.0268 \\ -0.0445 & 0.1616 & 0.7666 & 0.7603 & 0.5285 & -0.8197 & -0.1029 & 0.0548 & -0.3055 & -0.6555 \\ 0.0884 & -0.1275 & 0.6668 & -0.6647 & -0.9396 & -0.7912 & 0.5025 & -0.8248 & -0.2251 & -0.4477 \\ -0.1010 & -0.0432 & -0.5046 & -0.1954 & -0.4798 & -0.8736 & 0.0255 & -0.7219 & -0.5972 & -0.3260 \end{bmatrix}$$

$$\mathbf{b}^{(1)} = \begin{bmatrix} -0.1191 & -0.5056 & -1.0601 & -0.7060 & 0.9500 & 0.5705 & -0.3260 & 0.3845 & -0.6335 & -0.3670 \end{bmatrix}$$

$$(\mathbf{w}^{(2)})^{\mathrm{T}} = \begin{bmatrix} -0.0184 & -0.9373 & 1.9788 & -1.8868 & -1.4114 & 1.0739 & 0.0978 & -0.6521 & -0.7891 & -0.3542 \end{bmatrix} \text{ and } b^{(2)} = 0.4057$$

$$\mu_c = 0.4749 \text{ and } \sigma_c = 0.2342$$

TABLE 86: As in Table 85 but for $a_{ys}(412)$.

$$\boldsymbol{\mu_l} = \begin{bmatrix} -2.7696 & -2.7052 & -2.5144 & -2.4664 & -2.3741 & -2.9288 \end{bmatrix}$$

$$\boldsymbol{\sigma_l} = \begin{bmatrix} 0.1984 & 0.2304 & 0.2540 & 0.2602 & 0.2592 & 0.2880 \end{bmatrix}$$

$$\mathbf{w}^{(1)} = \begin{bmatrix} -0.2537 & -0.1613 & 0.3847 & -1.3565 & 0.2768 & -0.6131 & -0.7788 & 0.0423 & -0.1816 & -0.5721 \\ 0.3916 & -0.2344 & 0.9543 & 0.8941 & 1.2503 & 0.5793 & -1.0537 & -0.5553 & 0.5765 & 0.5958 \\ 0.0039 & -0.2112 & 1.1094 & -0.2809 & 0.2177 & 0.1426 & -0.6358 & 0.3453 & -0.2664 & 0.1149 \\ 0.7821 & -0.4798 & 0.6188 & -0.2958 & -0.0129 & 0.1235 & -0.2524 & -0.4879 & -0.2422 & -0.1009 \\ 0.8137 & -0.5701 & 0.5603 & -0.3306 & 0.9099 & 0.5415 & 0.3952 & -1.2536 & 0.4567 & 0.2255 \\ -0.7573 & -0.8351 & -0.8402 & 1.4743 & -2.2100 & -0.3337 & 0.3585 & -2.0548 & -0.1656 & 0.0520 \end{bmatrix}$$

$$\mathbf{b}^{(1)} = \begin{bmatrix} -0.1957 & -0.6103 & 1.1490 & -0.7676 & -0.3750 & 0.2517 & -0.1808 & -1.3061 & -0.0471 & 0.0442 \end{bmatrix}$$

$$(\mathbf{w}^{(2)})^{\mathrm{T}} = \begin{bmatrix} 0.9607 & 0.0794 & -1.8675 & 1.6417 & 1.4929 & 0.8692 & 1.0942 & -1.1515 & 0.7971 & 0.6691 \end{bmatrix} \text{ and } b^{(2)} = 1.3578$$

$$\mu_c = \text{-}0.6159 \text{ and } \sigma_c = 0.1041$$

TABLE 87: As in Table 85 but for TSM.

$$\boldsymbol{\mu_l} = \begin{bmatrix} -2.7696 & -2.7052 & -2.5144 & -2.4664 & -2.3741 & -2.9288 \end{bmatrix}$$

$$\boldsymbol{\sigma_l} = \begin{bmatrix} 0.1984 & 0.2304 & 0.2540 & 0.2602 & 0.2592 & 0.2880 \end{bmatrix}$$

$$\mathbf{w}^{(1)} = \begin{bmatrix} -0.0784 & 0.8005 & -0.6057 & -0.0897 & -0.4079 & 0.0089 & -0.1985 & 0.1899 & 0.6380 & 0.7641 \\ 0.1317 & 0.0647 & 0.4939 & -0.1347 & 0.0701 & -0.2392 & 0.0597 & 0.1731 & -0.6439 & 1.0185 \\ -0.0489 & 0.5224 & -0.0934 & -0.0717 & -0.5148 & 0.2877 & 0.0562 & 0.0328 & -0.0759 & 0.2945 \\ -0.0362 & -0.0642 & 0.2843 & 0.2075 & -0.1974 & 0.2483 & 0.4334 & 0.4493 & -0.2184 & -0.1329 \\ 0.4203 & -0.4965 & 0.3596 & -0.1163 & -0.2954 & -0.2188 & 0.2091 & -0.0421 & 0.4032 & -1.0213 \\ -0.0194 & -0.3993 & 0.0687 & -0.1382 & 0.6063 & 0.1878 & 0.0494 & -0.0597 & 0.2762 & -1.0861 \end{bmatrix}$$

$$\mathbf{b}^{(1)} = \begin{bmatrix} 0.1543 & 0.2797 & 0.1740 & 0.2760 & 0.7227 & -0.0879 & -0.0068 & 0.2724 & -0.1710 & -0.0843 \end{bmatrix}$$

$$(\mathbf{w}^{(2)})^{\mathrm{T}} = \begin{bmatrix} -0.1088 & 0.9958 & -0.7852 & -0.0798 & -0.8495 & 0.1036 & -0.2545 & 0.1094 & 1.0241 & -1.4562 \end{bmatrix} \text{ and } b^{(2)} = 0.3365$$

$$\mu_c = 0.3249 \text{ and } \sigma_c = 0.2816$$

TABLE 88: As in Table 82 but for the center wavelengths of the MODIS sensor (see Table. 2).

$$\boldsymbol{\mu_l} = \begin{bmatrix} -2.7696 & -2.7052 & -2.5310 & -2.3712 & -2.4027 & -2.9269 \end{bmatrix}$$

$$\boldsymbol{\sigma_l} = \begin{bmatrix} 0.1984 & 0.2304 & 0.2571 & 0.2497 & 0.2623 & 0.2878 \end{bmatrix}$$

$$\mathbf{w}^{(1)} = \begin{bmatrix} -0.6412 & 1.0088 & 0.2384 & -0.5208 & -0.7585 & 0.1544 & -0.2579 & -0.1593 & 0.5050 & 0.1855 \\ 0.7946 & -0.3468 & 0.5412 & -0.6804 & 0.0261 & -0.4992 & 0.4981 & -0.7915 & -0.1249 & 0.4207 \\ 0.7436 & -1.1871 & 0.1438 & -0.8483 & 0.3781 & -0.6360 & 0.7846 & -0.7668 & -0.1027 & -0.3857 \\ 0.2130 & 0.9705 & 0.8045 & 1.4288 & -1.0051 & 0.6795 & -1.1631 & -0.5247 & 0.3904 & 0.6380 \\ -0.2956 & 0.0052 & 0.9463 & -0.3112 & 0.0535 & 0.1848 & 0.2839 & -0.9702 & 0.0564 & 0.2243 \\ -0.3811 & 0.3776 & 0.0236 & 0.2148 & 0.1611 & -0.0404 & 0.1900 & -0.7181 & 0.8034 & 0.2436 \end{bmatrix}$$

$$\mathbf{b}^{(1)} = \begin{bmatrix} -1.0452 & -0.4423 & -0.4908 & -0.9501 & -0.2286 & 0.1665 & -0.1498 & 0.5356 & -0.5908 & -0.1385 \end{bmatrix}$$

$$(\mathbf{w}^{(2)})^{\mathrm{T}} = \begin{bmatrix} -1.5184 & 1.5738 & -0.3388 & 2.0503 & -1.1459 & 1.1852 & -1.7236 & 0.8875 & 0.7394 & 0.5550 \end{bmatrix} \text{ and } b^{(2)} = 0.2118$$

$$\mu_c = 0.4749 \text{ and } \sigma_c = 0.2342$$

TABLE 89: As in Table 88 but for $a_{ys}(412)$.

$$\boldsymbol{\mu_l} = \begin{bmatrix} -2.7696 & -2.7052 & -2.5310 & -2.3712 & -2.4027 & -2.9269 \end{bmatrix}$$

$$\boldsymbol{\sigma_l} = \begin{bmatrix} 0.1984 & 0.2304 & 0.2571 & 0.2497 & 0.2623 & 0.2878 \end{bmatrix}$$

$$\mathbf{w}^{(1)} = \begin{bmatrix} 0.5592 & -0.0877 & 0.4625 & 0.3197 & -0.8436 & -0.4591 & 0.4971 & 0.2481 & -0.2821 & -0.6298 \\ -0.1731 & 0.1529 & 0.4694 & -0.4352 & -0.5764 & -0.7803 & 0.2907 & -1.0283 & -0.1178 & 0.0228 \\ -0.1921 & 0.1723 & 0.4802 & 0.1095 & -1.0338 & -1.1725 & -0.1966 & -0.4756 & -0.4434 & -0.4988 \\ -0.5227 & -0.0627 & 0.9600 & -0.5653 & -0.0475 & -0.3828 & 0.3798 & -1.5467 & 0.0965 & 0.4257 \\ -0.2135 & 0.0287 & 0.6378 & -0.8265 & 0.2122 & -0.6399 & -0.1818 & 0.5650 & -0.0585 & 0.0045 \\ -0.0762 & 0.3778 & -0.1276 & -2.1831 & 0.6436 & 0.4111 & 1.1142 & 1.7948 & -1.5405 & 1.0702 \end{bmatrix}$$

$$\mathbf{b}^{(1)} = \begin{bmatrix} 0.2574 & 0.6858 & -0.7719 & -1.2713 & -0.2978 & -1.2566 & -0.1735 & 0.2752 & 0.1471 & -0.6562 \end{bmatrix}$$

$$(\mathbf{w}^{(2)})^{\mathrm{T}} = \begin{bmatrix} -0.8729 & 0.6557 & 1.1191 & -1.5228 & 1.1050 & 1.5189 & -0.4655 & -1.4867 & 1.1713 & 1.6011 \end{bmatrix} \text{ and } b^{(2)} = 0.9411$$

$$\mu_c = \text{-}0.6159 \text{ and } \sigma_c = 0.1041$$

TABLE 90: As in Table 88 but for TSM.

$$\boldsymbol{\mu_l} = \begin{bmatrix} -2.7696 & -2.7052 & -2.5310 & -2.3712 & -2.4027 & -2.9269 \end{bmatrix}$$

$$\boldsymbol{\sigma_l} = \begin{bmatrix} 0.1984 & 0.2304 & 0.2571 & 0.2497 & 0.2623 & 0.2878 \end{bmatrix}$$

$$\mathbf{w}^{(1)} = \begin{bmatrix} -0.5727 & 0.0015 & 0.2740 & -0.0692 & 0.3208 & -0.2387 & -0.2668 & 0.7148 & 0.1496 & -0.0203 \\ -0.2827 & 0.2350 & 1.0228 & -1.1753 & 0.1684 & 0.2949 & -0.2975 & 0.3448 & -0.1059 & -0.0276 \\ 0.0355 & -0.0479 & 0.4804 & 0.3966 & 0.1178 & -0.6004 & -0.1879 & 0.3622 & 0.2499 & 0.2144 \\ 0.2052 & -0.1012 & 0.3749 & -0.3568 & 0.5220 & 0.0338 & 0.4273 & 0.3645 & -0.2888 & -0.1577 \\ 0.3423 & -0.1508 & -0.9011 & 0.7872 & 0.4057 & -0.1901 & 0.1275 & 0.0424 & -0.2370 & -0.1301 \\ -0.1540 & 0.2531 & -1.1388 & 1.0148 & -0.0486 & 0.3225 & -0.0201 & -1.0969 & -0.0770 & 0.2875 \end{bmatrix}$$

$$\mathbf{b}^{(1)} = \begin{bmatrix} -0.2562 & 0.0364 & -0.6169 & -0.4243 & -0.3082 & 0.3678 & -0.1525 & -0.4669 & 0.0579 & 0.2522 \end{bmatrix}$$

$$(\mathbf{w}^{(2)})^{\mathrm{T}} = \begin{bmatrix} -0.4996 & -0.2002 & -1.2213 & 1.2172 & -0.4340 & -0.5414 & -0.2398 & 1.1027 & 0.4567 & -0.0734 \end{bmatrix} \text{ and } b^{(2)} = 0.0933$$

$$\mu_c = 0.3249 \text{ and } \sigma_c = 0.2816$$

TABLE 91: As in Table 82 but for the center wavelengths of the MERIS sensor (see Table. 2).

$$\boldsymbol{\mu_l} = \begin{bmatrix} -2.7696 & -2.7052 & -2.5144 & -2.4664 & -2.3600 & -2.9269 \end{bmatrix}$$

$$\boldsymbol{\sigma_l} = \begin{bmatrix} 0.1984 & 0.2304 & 0.2540 & 0.2602 & 0.2583 & 0.2878 \end{bmatrix}$$

$$\mathbf{w}^{(1)} = \begin{bmatrix} 0.0984 & -1.0519 & 0.4275 & 0.1630 & -1.3843 & 0.1763 & 0.0239 & 0.4725 & -0.5437 & 0.2213 \\ 0.0101 & -0.7697 & 0.8833 & -0.1827 & -0.2251 & 0.1678 & 0.3181 & -0.1762 & -0.5730 & 0.7907 \\ 0.2998 & 0.0092 & 0.3368 & -0.4983 & 0.4630 & 0.3127 & 0.3118 & -1.0481 & -0.3159 & 0.7190 \\ -0.0818 & 0.1803 & -0.7417 & 0.0264 & 1.0453 & -0.0235 & -0.2528 & -0.5129 & 0.7175 & 0.8215 \\ -0.4285 & -0.1258 & -0.4998 & 0.3916 & -0.7616 & -0.5678 & -0.6622 & 0.4958 & 0.0344 & 0.7787 \\ 0.3208 & -0.2675 & 0.4160 & -0.1037 & -0.6744 & 0.1237 & 0.5661 & 0.3664 & -0.1001 & 0.3985 \end{bmatrix}$$

$$\mathbf{b}^{(1)} = \begin{bmatrix} -0.0044 & -0.7839 & 0.8445 & 0.6190 & 0.8281 & 0.0440 & 0.2011 & 0.5623 & -0.8168 & -0.5986 \end{bmatrix}$$

$$(\mathbf{w}^{(2)})^{\mathrm{T}} = \begin{bmatrix} -0.4749 & -1.3562 & -1.3441 & 0.9458 & -2.0697 & -0.5890 & -0.7474 & 1.4411 & 0.9501 & -0.8394 \end{bmatrix} \text{ and } b^{(2)} = 0.6672$$

$$\mu_c = 0.4749 \text{ and } \sigma_c = 0.2342$$

TABLE 92: As in Table 91 but for $a_{ys}(412)$.

$$\boldsymbol{\mu_l} = \begin{bmatrix} -2.7696 & -2.7052 & -2.5144 & -2.4664 & -2.3600 & -2.9269 \end{bmatrix}$$

$$\boldsymbol{\sigma_l} = \begin{bmatrix} 0.1984 & 0.2304 & 0.2540 & 0.2602 & 0.2583 & 0.2878 \end{bmatrix}$$

$$\mathbf{w}^{(1)} = \begin{bmatrix} 0.5076 & 0.1690 & -0.2424 & 0.8953 & -0.1024 & -0.3432 & -0.4397 & 0.2676 & 1.1450 & 0.2872 \\ 0.4981 & 1.2310 & 0.2109 & 0.4415 & 0.1956 & 0.0486 & 0.6378 & -0.4539 & -0.5530 & -0.7220 \\ 0.7565 & 0.2614 & -0.0820 & 0.6885 & 0.1027 & -0.5298 & 0.2175 & -0.1691 & -0.5084 & -0.6111 \\ 1.2788 & 0.3341 & -0.4767 & 0.7839 & 0.3521 & -0.3903 & -0.1036 & -0.1085 & -0.0825 & -0.7728 \\ 0.3398 & 0.6384 & 0.0963 & -0.9850 & 0.8304 & 0.3573 & -0.0487 & -0.6964 & -0.1180 & -0.6840 \\ -0.7513 & -2.1808 & -1.3206 & -0.0439 & 2.0679 & 1.2490 & 0.2563 & 0.1697 & -0.4331 & 0.2943 \end{bmatrix}$$

$$\mathbf{b}^{(1)} = \begin{bmatrix} 1.0699 & -0.3377 & 0.2861 & -0.0131 & 1.1002 & -0.9662 & 0.4345 & 0.2519 & 0.0222 & 0.4741 \end{bmatrix}$$

$$(\mathbf{w}^{(2)})^{\mathrm{T}} = \begin{bmatrix} -2.0972 & 1.4531 & 1.1522 & -1.2741 & 1.2987 & 1.1715 & 0.6301 & -0.9601 & -1.0475 & -0.9396 \end{bmatrix} \text{ and } b^{(2)} = 1.0994$$

$$\mu_c = \text{-}0.6159 \text{ and } \sigma_c = 0.1041$$

TABLE 93: As in Table 91 but for TSM.

$$\boldsymbol{\mu_l} = \begin{bmatrix} -2.7696 & -2.7052 & -2.5144 & -2.4664 & -2.3600 & -2.9269 \end{bmatrix}$$

$$\boldsymbol{\sigma_l} = \begin{bmatrix} 0.1984 & 0.2304 & 0.2540 & 0.2602 & 0.2583 & 0.2878 \end{bmatrix}$$

$$\mathbf{w}^{(1)} = \begin{bmatrix} 0.2411 & 0.5090 & -0.0355 & 0.0778 & 1.3005 & 0.4550 & 0.3087 & -0.1102 & 0.0636 & -0.0681 \\ 0.2333 & 1.1339 & -0.8398 & 0.0564 & -0.1438 & 0.3275 & 0.5963 & 0.2819 & 0.2135 & 0.0252 \\ 0.1301 & 0.1579 & 0.0637 & 0.2512 & 0.2008 & 0.3886 & -0.3384 & 0.2129 & -0.0134 & 0.0125 \\ 0.2712 & 0.2621 & 0.0854 & 0.2140 & -0.2667 & 0.4889 & 0.0582 & 0.0917 & 0.1132 & 0.5063 \\ 0.1531 & -1.0219 & 0.6494 & 0.0616 & -0.4859 & -0.0975 & -0.3128 & 0.1147 & -0.0639 & -0.0246 \\ 0.2886 & -1.1715 & 0.6698 & 0.1055 & -0.2034 & -0.8325 & -0.3857 & 0.0754 & -0.1069 & 0.1091 \end{bmatrix}$$

$$\mathbf{b}^{(1)} = \begin{bmatrix} -0.1759 & -0.3001 & -0.5474 & 0.0583 & 0.2430 & -0.4472 & -0.1025 & -0.2110 & 0.0653 & 0.1228 \end{bmatrix}$$

$$(\mathbf{w}^{(2)})^{\mathrm{T}} = \begin{bmatrix} -0.3587 & -1.2644 & 0.9356 & -0.1570 & 1.1261 & 1.0376 & -0.5213 & -0.0882 & -0.1866 & -0.2719 \end{bmatrix} \text{ and } b^{(2)} = 0.0634$$

$$\mu_c = 0.3249 \text{ and } \sigma_c = 0.2816$$

3.8 Baltic Sea

Six BiOMaP campaigns were executed in the Baltic Sea between 2004 and 2008 (Figure 17(a)), for a total number of 274 stations. The generalization performance shown in Panels 15(b)–15(d) support the operational use of the MLP with ten hidden units. The resulting agreement between modeled and measured values is shown in Figure 18 and Table 94.

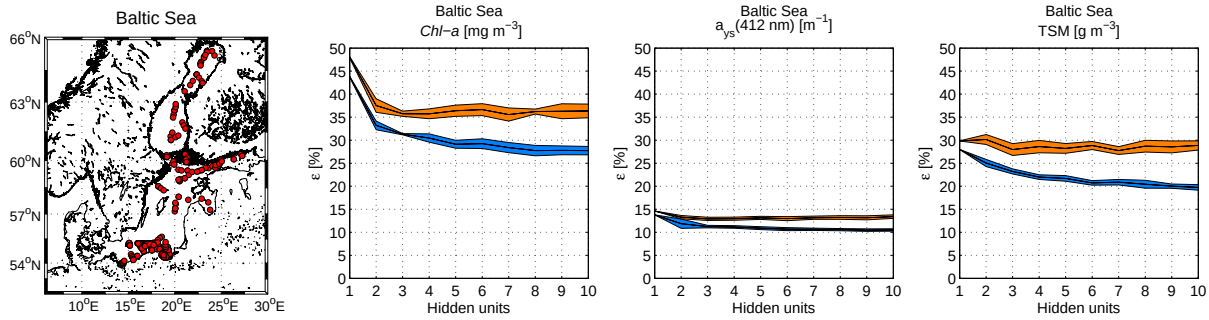

(a) (b) (c) (d)

FIGURE 17: As in Figure 3, but for the Baltic Sea.

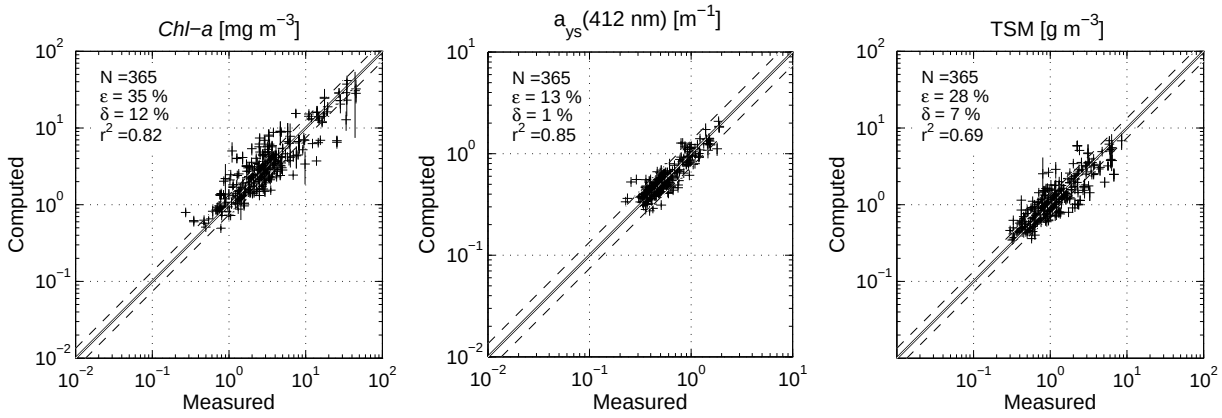

(a) (b) (c)

FIGURE 18: As in Figure 4, but for the Baltic Sea. Results based on the MLP with ten units in the hidden layer.

TABLE 94: As in Table 3, but for the Baltic Sea. Results based on the MLP with ten units in the hidden layer.

	N	ϵ [%]	δ [%]	r^2
Chl-a	365	34.9(27.7)	11.1(5.6)	84.1(89.2)
$a_{ys}(412)$	365	12.8(10.4)	0.9(1.1)	86.4(91.4)
TSM	365	27.8(19.3)	7.1(2.8)	74.3(90.1)

TABLE 95: Parameter sets to compute data pre- and post-processing, as well as MLP weights to derive *Chl-a* values in the Baltic Sea. Input R_{RS} wavelengths are those of the in-situ measurements (see Table. 2).

$$\boldsymbol{\mu_I} = \begin{bmatrix} -3.1603 & -3.0312 & -2.8155 & -2.7409 & -2.6652 & -3.1614 \end{bmatrix}$$

$$\boldsymbol{\sigma_I} = \begin{bmatrix} 0.2588 & 0.1838 & 0.1592 & 0.1607 & 0.1756 & 0.2461 \end{bmatrix}$$

$$\mathbf{w}^{(1)} = \begin{bmatrix} -0.7985 & 0.2080 & -0.4472 & 0.4574 & 0.4361 & -0.1427 & -0.3852 & 0.2818 & -0.5851 & -0.2278 \\ 0.0232 & -0.1921 & -0.0594 & -0.0531 & 1.0587 & -0.2680 & -0.2595 & 1.9991 & 0.8481 & -0.2425 \\ 1.0904 & 0.4620 & 0.2267 & 0.5697 & 0.0892 & -0.0123 & 0.2390 & 0.7510 & 0.4695 & 0.2861 \\ -0.2053 & 1.6031 & 0.4763 & 0.2052 & -0.0905 & -0.7447 & 0.4032 & -0.1785 & 0.7916 & 0.0340 \\ -0.7415 & -0.2967 & 1.0456 & 0.1586 & 0.1314 & 1.0432 & 0.3897 & -0.3688 & -0.6143 & 0.1766 \\ -0.4006 & -0.5703 & 0.0161 & 0.8207 & 1.1073 & 1.0108 & 0.6197 & -0.5683 & -0.3330 & 0.5511 \end{bmatrix}$$

$$\mathbf{b}^{(1)} = \begin{bmatrix} 0.9228 & -0.0448 & 0.9684 & -0.6415 & -0.7833 & 0.3443 & -0.0358 & 0.1046 & -0.3144 & -0.2158 \end{bmatrix}$$

$$(\mathbf{w}^{(2)})^{\mathrm{T}} = \begin{bmatrix} -0.6977 & -1.4963 & 0.7168 & -0.0015 & 0.5500 & -0.6762 & 0.3854 & 0.9912 & -1.0978 & 0.1195 \end{bmatrix} \text{ and } b^{(2)} = 0.0222$$

$$\mu_c = 0.4514 \text{ and } \sigma_c = 0.4222$$

TABLE 96: As in Table 95 but for $a_{ys}(412)$.

$$\boldsymbol{\mu_I} = \begin{bmatrix} -3.1603 & -3.0312 & -2.8155 & -2.7409 & -2.6652 & -3.1614 \end{bmatrix}$$

$$\boldsymbol{\sigma_I} = \begin{bmatrix} 0.2588 & 0.1838 & 0.1592 & 0.1607 & 0.1756 & 0.2461 \end{bmatrix}$$

$$\mathbf{w}^{(1)} = \begin{bmatrix} 0.1930 & 0.0512 & -0.2556 & -0.8239 & 0.0496 & 0.1965 & 0.0057 & -0.3002 & 0.2949 & -0.6945 \\ 0.2555 & -0.0472 & 1.6211 & -0.3791 & -0.5096 & 0.0137 & 0.1360 & -0.0862 & -0.4906 & 0.0386 \\ 0.1090 & 0.3578 & 0.0186 & 0.0836 & 0.4915 & -0.7753 & 0.2159 & 0.3804 & 0.1159 & -0.0237 \\ -0.1516 & 0.2401 & 0.2633 & -0.2715 & -0.4062 & -0.5634 & 0.2294 & -0.1420 & 0.0483 & 0.2814 \\ 0.4679 & 0.4561 & -0.4512 & 0.6787 & -0.4913 & -0.5848 & 0.1587 & -0.2098 & -0.3168 & 0.1732 \\ 0.7253 & 0.1659 & 0.4558 & 0.6019 & 1.2424 & 0.5534 & -0.3175 & 0.6177 & 0.1593 & 0.1621 \end{bmatrix}$$

$$\mathbf{b}^{(1)} = \begin{bmatrix} -0.2005 & -0.7520 & -1.0067 & 0.6829 & -1.2008 & 0.5185 & 0.8796 & -0.0811 & -0.0332 & -0.4301 \end{bmatrix}$$

$$(\mathbf{w}^{(2)})^{\mathrm{T}} = \begin{bmatrix} -0.1821 & 0.3365 & -1.3546 & 0.5618 & 1.2330 & -0.8007 & -0.6774 & 0.6307 & 0.3340 & -0.5197 \end{bmatrix} \text{ and } b^{(2)} = 0.6044$$

$$\mu_c = \text{-}0.2714 \text{ and } \sigma_c = 0.1777$$

TABLE 97: As in Table 95 but for TSM.

$$\boldsymbol{\mu_I} = \begin{bmatrix} -3.1603 & -3.0312 & -2.8155 & -2.7409 & -2.6652 & -3.1614 \end{bmatrix}$$

$$\boldsymbol{\sigma_I} = \begin{bmatrix} 0.2588 & 0.1838 & 0.1592 & 0.1607 & 0.1756 & 0.2461 \end{bmatrix}$$

$$\mathbf{w}^{(1)} = \begin{bmatrix} 0.8799 & 0.1325 & -0.5160 & -0.0215 & 0.2843 & -0.3127 & -0.5551 & -0.8073 & 0.0662 & -1.0059 \\ -0.2668 & -0.2682 & 0.1474 & -0.2924 & -0.0348 & 0.1547 & -0.0387 & -1.1498 & 0.2483 & 0.6541 \\ 0.0785 & 0.6948 & 0.1295 & -0.0048 & 0.0278 & -0.5767 & 0.4874 & -0.0208 & 0.6581 & 1.1407 \\ -0.2297 & 0.5088 & 0.6512 & 1.0914 & -0.1142 & -0.4780 & 0.1861 & 0.4632 & 0.0435 & 0.7652 \\ 0.5106 & 0.5540 & 0.3643 & 0.4926 & 0.8779 & 0.3578 & 0.0392 & -0.5037 & -0.1467 & -0.1592 \\ -0.3760 & 0.3051 & -0.4916 & 0.8374 & 0.5455 & -0.6298 & -1.1947 & 0.1349 & 0.3192 & -0.3973 \end{bmatrix}$$

$$\mathbf{b}^{(1)} = \begin{bmatrix} -0.8074 & -0.2520 & -0.9229 & -0.3941 & 1.6435 & -0.4803 & 1.1183 & -0.4103 & 0.7893 & -0.2635 \end{bmatrix}$$

$$(\mathbf{w}^{(2)})^{\mathrm{T}} = \begin{bmatrix} -0.9541 & 0.3903 & 1.1452 & 0.5262 & 1.2554 & 0.8078 & -0.7953 & -1.1514 & -0.9843 & -1.1518 \end{bmatrix} \text{ and } b^{(2)} = 0.1440$$

$$\mu_c = 0.0513 \text{ and } \sigma_c = 0.3198$$

TABLE 98: As in Table 95 but for the center wavelengths of the SeaWiFS sensor (see Table. 2).

$$\boldsymbol{\mu_l} = \begin{bmatrix} -3.1603 & -3.0312 & -2.8155 & -2.7409 & -2.6652 & -3.1631 \end{bmatrix}$$

$$\boldsymbol{\sigma_l} = \begin{bmatrix} 0.2588 & 0.1838 & 0.1592 & 0.1607 & 0.1756 & 0.2456 \end{bmatrix}$$

$$\mathbf{w}^{(1)} = \begin{bmatrix} 0.1868 & -0.9093 & 0.2180 & -0.2896 & 1.1221 & 0.5478 & -0.7945 & 0.7704 & -1.2982 & 0.1917 \\ -0.1943 & -0.1472 & 1.0274 & -0.1184 & 1.5555 & -0.7311 & 0.0528 & 0.7405 & -0.3475 & 0.0059 \\ -0.2410 & 0.4158 & 0.3454 & 0.4016 & 1.0509 & -0.5352 & 0.6449 & 0.3121 & -0.5122 & 0.6875 \\ 0.4301 & 0.5858 & -0.0123 & -0.0461 & -0.5946 & -1.4172 & 0.5472 & -0.4534 & -0.7762 & 0.0233 \\ 0.7297 & 0.7958 & -0.1054 & 0.8327 & -0.2595 & 0.6515 & -1.0174 & -0.0358 & 0.3506 & -0.2278 \\ -0.1574 & 1.4517 & 0.3568 & 0.3412 & -0.7900 & 0.5216 & -0.7115 & 0.3328 & 0.5828 & -0.1058 \end{bmatrix}$$

$$\mathbf{b}^{(1)} = \begin{bmatrix} 0.7402 & -0.7872 & -0.4397 & -0.6580 & -0.1960 & 0.2127 & 1.6847 & -0.4372 & 0.5835 & 0.1073 \end{bmatrix}$$

$$(\mathbf{w}^{(2)})^{\mathrm{T}} = \begin{bmatrix} 0.9423 & 0.5984 & 0.5198 & -0.8234 & 1.2079 & 0.9650 & -0.7519 & 0.5487 & 1.2326 & -0.8612 \end{bmatrix} \text{ and } b^{(2)} = \text{-0.1091}$$

$$\mu_c = 0.4514 \text{ and } \sigma_c = 0.4222$$

TABLE 99: As in Table 98 but for $a_{ys}(412)$.

$$\boldsymbol{\mu_l} = \begin{bmatrix} -3.1603 & -3.0312 & -2.8155 & -2.7409 & -2.6652 & -3.1631 \end{bmatrix}$$

$$\boldsymbol{\sigma_l} = \begin{bmatrix} 0.2588 & 0.1838 & 0.1592 & 0.1607 & 0.1756 & 0.2456 \end{bmatrix}$$

$$\mathbf{w}^{(1)} = \begin{bmatrix} -0.3173 & 0.1763 & 0.0515 & 0.0415 & 0.8513 & 0.9058 & 0.1346 & -0.0645 & -0.3436 & -0.0355 \\ -0.2166 & 0.2109 & -0.2675 & -1.4491 & 0.0250 & -0.5095 & -0.2771 & 0.3483 & -0.0548 & -0.4939 \\ 0.3811 & 0.1517 & 0.6996 & -0.2879 & 0.3080 & 0.3107 & 0.3925 & -0.2735 & 0.3332 & -0.1352 \\ -0.1906 & -0.2383 & 0.7665 & -0.2580 & 0.1232 & -0.2816 & -0.3506 & 0.5576 & -0.3060 & -0.2607 \\ 0.4349 & 0.5113 & 0.4099 & 0.6057 & -0.6685 & -0.3681 & -0.4851 & 0.3009 & 0.0641 & 0.1868 \\ 0.2929 & -0.5119 & -0.4785 & -0.4781 & -0.5618 & -0.0864 & 0.0290 & -1.1621 & 0.6542 & 0.3910 \end{bmatrix}$$

$$\mathbf{b}^{(1)} = \begin{bmatrix} -0.4017 & 0.3960 & -0.5737 & 1.0658 & -0.7492 & 0.2209 & 0.1040 & 1.3030 & -0.3968 & -0.2167 \end{bmatrix}$$

$$(\mathbf{w}^{(2)})^{\mathrm{T}} = \begin{bmatrix} 0.4234 & -0.5069 & 1.0793 & 1.1492 & -0.7746 & 0.6952 & 0.7860 & -1.2056 & 0.5249 & -0.0356 \end{bmatrix} \text{ and } b^{(2)} = 0.5640$$

$$\mu_c = \text{-0.2714 and } \sigma_c = 0.1777$$

TABLE 100: As in Table 98 but for TSM.

$$\boldsymbol{\mu_l} = \begin{bmatrix} -3.1603 & -3.0312 & -2.8155 & -2.7409 & -2.6652 & -3.1631 \end{bmatrix}$$

$$\boldsymbol{\sigma_l} = \begin{bmatrix} 0.2588 & 0.1838 & 0.1592 & 0.1607 & 0.1756 & 0.2456 \end{bmatrix}$$

$$\mathbf{w}^{(1)} = \begin{bmatrix} 0.0375 & -0.8422 & 0.4576 & 0.2337 & -0.6487 & 0.1822 & -0.1194 & 0.2783 & 0.5292 & 1.8111 \\ 0.0712 & 0.9724 & 0.1175 & -0.4551 & -0.9626 & -0.6575 & -0.2390 & 0.5391 & -0.0368 & -0.4462 \\ -0.7088 & 0.9127 & -0.4352 & 0.0628 & -0.1094 & 0.5622 & 0.1012 & 0.1609 & 0.1796 & -0.5924 \\ -0.7871 & 0.1878 & -0.2647 & 0.0603 & 0.1910 & 0.7706 & 0.6325 & -0.1589 & 0.2085 & -0.1519 \\ 0.1616 & 0.5356 & -0.8239 & -0.6722 & 0.0098 & 0.7062 & 0.2734 & -0.2374 & 0.1685 & 1.0090 \\ 0.4577 & -0.3184 & 0.5522 & -0.2467 & -1.0250 & -0.7254 & 0.2531 & 1.2620 & 0.3423 & -0.0452 \end{bmatrix}$$

$$\mathbf{b}^{(1)} = \begin{bmatrix} 0.3309 & -1.0690 & 0.9159 & -0.9046 & 0.7153 & 0.4342 & -0.2024 & 0.5288 & 0.1879 & 0.4778 \end{bmatrix}$$

$$(\mathbf{w}^{(2)})^{\mathrm{T}} = \begin{bmatrix} 0.2315 & -1.1198 & -1.0767 & -1.0545 & -0.8662 & -1.1208 & 1.3661 & -0.9597 & -0.7248 & 1.2828 \end{bmatrix} \text{ and } b^{(2)} = 0.2117$$

$$\mu_c = 0.0513 \text{ and } \sigma_c = 0.3198$$

TABLE 101: As in Table 95 but for the center wavelengths of the MODIS sensor (see Table. 2).

$$\boldsymbol{\mu_l} = \begin{bmatrix} -3.1603 & -3.0312 & -2.8371 & -2.6176 & -2.7025 & -3.1614 \end{bmatrix}$$

$$\boldsymbol{\sigma_l} = \begin{bmatrix} 0.2588 & 0.1838 & 0.1614 & 0.1558 & 0.1751 & 0.2461 \end{bmatrix}$$

$$\mathbf{w}^{(1)} = \begin{bmatrix} -1.0999 & 0.0018 & -1.1860 & 0.2371 & 0.5948 & 0.6337 & -0.5774 & -0.7164 & -0.7737 & -0.4759 \\ 0.4052 & -0.1184 & -1.3795 & 0.0345 & -0.4129 & 0.5126 & -0.1083 & -0.1091 & -0.2941 & 1.5085 \\ 1.1483 & 0.3994 & -0.5272 & 0.4435 & -1.1047 & -0.5173 & 0.6019 & -0.2984 & -0.0982 & 0.7337 \\ -0.7579 & -0.1544 & 0.3897 & 0.0809 & -0.0793 & 0.5126 & 0.6920 & 0.8392 & -0.0870 & 0.5022 \\ -0.2998 & -0.1955 & 0.4281 & 0.8574 & -0.0041 & 0.1987 & 0.3110 & -0.0671 & 0.1721 & 0.3166 \\ 0.2345 & -0.4634 & 0.4958 & -0.6631 & 0.0217 & 1.0711 & 0.2831 & -0.0981 & -0.0959 & -0.9268 \end{bmatrix}$$

$$\mathbf{b}^{(1)} = \begin{bmatrix} -0.1572 & 0.7094 & 0.0344 & 0.2440 & 0.7260 & -1.2103 & 0.5018 & 0.2590 & 0.1194 & -0.5805 \end{bmatrix}$$

$$(\mathbf{w}^{(2)})^{\mathrm{T}} = \begin{bmatrix} -1.0145 & -0.4486 & -0.8979 & -0.9070 & 0.6738 & 0.7729 & 0.8038 & 1.0811 & -0.0765 & -0.7864 \end{bmatrix} \text{ and } b^{(2)} = \text{-0.3863}$$

$$\mu_c = 0.4514 \text{ and } \sigma_c = 0.4222$$

TABLE 102: As in Table 101 but for $a_{ys}(412)$.

$$\boldsymbol{\mu_l} = \begin{bmatrix} -3.1603 & -3.0312 & -2.8371 & -2.6176 & -2.7025 & -3.1614 \end{bmatrix}$$

$$\boldsymbol{\sigma_l} = \begin{bmatrix} 0.2588 & 0.1838 & 0.1614 & 0.1558 & 0.1751 & 0.2461 \end{bmatrix}$$

$$\mathbf{w}^{(1)} = \begin{bmatrix} -0.6684 & -0.2755 & -0.3662 & -0.5814 & 0.0968 & -0.0143 & 0.1459 & 0.0251 & 0.0019 & -0.4653 \\ 0.2465 & -0.4216 & 1.9607 & 0.1125 & 0.6207 & 0.2419 & -0.3652 & -0.2421 & 0.1049 & -1.0810 \\ 0.5871 & -1.3328 & -0.0262 & -0.7090 & 0.6192 & 0.1661 & -0.1383 & 0.1087 & 0.5541 & 0.0260 \\ 0.1583 & 0.1669 & -0.3160 & 0.3005 & 0.3326 & 0.9978 & 0.3305 & -0.5614 & 0.4472 & 0.4950 \\ 0.1725 & 0.3825 & -0.0740 & -0.8965 & -0.0471 & 0.2257 & -0.6488 & -0.2089 & 0.2740 & 0.3184 \\ 0.1801 & -0.1678 & 0.4143 & -0.1952 & 0.3902 & -0.4408 & 0.8651 & 1.1856 & -0.2717 & 0.7425 \end{bmatrix}$$

$$\mathbf{b}^{(1)} = \begin{bmatrix} -0.4502 & 0.1600 & -0.8898 & -0.4737 & 0.3574 & -0.5849 & -0.7296 & -1.2944 & -0.5112 & 0.6868 \end{bmatrix}$$

$$(\mathbf{w}^{(2)})^{\mathrm{T}} = \begin{bmatrix} -0.1280 & 0.3332 & -1.4321 & 0.7998 & 0.7155 & 0.7469 & 1.0271 & 0.9410 & 0.5959 & 0.6273 \end{bmatrix} \text{ and } b^{(2)} = 0.7583$$

$$\mu_c = \text{-0.2714 and } \sigma_c = 0.1777$$

TABLE 103: As in Table 101 but for TSM.

$$\boldsymbol{\mu_l} = \begin{bmatrix} -3.1603 & -3.0312 & -2.8371 & -2.6176 & -2.7025 & -3.1614 \end{bmatrix}$$

$$\boldsymbol{\sigma_l} = \begin{bmatrix} 0.2588 & 0.1838 & 0.1614 & 0.1558 & 0.1751 & 0.2461 \end{bmatrix}$$

$$\mathbf{w}^{(1)} = \begin{bmatrix} -0.2055 & -0.4678 & 0.8230 & -0.3262 & -0.0125 & 0.3435 & -1.1050 & 0.6805 & -0.6848 & 0.5439 \\ 0.4139 & 0.8167 & -0.5640 & -0.0111 & -0.6443 & -0.0835 & 0.3802 & 1.0988 & 0.3598 & -0.4910 \\ -1.3477 & 0.4165 & -0.7831 & -0.0223 & 0.0001 & 0.3763 & 0.3080 & -0.9137 & -0.3495 & -0.0489 \\ 0.0333 & 0.1758 & -0.1877 & 0.3117 & 1.1698 & -0.7578 & -0.5076 & 0.1636 & 0.4568 & 0.2367 \\ -0.2383 & 0.4768 & -0.6637 & -0.2502 & 0.5305 & -0.7199 & -0.1861 & -0.8471 & -0.0861 & 0.3859 \\ -0.0848 & 0.0308 & 0.5542 & -0.0919 & 0.1125 & 0.5122 & -0.0031 & 1.3408 & -0.1794 & 0.3139 \end{bmatrix}$$

$$\mathbf{b}^{(1)} = \begin{bmatrix} -0.7963 & -1.1903 & 0.1412 & 0.3728 & -0.4604 & 0.5292 & -0.4910 & -1.2150 & 0.6195 & 0.9351 \end{bmatrix}$$

$$(\mathbf{w}^{(2)})^{\mathrm{T}} = \begin{bmatrix} 0.8153 & -0.9288 & 0.8387 & 0.5211 & 0.9663 & -1.2140 & -0.9457 & 1.2807 & 1.0115 & 0.7433 \end{bmatrix} \text{ and } b^{(2)} = \text{-0.1370}$$

$$\mu_c = 0.0513 \text{ and } \sigma_c = 0.3198$$

TABLE 104: As in Table 95 but for the center wavelengths of the MERIS sensor (see Table. 2).

$$\boldsymbol{\mu_l} = \begin{bmatrix} -3.1603 & -3.0312 & -2.8155 & -2.7409 & -2.6463 & -3.1614 \end{bmatrix}$$

$$\boldsymbol{\sigma_l} = \begin{bmatrix} 0.2588 & 0.1838 & 0.1592 & 0.1607 & 0.1759 & 0.2461 \end{bmatrix}$$

$$\mathbf{w}^{(1)} = \begin{bmatrix} -0.7072 & -0.2204 & 0.9090 & 0.3643 & -1.4705 & 0.0090 & 0.1030 & -0.6208 & 0.2619 & 0.1655 \\ -0.0753 & 0.2378 & 1.5443 & 0.6680 & 0.5713 & -0.0077 & -0.0471 & 0.1630 & -0.5746 & 0.3792 \\ 0.7791 & -0.2971 & 0.6546 & 0.3460 & 0.5344 & 0.3378 & -0.1154 & 0.3745 & -0.9493 & 0.0325 \\ 0.6311 & -0.8868 & -0.0850 & 0.3413 & 0.4146 & 0.2358 & -0.1743 & 0.5854 & -1.2518 & -0.0784 \\ 0.4200 & 0.3335 & -0.3470 & -0.0486 & -0.6309 & 0.4759 & -0.7051 & -1.0131 & 0.1823 & 0.3971 \\ 0.3617 & 0.2524 & -0.7843 & 1.2379 & 0.3234 & 0.5330 & -0.1382 & -0.7602 & 0.8294 & 0.6521 \end{bmatrix}$$

$$\mathbf{b}^{(1)} = \begin{bmatrix} 0.2944 & -0.1026 & 0.0862 & -0.8597 & -0.1240 & -0.0209 & -0.9468 & 1.4278 & 0.4159 & -0.5515 \end{bmatrix}$$

$$(\mathbf{w}^{(2)})^{\mathrm{T}} = \begin{bmatrix} 0.5877 & 1.4647 & 0.8927 & 0.7731 & -0.3996 & -0.6302 & -0.8200 & -0.6686 & 0.9682 & -0.1651 \end{bmatrix} \text{ and } b^{(2)} = \text{-0.0951}$$

$\mu_c = 0.4514$ and $\sigma_c = 0.4222$

TABLE 105: As in Table 104 but for $a_{ys}(412)$.

$$\boldsymbol{\mu_l} = \begin{bmatrix} -3.1603 & -3.0312 & -2.8155 & -2.7409 & -2.6463 & -3.1614 \end{bmatrix}$$

$$\boldsymbol{\sigma_l} = \begin{bmatrix} 0.2588 & 0.1838 & 0.1592 & 0.1607 & 0.1759 & 0.2461 \end{bmatrix}$$

$$\mathbf{w}^{(1)} = \begin{bmatrix} -0.1857 & -0.4094 & 0.1750 & -0.1390 & 0.2209 & 0.2343 & 0.8843 & -0.1423 & -0.2903 & -0.3695 \\ 0.2368 & 0.2147 & 0.5541 & 0.5134 & -0.2070 & 1.1400 & 0.0086 & 0.2262 & 0.4242 & 0.4253 \\ -0.7331 & -0.0208 & -0.9763 & -0.8208 & 0.3245 & 0.4250 & -0.5372 & -0.4318 & -0.1319 & 0.1158 \\ -0.4191 & -0.4317 & -0.1000 & -0.0248 & -0.0333 & 0.2176 & -0.3299 & 0.4322 & 0.1290 & 0.1623 \\ -0.6067 & 0.8939 & 0.0970 & -0.1241 & -0.4318 & -0.4004 & 0.3556 & 0.4827 & 0.3508 & 0.2153 \\ 0.5767 & 0.2848 & 0.2073 & -0.2469 & -0.1212 & 0.2937 & 0.6879 & -1.0188 & -0.4646 & -0.5677 \end{bmatrix}$$

$$\mathbf{b}^{(1)} = \begin{bmatrix} 0.5364 & 0.2169 & 0.0405 & -0.6921 & -0.1090 & -1.1226 & -0.3605 & 0.8051 & 0.2126 & 0.7301 \end{bmatrix}$$

$$(\mathbf{w}^{(2)})^{\mathrm{T}} = \begin{bmatrix} -1.0357 & 0.8119 & -0.1699 & 0.6091 & -0.2334 & -1.1913 & -0.6154 & -1.2203 & -0.8043 & -0.9919 \end{bmatrix} \text{ and } b^{(2)} = 1.1131$$

$\mu_c = \text{-0.2714}$ and $\sigma_c = 0.1777$

TABLE 106: As in Table 104 but for TSM.

$$\boldsymbol{\mu_l} = \begin{bmatrix} -3.1603 & -3.0312 & -2.8155 & -2.7409 & -2.6463 & -3.1614 \end{bmatrix}$$

$$\boldsymbol{\sigma_l} = \begin{bmatrix} 0.2588 & 0.1838 & 0.1592 & 0.1607 & 0.1759 & 0.2461 \end{bmatrix}$$

$$\mathbf{w}^{(1)} = \begin{bmatrix} -0.2578 & 0.0494 & -0.2704 & 0.9695 & 0.6953 & 0.3961 & -0.0733 & -0.0259 & 0.1877 & -0.7190 \\ 0.4994 & -0.0518 & 0.0518 & -0.5054 & 1.3984 & -0.1293 & -0.2548 & -0.6572 & -0.1098 & 0.3341 \\ -0.2831 & 0.6544 & -0.1280 & -0.1760 & -0.2860 & 0.1042 & -0.1665 & -0.6461 & -0.1713 & 0.9656 \\ 0.3232 & 0.1779 & 0.4426 & 0.5359 & -0.2190 & -0.2430 & -0.2918 & 0.1677 & 0.7338 & 1.0954 \\ 0.6289 & -0.2556 & 0.0721 & -0.0899 & 0.4702 & 0.3711 & -0.3588 & 0.3165 & 0.5960 & -0.1547 \\ 0.3153 & 0.7193 & 0.2371 & -0.2979 & -0.0862 & 0.0222 & 0.2878 & -1.0786 & 0.5394 & -0.5779 \end{bmatrix}$$

$$\mathbf{b}^{(1)} = \begin{bmatrix} 0.9996 & -0.0096 & -0.8905 & -0.9013 & 0.4014 & 0.0729 & -0.2236 & -0.8338 & -0.3438 & 0.0012 \end{bmatrix}$$

$$(\mathbf{w}^{(2)})^{\mathrm{T}} = \begin{bmatrix} 1.2370 & -0.2074 & 1.0472 & -0.7250 & 1.0860 & 0.6968 & 0.4282 & 1.1751 & 0.7273 & -1.0470 \end{bmatrix} \text{ and } b^{(2)} = \text{-0.1196}$$

$\mu_c = 0.0513$ and $\sigma_c = 0.3198$

3.9 BiOMaP

Results of this section are derived by jointly considering the entire set of BiOMaP data (Figure 19(a)). The MLP architecture selected on the basis of trends shown in Panels 19(b)–19(d) has ten hidden units. Validation details (Figure 20 and Table 107) show uncertainties in some cases higher than those observed in the previous basin-specific analyses.

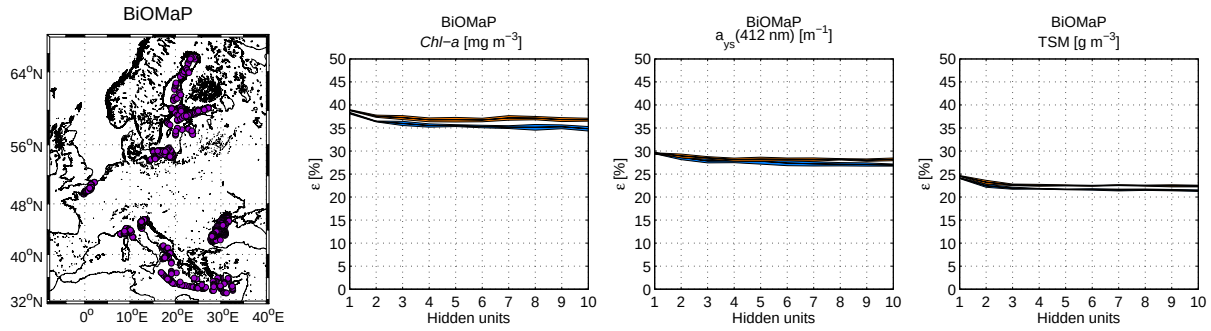

(a) (b) (c) (d)

FIGURE 19: As in Figure 3, but for the BiOMaP data ensemble.

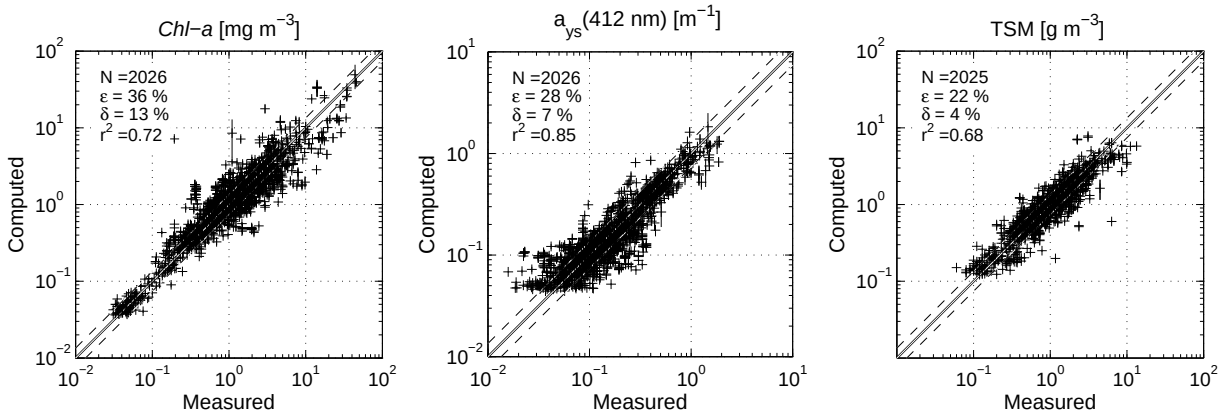

(a) (b) (c)

FIGURE 20: As in Figure 4, but for the BiOMaP data ensemble. Results based on the MLP with ten units in the hidden layer.

TABLE 107: As in Table 3, but for the BiOMaP data ensemble. Results based on the MLP with ten units in the hidden layer.

	N	ϵ [%]	δ [%]	r^2
Chl-a	2026	36.6(35.0)	12.2(10.4)	65.1(77.0)
$a_{ys}(412)$	2026	28.3(26.9)	7.4(6.0)	81.9(88.2)
TSM	2025	22.5(21.3)	3.8(4.0)	68.2(80.2)

TABLE 108: Parameter sets to compute data pre- and post-processing, as well as MLP weights to derive *Chl-a* values from the ensemble of BiOMaP data. Input R_{RS} wavelengths are those of the in-situ measurements (see Table. 2).

$$\boldsymbol{\mu_l} = \begin{bmatrix} -2.5403 & -2.4745 & -2.3595 & -2.3615 & -2.4037 & -3.1563 \end{bmatrix}$$

$$\boldsymbol{\sigma_l} = \begin{bmatrix} 0.3593 & 0.3241 & 0.2719 & 0.2479 & 0.2525 & 0.3261 \end{bmatrix}$$

$$\mathbf{w}^{(1)} = \begin{bmatrix} -0.0279 & 0.0611 & -0.2328 & -0.4924 & -0.4391 & 0.7419 & 0.3623 & 0.5212 & 0.2583 & 0.2317 \\ -0.2120 & 0.1132 & 0.3102 & 0.2467 & -0.5775 & -0.6760 & -0.2664 & -1.2009 & 0.8307 & 0.0966 \\ -0.1585 & -0.2859 & -0.0273 & 0.4421 & 0.2078 & -0.0502 & 0.6433 & 0.3362 & 0.0821 & 0.5006 \\ -0.1785 & 0.2197 & 0.0666 & -0.1310 & -0.8315 & -0.7425 & 0.2242 & -0.0203 & -0.0185 & -0.2533 \\ 0.3505 & 0.3476 & 0.3562 & -0.2888 & -0.1646 & -0.2453 & 0.5885 & -0.2510 & -0.4173 & -0.2671 \\ 0.5125 & 0.1725 & -0.1269 & -0.2036 & -0.6752 & 0.2899 & -0.3724 & 0.1588 & -0.0955 & 0.9892 \end{bmatrix}$$

$$\mathbf{b}^{(1)} = \begin{bmatrix} -1.1681 & 0.8610 & 0.6547 & -0.3884 & -0.2981 & -0.8913 & 0.3377 & 0.4050 & -1.5516 & 0.3314 \end{bmatrix}$$

$$(\mathbf{w}^{(2)})^{\mathrm{T}} = \begin{bmatrix} 0.9014 & 0.3209 & 0.2997 & -0.4214 & 0.3679 & 1.2693 & 0.9067 & 0.9547 & -0.9281 & 0.4830 \end{bmatrix} \text{ and } b^{(2)} = \text{-0.4645}$$

$$\mu_c = \text{0.0036 and } \sigma_c = 0.5210$$

TABLE 109: As in Table 108 but for $a_{ys}(412)$.

$$\boldsymbol{\mu_l} = \begin{bmatrix} -2.5403 & -2.4745 & -2.3595 & -2.3615 & -2.4037 & -3.1563 \end{bmatrix}$$

$$\boldsymbol{\sigma_l} = \begin{bmatrix} 0.3593 & 0.3241 & 0.2719 & 0.2479 & 0.2525 & 0.3261 \end{bmatrix}$$

$$\mathbf{w}^{(1)} = \begin{bmatrix} 0.4304 & 0.4065 & 0.0555 & 0.2197 & -1.1300 & 0.3191 & 0.5756 & -0.2993 & 0.3478 & 0.7213 \\ -0.2360 & 0.1492 & 0.0172 & -0.5776 & 0.6294 & 0.0131 & 0.3772 & 1.0398 & -0.7630 & -0.0102 \\ 0.2660 & -0.6472 & 0.2544 & -0.3795 & 0.3166 & 0.0372 & -0.1602 & -0.4500 & -0.2571 & 0.0358 \\ 0.1624 & 0.5831 & -0.1946 & -0.2295 & -1.0181 & 0.3116 & 0.0414 & 0.1313 & 0.1591 & -0.4038 \\ 0.5756 & 0.8049 & -0.0187 & 0.4452 & 0.7925 & 0.1905 & 0.5266 & 0.3129 & -0.2756 & 0.2984 \\ -0.4559 & -0.2649 & 0.4982 & 0.7215 & 0.2562 & 0.0916 & -0.3111 & 0.4633 & 0.7209 & -0.2320 \end{bmatrix}$$

$$\mathbf{b}^{(1)} = \begin{bmatrix} -0.6071 & 0.3596 & -0.0769 & 0.3963 & 0.2620 & -0.2011 & -0.4806 & -0.5190 & -1.8838 & 0.2743 \end{bmatrix}$$

$$(\mathbf{w}^{(2)})^{\mathrm{T}} = \begin{bmatrix} -0.1954 & -0.1662 & -0.2599 & -0.7822 & 1.7944 & -0.4391 & 0.2504 & 0.6312 & 1.3676 & -0.2452 \end{bmatrix} \text{ and } b^{(2)} = 1.2818$$

$$\mu_c = \text{-0.8057 and } \sigma_c = 0.3564$$

TABLE 110: As in Table 108 but for TSM.

$$\boldsymbol{\mu_l} = \begin{bmatrix} -2.5404 & -2.4745 & -2.3595 & -2.3614 & -2.4035 & -3.1560 \end{bmatrix}$$

$$\boldsymbol{\sigma_l} = \begin{bmatrix} 0.3594 & 0.3242 & 0.2720 & 0.2480 & 0.2524 & 0.3258 \end{bmatrix}$$

$$\mathbf{w}^{(1)} = \begin{bmatrix} 0.6390 & -0.0273 & -0.2412 & -0.2976 & 0.6994 & -0.4537 & -0.5120 & -0.5319 & -0.6078 & 0.3328 \\ -0.6666 & 0.0824 & -0.7753 & 0.2751 & -0.0017 & 0.2482 & 0.4161 & 0.7394 & 0.0904 & -0.0921 \\ -0.0959 & 0.1107 & -0.4213 & -0.0508 & -0.2324 & -0.2920 & -0.0434 & -0.0590 & 0.1559 & 0.1398 \\ -0.3026 & 0.1148 & -0.3164 & -0.3171 & -0.5334 & 0.3099 & -0.2069 & 0.0054 & -0.0199 & -0.4937 \\ -0.1055 & -0.3796 & -0.1448 & 0.0951 & 0.6140 & -0.3382 & -0.0424 & -0.5344 & 0.5182 & 0.1010 \\ -0.6134 & 0.1260 & 0.3031 & 0.7406 & 0.5391 & 0.1952 & 0.0709 & 0.0163 & -0.1095 & 0.5748 \end{bmatrix}$$

$$\mathbf{b}^{(1)} = \begin{bmatrix} 0.0846 & -0.0408 & -0.5371 & -1.3595 & 0.1803 & 0.1769 & 0.2192 & -0.7827 & 1.3126 & -0.1033 \end{bmatrix}$$

$$(\mathbf{w}^{(2)})^{\mathrm{T}} = \begin{bmatrix} 0.5924 & -0.5680 & -0.2894 & 1.3096 & 0.7996 & 0.6485 & 0.4277 & -0.7697 & 0.8240 & 0.4850 \end{bmatrix} \text{ and } b^{(2)} = \text{-0.5050}$$

$$\mu_c = \text{-0.0299 and } \sigma_c = 0.3367$$

TABLE 111: As in Table 108 but for the center wavelengths of the SeaWiFS sensor (see Table. 2).

$$\boldsymbol{\mu_l} = \begin{bmatrix} -2.5403 & -2.4745 & -2.3595 & -2.3615 & -2.4037 & -3.1572 \end{bmatrix}$$

$$\boldsymbol{\sigma_l} = \begin{bmatrix} 0.3593 & 0.3241 & 0.2719 & 0.2479 & 0.2525 & 0.3257 \end{bmatrix}$$

$$\mathbf{w}^{(1)} = \begin{bmatrix} 0.0491 & 0.4866 & -0.1683 & -0.2845 & -0.1405 & -0.3640 & 0.4330 & 0.7380 & -0.9847 & 0.6849 \\ -1.0094 & -0.2117 & 0.2513 & -0.2560 & -0.3130 & 0.5929 & -0.7773 & -0.3810 & -0.5642 & -1.1973 \\ -0.2889 & -0.7294 & 0.1505 & -0.0667 & -0.3592 & 0.3756 & -0.6689 & 0.1486 & 0.2936 & 0.2540 \\ -0.2673 & -0.3945 & -0.5053 & -0.0339 & 0.2045 & -0.1675 & -0.3317 & -0.2066 & 0.4203 & -0.1947 \\ 0.1806 & -0.1329 & 0.3837 & -0.0772 & -0.1808 & 0.7180 & -0.2541 & 0.0108 & -0.5290 & 0.3108 \\ 0.4106 & 0.5881 & 0.2581 & 0.0748 & 0.1797 & 0.3315 & -0.5502 & 0.3632 & -0.6018 & -0.0274 \end{bmatrix}$$

$$\mathbf{b}^{(1)} = \begin{bmatrix} -0.3129 & -0.8323 & -0.2775 & 0.4532 & 0.6028 & -0.1353 & 0.8519 & -0.0890 & 0.5780 & 0.3782 \end{bmatrix}$$

$$(\mathbf{w}^{(2)})^{\mathrm{T}} = \begin{bmatrix} -0.6586 & 0.9122 & 0.9960 & 0.4480 & 0.4968 & -0.0864 & -0.6728 & 1.2672 & 0.9472 & 1.5078 \end{bmatrix} \text{ and } b^{(2)} = \text{-0.2219}$$

$$\mu_c = \text{0.0036 and } \sigma_c = 0.5210$$

TABLE 112: As in Table 111 but for $a_{ys}(412)$.

$$\boldsymbol{\mu_l} = \begin{bmatrix} -2.5403 & -2.4745 & -2.3595 & -2.3615 & -2.4037 & -3.1572 \end{bmatrix}$$

$$\boldsymbol{\sigma_l} = \begin{bmatrix} 0.3593 & 0.3241 & 0.2719 & 0.2479 & 0.2525 & 0.3257 \end{bmatrix}$$

$$\mathbf{w}^{(1)} = \begin{bmatrix} -0.7031 & -0.5495 & 0.0489 & -1.1762 & -0.1627 & 0.0014 & 0.1203 & 0.3149 & 0.1549 & 0.9224 \\ 0.2324 & -0.1517 & -0.4348 & 0.7679 & 0.0522 & -0.4161 & -0.4269 & -0.4578 & -0.1338 & -0.3955 \\ 0.2862 & -0.5360 & 0.4926 & -0.0717 & -0.2656 & -0.0882 & -0.3683 & -0.4919 & 0.1031 & -0.3892 \\ 0.7141 & -0.0649 & 0.8300 & -0.7666 & -0.0199 & 0.3989 & -0.0994 & 0.0481 & 0.2059 & 0.4603 \\ 0.2315 & -0.3480 & -0.1430 & 0.4888 & -0.4964 & -0.4761 & 0.1260 & -0.2294 & 0.3208 & -0.4549 \\ 0.2579 & -0.5541 & 0.0752 & 0.5426 & -0.1882 & -0.3119 & 0.8793 & 0.7436 & 0.3557 & -0.2796 \end{bmatrix}$$

$$\mathbf{b}^{(1)} = \begin{bmatrix} 0.1900 & -0.1534 & 0.0969 & 0.2964 & -0.5899 & 0.5090 & 0.4384 & -1.8790 & -0.2030 & -0.3546 \end{bmatrix}$$

$$(\mathbf{w}^{(2)})^{\mathrm{T}} = \begin{bmatrix} 0.3805 & -0.0865 & -0.5242 & 1.2402 & 0.5671 & -0.3471 & -1.0328 & 1.2903 & 0.0030 & -0.8292 \end{bmatrix} \text{ and } b^{(2)} = 1.2762$$

$$\mu_c = \text{-0.8057 and } \sigma_c = 0.3564$$

TABLE 113: As in Table 111 but for TSM.

$$\boldsymbol{\mu_l} = \begin{bmatrix} -2.5404 & -2.4745 & -2.3595 & -2.3614 & -2.4035 & -3.1569 \end{bmatrix}$$

$$\boldsymbol{\sigma_l} = \begin{bmatrix} 0.3594 & 0.3242 & 0.2720 & 0.2480 & 0.2524 & 0.3254 \end{bmatrix}$$

$$\mathbf{w}^{(1)} = \begin{bmatrix} 0.0782 & 0.4709 & 0.3544 & 0.4321 & 0.6549 & -0.0352 & 0.1509 & -0.0085 & -0.9334 & -0.5372 \\ 0.7908 & 0.1811 & 0.4918 & 0.4260 & -0.5453 & 0.0335 & -0.4629 & -0.0411 & -0.1627 & -0.6687 \\ -0.1506 & -0.0703 & -0.4881 & -0.2781 & -0.0311 & -0.0516 & -0.2081 & -0.1080 & 0.3158 & 0.7620 \\ -0.4915 & -0.3747 & -0.4674 & 0.0639 & -0.4837 & 0.3698 & 0.2967 & -0.3986 & 0.3296 & -0.0335 \\ -0.4500 & -0.0092 & 0.2218 & -0.3886 & 0.6845 & -0.8732 & 0.1736 & 0.5924 & -0.1345 & 0.8327 \\ 0.9036 & -0.1164 & 0.7129 & -0.2751 & 0.1496 & 0.2441 & -0.0540 & 0.2522 & -0.4104 & -0.0000 \end{bmatrix}$$

$$\mathbf{b}^{(1)} = \begin{bmatrix} -0.8505 & -1.4494 & -0.3791 & 1.4502 & 0.3755 & -0.4971 & 0.5080 & -0.2105 & 0.7306 & -0.1028 \end{bmatrix}$$

$$(\mathbf{w}^{(2)})^{\mathrm{T}} = \begin{bmatrix} 1.0730 & -0.6018 & 0.2790 & -1.1153 & 1.0089 & -0.8104 & 0.4755 & 0.1530 & 0.5690 & -0.4202 \end{bmatrix} \text{ and } b^{(2)} = 0.0206$$

$$\mu_c = \text{-0.0299 and } \sigma_c = 0.3367$$

TABLE 114: As in Table 108 but for the center wavelengths of the MODIS sensor (see Table. 2).

$$\boldsymbol{\mu_l} = \begin{bmatrix} -2.5403 & -2.4745 & -2.3744 & -2.2809 & -2.4267 & -3.1563 \end{bmatrix}$$

$$\boldsymbol{\sigma_l} = \begin{bmatrix} 0.3593 & 0.3241 & 0.2756 & 0.2333 & 0.2537 & 0.3261 \end{bmatrix}$$

$$\mathbf{w}^{(1)} = \begin{bmatrix} 0.0347 & 0.1613 & -0.4990 & 0.5887 & -0.1537 & 0.1261 & 0.5574 & 0.0513 & -0.0407 & 0.7002 \\ -0.8378 & -0.0019 & 0.3261 & -0.4613 & 0.0563 & -0.0332 & -0.0353 & -1.0463 & 0.1909 & -0.4554 \\ -0.1364 & -0.1936 & 0.4005 & -0.3470 & -0.0140 & 0.4832 & -0.1249 & -0.3254 & 0.0107 & 0.3789 \\ 0.5226 & -0.3810 & -0.1093 & 0.2929 & -0.4773 & -0.2472 & -0.0643 & 0.8257 & -0.3998 & 0.2462 \\ 0.0103 & -0.2462 & 0.0523 & -0.3829 & -0.8642 & -0.3297 & 0.3042 & 0.0011 & 0.0271 & -0.1402 \\ -0.7108 & 0.3262 & -0.1599 & 0.5753 & -0.3017 & -0.2092 & 0.2179 & -0.2204 & -0.1630 & 0.4709 \end{bmatrix}$$

$$\mathbf{b}^{(1)} = \begin{bmatrix} 0.2722 & -0.8881 & -0.1767 & -0.4859 & -0.2977 & 0.4622 & 0.2034 & 1.1366 & -0.0700 & 0.2567 \end{bmatrix}$$

$$(\mathbf{w}^{(2)})^{\mathrm{T}} = \begin{bmatrix} 0.6497 & 0.7509 & -0.1783 & 1.0605 & 0.3542 & -0.5978 & 0.2642 & 1.3622 & -0.8507 & 0.7048 \end{bmatrix} \text{ and } b^{(2)} = \text{-0.1939}$$

$$\mu_c = 0.0036 \text{ and } \sigma_c = 0.5210$$

TABLE 115: As in Table 114 but for $a_{ys}(412)$.

$$\boldsymbol{\mu_l} = \begin{bmatrix} -2.5403 & -2.4745 & -2.3744 & -2.2809 & -2.4267 & -3.1563 \end{bmatrix}$$

$$\boldsymbol{\sigma_l} = \begin{bmatrix} 0.3593 & 0.3241 & 0.2756 & 0.2333 & 0.2537 & 0.3261 \end{bmatrix}$$

$$\mathbf{w}^{(1)} = \begin{bmatrix} 0.8249 & -0.3216 & 0.1204 & 0.3124 & -0.4696 & -0.1878 & 0.3423 & 0.2131 & -0.6949 & 0.0698 \\ -0.4297 & 0.6563 & -0.0835 & 0.2391 & 0.1597 & 0.2333 & -0.1735 & -0.2020 & 0.2692 & -0.0579 \\ -0.0768 & -0.4757 & -0.3721 & -0.9317 & -0.5317 & -1.1310 & 0.4423 & -0.0338 & 0.3933 & 0.0786 \\ -1.1809 & -0.3450 & -0.4017 & 0.6288 & 0.3529 & 0.0965 & -0.5816 & -0.0335 & -0.2824 & -0.1143 \\ 0.3547 & 0.0881 & -0.0882 & -0.4716 & 0.1346 & 0.8640 & 0.3793 & 0.6102 & 0.4896 & 0.3529 \\ 0.9310 & 0.3648 & -0.2386 & 0.2923 & 0.1897 & 0.0364 & -0.3939 & -0.3458 & 0.7943 & -0.2225 \end{bmatrix}$$

$$\mathbf{b}^{(1)} = \begin{bmatrix} 0.3845 & -0.1208 & -0.2933 & 0.0158 & 0.2129 & -0.3418 & -0.8361 & 0.3513 & -1.0418 & 0.0301 \end{bmatrix}$$

$$(\mathbf{w}^{(2)})^{\mathrm{T}} = \begin{bmatrix} -1.6256 & 0.3887 & 0.0234 & 1.2775 & 1.0322 & 1.1401 & -0.8459 & -0.4797 & 0.2945 & -0.3146 \end{bmatrix} \text{ and } b^{(2)} = 0.2917$$

$$\mu_c = \text{-0.8057 and } \sigma_c = 0.3564$$

TABLE 116: As in Table 114 but for TSM.

$$\boldsymbol{\mu_l} = \begin{bmatrix} -2.5404 & -2.4745 & -2.3744 & -2.2808 & -2.4266 & -3.1560 \end{bmatrix}$$

$$\boldsymbol{\sigma_l} = \begin{bmatrix} 0.3594 & 0.3242 & 0.2756 & 0.2333 & 0.2536 & 0.3258 \end{bmatrix}$$

$$\mathbf{w}^{(1)} = \begin{bmatrix} -0.7499 & 0.2611 & 0.2025 & 0.6948 & -0.2992 & -0.1413 & -0.4742 & -0.8663 & -0.1199 & 0.4977 \\ -0.5696 & -0.2502 & -0.2683 & 0.3902 & -0.6933 & 0.3773 & -0.2608 & 0.0455 & 0.3290 & -0.4868 \\ -0.3625 & 0.0540 & 0.0662 & -0.9074 & -0.4091 & 0.2794 & -0.3712 & -0.1893 & 0.0284 & 0.4693 \\ 0.0981 & -0.1045 & -0.2987 & 0.3343 & 0.3660 & -0.1538 & 0.0520 & -0.3559 & 0.0978 & -0.3834 \\ -0.3906 & -0.3956 & 0.0319 & -0.3594 & -0.2478 & -0.2912 & 0.5335 & 0.1220 & -0.4260 & 0.0302 \\ -0.0740 & -0.2359 & 0.6953 & -0.2819 & 0.8622 & -0.1962 & 0.7371 & -0.2475 & -0.0044 & -0.1748 \end{bmatrix}$$

$$\mathbf{b}^{(1)} = \begin{bmatrix} -0.1912 & -1.0349 & -0.8925 & -0.2119 & -0.0021 & -0.2566 & -0.3721 & 0.4753 & -0.4773 & -0.2791 \end{bmatrix}$$

$$(\mathbf{w}^{(2)})^{\mathrm{T}} = \begin{bmatrix} -0.2244 & -0.5682 & 1.5556 & 0.7081 & -0.1245 & -0.9812 & -0.0258 & 0.3222 & -0.8491 & -0.6553 \end{bmatrix} \text{ and } b^{(2)} = \text{-0.1664}$$

$$\mu_c = \text{-0.0299 and } \sigma_c = 0.3367$$

TABLE 117: As in Table 108 but for the center wavelengths of the MERIS sensor (see Table. 2).

$$\boldsymbol{\mu_l} = \begin{bmatrix} -2.5403 & -2.4745 & -2.3595 & -2.3615 & -2.3925 & -3.1563 \end{bmatrix}$$

$$\boldsymbol{\sigma_l} = \begin{bmatrix} 0.3593 & 0.3241 & 0.2719 & 0.2479 & 0.2521 & 0.3261 \end{bmatrix}$$

$$\mathbf{w}^{(1)} = \begin{bmatrix} 0.1716 & 0.1336 & -0.4920 & -0.6883 & 0.0976 & -0.0098 & -0.3310 & 0.6028 & 0.8591 & 0.0297 \\ 0.0761 & -0.2900 & 0.2512 & 0.5782 & -0.2407 & 0.0580 & -0.6936 & -0.1667 & -0.7111 & -0.6831 \\ -0.5312 & -0.4037 & 0.1193 & -0.9150 & 0.1808 & -0.1721 & -0.1258 & -0.0732 & 0.1800 & 0.3276 \\ -0.7696 & 0.1489 & -0.2347 & -0.4740 & -0.7783 & -0.2836 & 0.0199 & -0.1983 & -0.3555 & -0.0423 \\ -0.3791 & 0.3524 & 0.4108 & 0.8186 & 0.1620 & -0.0868 & 0.2577 & 0.3384 & -0.1098 & -0.4637 \\ 0.1067 & -0.0456 & 0.3741 & 0.4124 & 0.1035 & 0.3661 & 0.0702 & 0.2337 & 0.3927 & -0.2392 \end{bmatrix}$$

$$\mathbf{b}^{(1)} = \begin{bmatrix} 0.4299 & 0.4575 & -0.4638 & 0.2796 & -0.3146 & -0.0165 & 1.0760 & 0.4546 & -0.1807 & -0.0051 \end{bmatrix}$$

$$(\mathbf{w}^{(2)})^{\mathrm{T}} = \begin{bmatrix} -0.6037 & 0.7488 & 0.8067 & -0.6448 & 1.0434 & 0.3027 & 0.9847 & 0.8700 & 1.0479 & 0.7281 \end{bmatrix} \text{ and } b^{(2)} = \text{-0.2436}$$

$$\mu_c = \text{0.0036 and } \sigma_c = 0.5210$$

TABLE 118: As in Table 117 but for $a_{ys}(412)$.

$$\boldsymbol{\mu_l} = \begin{bmatrix} -2.5403 & -2.4745 & -2.3595 & -2.3615 & -2.3925 & -3.1563 \end{bmatrix}$$

$$\boldsymbol{\sigma_l} = \begin{bmatrix} 0.3593 & 0.3241 & 0.2719 & 0.2479 & 0.2521 & 0.3261 \end{bmatrix}$$

$$\mathbf{w}^{(1)} = \begin{bmatrix} 0.4705 & -0.0333 & -0.7576 & 1.1616 & -0.1439 & -0.0506 & -0.5946 & 0.3930 & 0.0166 & -0.1670 \\ -0.1486 & 0.5243 & 1.3232 & -0.8026 & 0.1540 & -0.6336 & -0.1792 & 0.3089 & -0.2271 & 0.6198 \\ -0.0520 & 1.0840 & -0.0799 & 0.1587 & -0.6406 & -0.0457 & 0.4497 & 0.0126 & 0.5698 & -0.2094 \\ -0.2418 & 0.2310 & -0.0557 & 0.7669 & -0.2584 & 0.1388 & -0.2378 & -0.0873 & 0.6292 & 0.0068 \\ 0.3816 & 0.0684 & 0.3181 & -0.3243 & 0.1542 & -0.3167 & 0.1879 & -0.1307 & -0.2485 & 0.2601 \\ 0.3249 & -0.4123 & -0.8033 & -0.5103 & -0.1822 & 0.6087 & 0.2706 & 0.3146 & -0.0418 & 0.4396 \end{bmatrix}$$

$$\mathbf{b}^{(1)} = \begin{bmatrix} -0.7622 & -0.2401 & -0.2309 & -0.3835 & -0.1926 & -1.4228 & 0.0881 & -0.0461 & -0.0265 & -0.3167 \end{bmatrix}$$

$$(\mathbf{w}^{(2)})^{\mathrm{T}} = \begin{bmatrix} 0.3820 & 0.4471 & 1.4082 & -1.5795 & 0.4151 & 1.2106 & 0.5946 & 0.0705 & -0.5392 & 0.4749 \end{bmatrix} \text{ and } b^{(2)} = 1.1733$$

$$\mu_c = \text{-0.8057 and } \sigma_c = 0.3564$$

TABLE 119: As in Table 117 but for TSM.

$$\boldsymbol{\mu_l} = \begin{bmatrix} -2.5404 & -2.4745 & -2.3595 & -2.3614 & -2.3924 & -3.1560 \end{bmatrix}$$

$$\boldsymbol{\sigma_l} = \begin{bmatrix} 0.3594 & 0.3242 & 0.2720 & 0.2480 & 0.2520 & 0.3258 \end{bmatrix}$$

$$\mathbf{w}^{(1)} = \begin{bmatrix} -0.0018 & 0.0974 & 0.2093 & 0.0115 & 0.5281 & 0.1822 & -0.4053 & 0.8022 & 0.1993 & -0.5222 \\ -0.5233 & -0.0598 & 0.8192 & 0.1646 & -0.0659 & -0.7456 & 0.3819 & -0.1368 & -0.0378 & 0.4645 \\ -0.2464 & -0.1825 & 0.2709 & 0.0781 & -0.2162 & 0.0336 & -0.3096 & 0.3081 & -0.2648 & -0.0416 \\ -0.4900 & -0.2973 & -0.1357 & -0.7465 & -0.3303 & 0.0969 & -0.1941 & -0.6770 & 0.1515 & 0.3558 \\ -0.4493 & 0.8367 & 0.5178 & -0.8559 & 0.4974 & -0.1720 & -0.0842 & 0.6374 & 0.3999 & -0.8551 \\ -0.2315 & -0.2694 & -0.2074 & -0.0861 & 0.3965 & 0.0469 & 0.1585 & -0.3211 & -0.8769 & 0.1087 \end{bmatrix}$$

$$\mathbf{b}^{(1)} = \begin{bmatrix} 0.1187 & 0.4830 & 0.6260 & 0.0774 & -0.0564 & 0.3426 & -0.4462 & -1.0634 & 1.2278 & -0.5685 \end{bmatrix}$$

$$(\mathbf{w}^{(2)})^{\mathrm{T}} = \begin{bmatrix} -0.2591 & 0.8149 & 0.3938 & 0.5479 & 0.6702 & 0.0244 & 1.1885 & -0.6453 & -1.2634 & -1.2149 \end{bmatrix} \text{ and } b^{(2)} = \text{-0.0878}$$

$$\mu_c = \text{-0.0299 and } \sigma_c = 0.3367$$

TABLE 120: Summary of cross-validation results from the comparison between modeled and measured ocean color data products when considering individual basins and their ensemble (row data labeled ALLB). For each case, the number of measurement stations and the number of MLP hidden units are in the data columns labeled N and MLP, respectively. Values within brackets are obtained using all data for a single training.

Basin	N	MLP	Product	ϵ [%]	δ [%]	r^2
EMED	129	2	*Chl-a*	14.2(12.3)	1.4(1.1)	93.8(96.7)
			$a_{ys}(412)$	34.3(28.1)	9.8(5.9)	16.3(40.5)
			TSM	25.5(20.5)	6.1(3.4)	51.6(68.0)
LIGS	97	2	*Chl-a*	25.2(21.3)	4.7(4.2)	72.2(79.2)
			$a_{ys}(412)$	36.0(29.5)	8.2(7.6)	44.7(71.4)
			TSM	27.2(22.4)	7.0(6.1)	77.2(87.9)
NADR	107	2	*Chl-a*	37.8(24.6)	10.1(3.9)	49.2(78.2)
			$a_{ys}(412)$	26.3(14.5)	4.9(2.0)	39.1(78.3)
			TSM	32.7(23.5)	6.6(5.4)	53.8(85.2)
AAOT	1068	10	*Chl-a*	33.2(28.4)	7.4(6.6)	60.0(66.2)
			$a_{ys}(412)$	30.0(25.4)	8.0(6.2)	34.9(45.9)
			TSM	19.3(16.5)	4.0(2.6)	71.3(78.1)
VADR	1175	10	*Chl-a*	36.3(30.9)	10.4(6.4)	55.9(67.0)
			$a_{ys}(412)$	28.8(24.9)	7.5(5.1)	35.8(47.7)
			TSM	20.7(18.2)	3.5(2.8)	70.0(76.5)
BLKS	206	10	*Chl-a*	25.7(21.5)	4.8(4.0)	85.2(91.0)
			$a_{ys}(412)$	17.2(15.5)	1.6(2.9)	78.1(89.8)
			TSM	13.9(11.7)	1.2(1.3)	78.3(96.6)
ECHN	53	10	*Chl-a*	28.9(16.2)	2.9(2.2)	58.1(90.6)
			$a_{ys}(412)$	13.9(7.7)	-0.4(0.2)	53.6(86.0)
			TSM	19.4(11.4)	1.5(0.9)	66.9(93.0)
BLTS	365	10	*Chl-a*	34.9(27.7)	11.1(5.6)	84.1(89.2)
			$a_{ys}(412)$	12.8(10.4)	0.9(1.1)	86.4(91.4)
			TSM	27.8(19.3)	7.1(2.8)	74.3(90.1)
ALLB	2026	10	*Chl-a*	36.6(35.0)	12.2(10.4)	65.1(77.0)
			$a_{ys}(412)$	28.3(26.9)	7.4(6.0)	81.9(88.2)
			TSM	22.5(21.3)	3.8(4.0)	68.2(80.2)

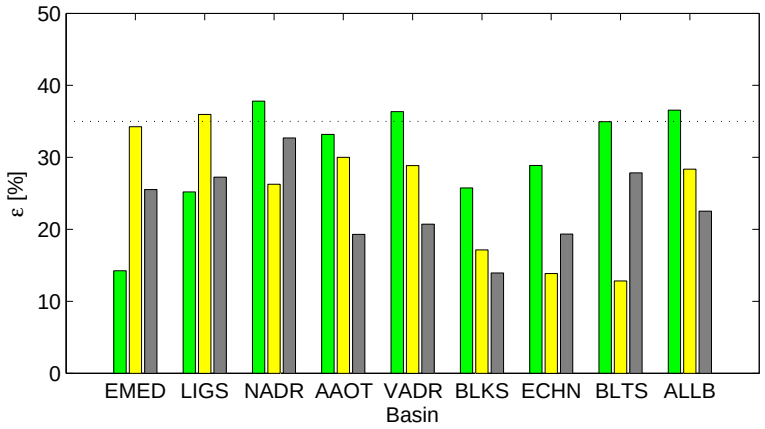

FIGURE 21: Cross-validation results at individual basins and for the BiOMaP data ensemble. Results for *Chl-a*, $a_{ys}(412)$ and TSM are in green, yellow and gray, respectively.

3.10 MLP performance analysis

Results from previous sections are summarized in Table 120 and Figure 21. The highest accuracy in retrieving *Chl-a* is observed in the Easter Mediterranean Sea and the Ligurian Sea (14 and 25 %, respectively). In the case of $a_{ys}(412)$, the MLP is the most performing in the English Channel and the Baltic Sea (14 and 13 %, respectively). The TSM retrieval is the most accurate in the Black Sea and for the data collected at

the Acqua Alta Oceanographic Tower (14 and 19 %). Instead, MLPs for the *Chl-a* retrieval are less performing when considering the BiOMaP data collected in the Northern Adriatic Sea and in the Baltic Sea. The $a_{ys}(412)$ and TSM retrieval is less accurate in the Ligurian Sea and Eastern Mediterranean Sea (note that here the absorption of the yellow substance and the concentration of the total suspended matter are extremely low). A reduced effectiveness in deriving TSM values can also be noticed in the Baltic Sea.

A remarkable similarity of the error distribution in retrieving *Chl-a*, $a_{ys}(412)$ and TSM has been found in the following basin subsets: 1) the Eastern Mediterranean and Ligurian Seas, 2) the Northern Adriatic and the Black Seas, and 3) the English Channel and the Baltic Sea. The reason is that seawater optical properties are mainly dominated by phytoplankton in the Eastern Mediterranean Sea and Ligurian Sea, by colored dissolved organic matter in the Baltic Sea and, although at a lesser degree, in the English Channel, and by sediment in the Black and partially in the Northern Adriatic Sea (Berthon et al., 2008).

It can also be observed that the performance of the MLP developed with the BiOMaP data ensemble does not systematically overcome results at individual basin level. From an operational perspective, this highlights the need of using specific algorithms for different water types, but it also raises the question of how water types have to be defined (e.g., D'Alimonte et al., 2007) in order to optimize the inversion scheme performance.

4 Cross-basin MLP applicability

This section complements the former performance analysis by applying MLP to water types different from thase used for the training (basin-specific or data ensemble). NOMAD data (Werdell and Bailey, 2005) are used as a benchmark of independent and globally distributed samples (GLOB). Results are presented through the scatter plots of Figure 22, where the modeled quantity is *Chl-a*. Figure insets give the overall performance with respect to the ensemble of NOMAD and BiOMaP data. Scatter plot legends instead specify the relative percent difference between measured and model quantities for each basin.

Overall results are in line with the MLP regression theory: the higher is the degree of specialization (training data mostly pertaining to a specific water type), the lower is the generalization capability. For instance, the performance of the MLP based on the data from the Northern Adriatic Sea (Panel 22(c)) shows better overall results with respect to the MLPs derived from the Baltic and the Black Seas (Panels 22(f) and 22(d), respectively). This can be explained by the variability of the optical properties in the Northern Adriatic Sea with respect to the other basins (Zibordi et al., 2011). When the algorithm of the Northern Adriatic Sea is applied to the data of the other basins, however, it produces results that are less accurate than those observed applying basin specific MLPs.

By the same token, the reduced generalization capability of the MLPs based on the Eastern Mediterranean Sea (Panels 22(a)), the Baltic (Panels 22(f)) and Black Sea data (Panels 22(d)) is the counterpart of their higher performance in specific water types. This is exemplified by the fact that the MLP for specific basins tends to saturate when applied to NOMAD data. As expected, the MLP with the best generalization properties is that developed on the basis of the ensemble of BiOMaP data (Panel 22(g)). Finally, it has to be noticed that the accuracy of the MLP trained with ALLB does not degrade much for most of the basins. Exceptions are the English Channel and the Baltic Sea, probably the most particular basins around Europe from the optical point of view (D'Alimonte et al., 2003).

5 Conclusions

This study presented MLP algorithms that use R_{RS} spectra to retrieve *Chl-a*, $a_{ys}(412)$ and TSM in different European seas, whereas accounting for the specificity of different space missions. MLPs were derived from data collected in the CoASTS (Zibordi et al., 2004) and BiOMaP (Zibordi et al., 2011) programs by the Joint Research Centre. Architecture selection and performance assessment were based on cross-validation to

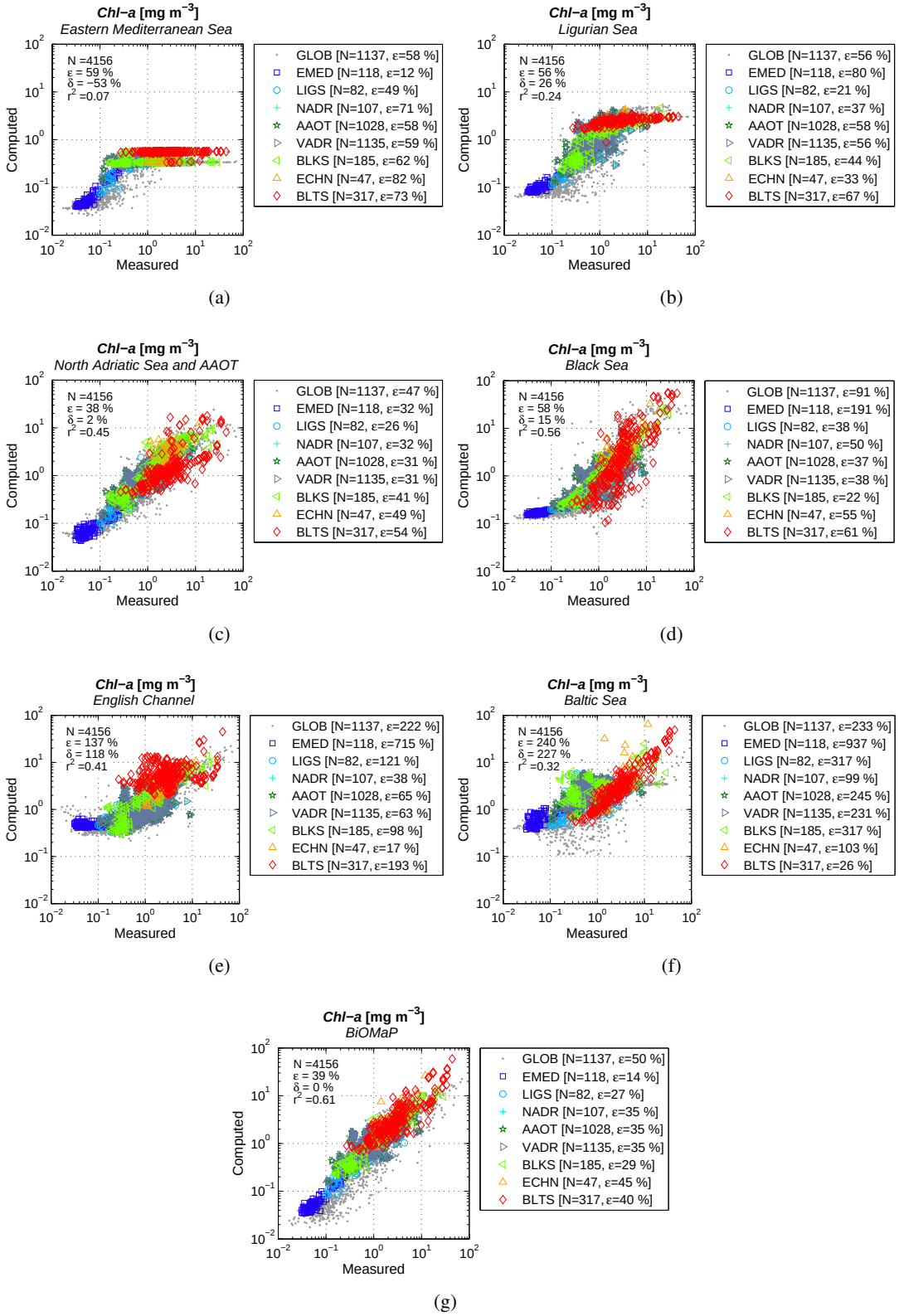

FIGURE 22: Assessment of the cross-basin applicability of the MLP algorithm for chlorophyll *a* retrieval. NOMAD data (labelled GLOB) are considered as benchmark to represent independent and globally distributed samples.

properly assess the MLP generalization capability (D'Alimonte and Zibordi, 2003; D'Alimonte et al., 2004; Kajiyama et al., 2011). The MLP parameters reported in this document are accompanied by theoretical elements, details on data pre- and post-processing methods, as well as examples of application programs written in MATLAB and C. Any user should be aware that MLP parameters might undergo future revisions upon the inclusion of new field measurements and further validation analyses.

This study clearly indicates the possibility to retrieve high level satellite ocean color products in optically complex waters through specific regional algorithms. However, this requires accurate in-situ measurements collected in different basins using state of the art instruments and measurement protocols (Zibordi et al., 2011). The study also indicates that regional algorithms might have a limited generalization capability. Water types might vary at a basin level due to subregional features, seasonal variability and environmental forcing. And this suggests caution on MLP application even to the same oceanographic region where in-situ data for the MLP development were collected. As a consequence, major efforts need to be undertaken to properly define ranges of applicability (e.g., through novelty detection schemes Bishop, 1994; D'Alimonte et al., 2003; D'Alimonte and Cornford, 2008), as well as to maintain validation program for satellite ocean color products.

Acknowledgements

This study has been supported by the European Space Agency within the framework of the MERIS Validation Activities under contract n. 12595/09/I-OL with the Departamento de Informática of the Universidade Nova de Lisboa; and contract n. 21653/08/I-OL with the Institute for Environment and Sustainability of the Joint Research Centre.

References

Berthon, J. F., Mélin, F., and Zibordi, G. (2008). Ocean Colour Remote Sensing of the Optically Complex European Seas. In Barale, V. and Gade, M., editors, *Remote Sensing of the European Seas*, Earth and Environmental Science, chapter 3, pages 35–52. Springer Netherlands, Dordrecht.

Bishop, C. M. (1994). Novelty Detection and Neural Network Validation. *IEE Proc.Vision and Image & Sig. Proc.*, 141:217–222.

Bishop, C. M. (1995). *Neural Networks for Pattern Recognition*. Oxford University Press.

Buiteveld, H., Hakvoort, J. H. M., and Donze, M. (1994). The optical properties of pure water. In *Ocean Optics XII*, volume 2258, pages 174–183. SPIE.

Campbell, J. W. (1995). The Lognormal Distribution as a Model for the Bio-optical Variability in the Sea. *J. Geophys. Res.*, 100:237–254.

Cherkassky, V. and Muller, F. (1998). *Learning from data*. Wiley-Interscience Publication.

D'Alimonte, D. and Cornford, D. (2008). Outlier Detection with Partial Information: Application to Emergency Mapping. *Stoch. Env. Res. Risk. A.*, 22(5):613–620.

D'Alimonte, D., Mélin, F., Zibordi, G., and Berthon, J.-F. (2003). Use of the Novelty Detection Technique to Identify the Range of Applicability of Empirical Ocean Colour Algorithms. *IEEE Trans. Geosc. Rem. Sens.*, 41:2833–2843.

D'Alimonte, D. and Zibordi, G. (2003). Phytoplankton Determination in an Optically Complex Coastal Region Using a Multilayer Perceptron Neural Network. *IEEE Trans. Geosc. Rem. Sens.*, 41(12):2861–2868.

D'Alimonte, D., Zibordi, G., and Berthon, J.-F. (2004). Determination of CDOM and NPPM Absorption Coefficient Spectra from Coastal Water Remote Sensing Reflectance. *IEEE Trans. Geosc. Rem. Sens.*, 42(8):1770–1777.

D'Alimonte, D., Zibordi, G., and Berthon, J.-F. (2007). A Statistical Index of Bio-optical Sea-water Types. *IEEE Trans. Geosc. Rem. Sens.*, 45:2644–2651.

Gordon, H. R. and Morel, A. (1983). Remote Assessment of Ocean Color for Interpretation of Satellite Visible

Imagery. In Barber, R. T., Mooers, C. N. K., Bowman, M. J., and Zeitzschel, B., editors, *Lecture Notes on Coastal and Estuarine Studies*, volume 4. Springer-Verlag, Berlin.

Haykin, S. (1994). *Neural Networks: A Comprehensive Foundation*. Macmillan, New York.

Kajiyama, T., D'Alimonte, D., and Cunha, J. C. (2011). Performance prediction of ocean color monte carlo simulations using multi-layer perceptron neural networks. In *International Conference on Computational Science (ICCS 2011)*. Accepted for publication.

Mélin, F. and Zibordi, G. (2007). Optically Based Technique for Producing Merged Spectra of Water-leaving Radiances from Ocean Color Remote Sensing. *Appl. Opt.*, 46(18):3856–3869.

Morel, A. and Prieur, L. (1977). Analysis of Variation in Ocean Colour. *Limnol. Oceanogr.*, 22:709–722.

Nabney, I. T. (2001). *Netlab: Algorithms for Pattern Recognition*. Springer-Verlag, London.

Pope, R. M. and Fry, E. S. (1997). Absorptium Spectrum (380-700 nm) of Pure Water: II. Integrating Cavity Measurements. *Appl. Opt.*, 36:8710–8723.

Werdell, P. J. and Bailey, S. W. (2005). An Improved In-situ Bio-optical Data Set for Ocean Color Algorithm Development and Satellite Data Product Validation. *Remote Sens. Environ.*, 98:122–140.

Zibordi, G., Berthon, J.-F., Mélin, F., and D'Alimonte, D. (2011). Cross-site consistent in situ measurements for satellite ocean color applications: the BiOMaP radiometric dataset. *Remote Sens. Environ.* Accepted for publication.

Zibordi, G., D'Alimonte, D., and Berthon, J.-F. (2004). An Evaluation of Depth Resolution Requirements for Optical Profiling in Coastal Waters. *J. of Atm. and Ocean. Tech.*, 21(7):1059–1073.

Zibordi, G., Mélin, F., and Berthon, J.-F. (2006). Comparison of SeaWiFS, MODIS and MERIS Radiometric Products at a Coastal Site. *Geophys. Res. Lett.*, 33:L06617.

A MLP functions in C

This section presents a set of C functions that implement the MLPs described in this document. The code listed hereafter includes header file, data pre- and post-processing solutions, the MLP mapping function and an example of application to retrieve *Chl-a* in the Northern Adriatic Sea.

A.1 Header file: mlp.h

```
/* mlp.h */

#define MAX_VALUES 8

int parse_input_values(int argc, char *argv[], double RRS[6], double val[MAX_VALUES]);

void preprocess(double RRS[6], double mu_l[6], double sigma_l[6], double x[6]);

double mlp_mapping(double x[6], double w1[6][10], double b1[10], double w2[10], double
    b2);

double postprocess(double y, double mu_c, double sigma_c);

void compare_output(double c, double val[MAX_VALUES], int n);
```

A.2 MLP mapping with data pre- and post-processing: mlp.c

```

/* mlp.h */

#include <stdio.h>
#include <stdlib.h>
#include <math.h>

#include "mlp.h"

int
parse_input_values(int argc, char *argv[], double RRS[6], double val[MAX_VALUES])
{
  int i, n;

  if (argc < 7) {
    fprintf(stderr, "Usage: %s RRS412 RRS442 RRS491 RRS511 RRS555 RRS665 [value ...]\n
        ", argv[0]);
    fprintf(stderr, "The first six arguments (required) are RRS values at 412, 422,
        491, 511,\n");
    fprintf(stderr, "555, and 665 nm.  Additional arguments are expected to be
        independently\n");
    fprintf(stderr, "measured/computed values of the modeled quantity (i.e., Chl-a,
        a_ys(412)\n");
    fprintf(stderr, "or TSM) used for comparison with the MLP mapping result.\n");
    return -1;
  }
  n = argc - 7;
  if (n > MAX_VALUES) {
    fprintf(stderr, "Error: too many benchmark values were given.\n");
    return -1;
  }
```

```
  for (i = 0; i < 6; i++)
    RRS[i] = strtod(argv[i+1], NULL);
  for (i = 0; i < n; i++)
    val[i] = strtod(argv[i+7], NULL);
  return n;
}

void
preprocess(double RRS[6], double mu_l[6], double sigma_l[6], double x[6])
{
  int i;

  for (i = 0; i < 6; i++)
    x[i] = (log10(RRS[i]) - mu_l[i]) / sigma_l[i];
}

double
mlp_mapping(double x[6], double w1[6][10], double b1[10], double w2[10], double b2)
{
  double tmp, y, z[10];
  int i, j;

  for (j = 0; j < 10; j++) {
    tmp = 0.0;
    for (i = 0; i < 6; i++)
      tmp += x[i] * w1[i][j];
    z[j] = tanh(tmp + b1[j]);
  }
  y = b2;
  for (j = 0; j < 10; j++)
    y += z[j] * w2[j];
  return y;
}

double
postprocess(double y, double mu_c, double sigma_c)
{
  return pow(10.0, y * sigma_c + mu_c);
}

void
compare_output(double c, double val[MAX_VALUES], int n)
{
  int i;

  /* MLP output */
  printf("%.4e", c);
  /* Comparison of the MLP output with other measured/computed values */
  for (i = 0; i < n; i++)
    printf("   %.4e (%7.2f %%)", val[i], (val[i] - c) / val[i] * 100.0);
  printf("\n");
}
```

A.3 *Chl-a* retrieval in the Northern Adriatic Sea (BiOMaP and CoASTS data): adriatic_chl.c

```
/* mlp_adriatic_chl.c */

#include "mlp.h"

double mu_1[6] =
  {-2.4140, -2.3562, -2.2420, -2.2459, -2.3001, -3.1077};
double sigma_1[6] =
  { 0.1266, 0.1376, 0.1410, 0.1531, 0.1913, 0.2898};
double w1[6][10] = {
  { 0.8171,  0.1020,  0.0055, -0.7657,  1.3000,  0.9552, -0.0389,  0.2977, -0.3111,
    -1.3794},
  { 0.7788, -0.8233, -0.1462,  1.0440, -0.0541,  0.5041,  0.2709, -0.2039, -0.9394,
    0.2407},
  {-0.5943,  0.2567,  0.1180, -0.0121, -0.5634,  0.0795,  0.3766, -0.0012, -0.2342,
    0.5870},
  { 0.9183, -0.2228, -0.2723, -0.3433,  0.7181, -0.3145, -0.2038, -0.8187, -0.7295,
    0.2357},
  { 1.1696,  0.0653, -0.0641, -0.4761,  0.2034, -0.4225,  0.5823,  0.5535, -0.9467,
    -1.6642},
  {-0.0250,  0.4470,  0.6222,  0.3024, -0.2759, -0.4216,  0.7834,  0.2380, -0.3021,
    -0.2630}};
double b1[10] =
  {0.6897,  0.4251, -0.1718, -0.5192,  0.0070, -0.0633, -0.0405, -0.7154, -0.0193,
    0.0832}};
double w2[10] =
  {-0.5005,  1.0459,  1.1365,  -1.5768, -0.0562,  0.5799,  0.7121,  1.1483, -0.9814,
    1.2666}};
double b2 = -0.0907;
double mu_c = -0.0185;
double sigma_c = 0.3270;

int
main(int argc, char *argv[])
{
  double RRS[6], x[6], y, c, val[MAX_VALUES];
  int n;

  if ((n = parse_input_values(argc, argv, RRS, val)) < 0)
    return -1;

  /* Pre-processing */
  preprocess(RRS, mu_1, sigma_1, x);

  /* MLP mapping */
  y = mlp_mapping(x, w1, b1, w2, b2);

  /* Post-processing */
  c = postprocess(y, mu_c, sigma_c);

  /* Comparison of the MLP output with other measured/computer values */
  compare_output(c, val, n);
  return 0;
}
```

European Commission

EUR 24920 EN – Joint Research Centre – Institute for Environment and Sustainability
Title: Bio-optical Algorithms for European Seas
Author(s): Davide D'Alimonte, Giuseppe Zibordi, Jean-François Berthon,
Elisabetta Canuti and Tamito Kajiyama
Luxembourg: Publications Office of the European Union
2011 – 59 pp. – 21.0 x 29.7 cm
EUR – Scientific and Technical Research series – ISSN 1831-9424 (online), ISSN-5593 (print)
ISBN 978-92-79-21028-0
doi:10.2788/56321

Abstract
The report presents and discusses the application of Multi Layer Perceptron (MLP) neural networks to derive Chlorophyll-a concentration (Chl-a), absorption of the yellow substance at 412 nm ($a_{ys}(412)$) and concentration of the total suspended matter (TSM) from remote sensing reflectance R_{RS} values. MLPs were developed on the basis of data collected within the framework of the Coastal Atmosphere and Sea Time Series (CoASTS) and Bio-Optical mapping of Marine Properties (BiOMaP) programs carried out by the Institute for Environment and Sustainability (IES), JRC of E.C., Italy. Investigated oceanographic regions include the Eastern Mediterranean Sea, the Ligurian Sea, the Northern Adriatic Sea, the Western Black Sea, the English Channel and the Baltic Sea. The study verifies the applicability of MLPs to retrieve ocean color data products in each basin. For instance, the highest accuracy in retrieving Chl-a has been found in the Easter Mediterranean Sea and the Ligurian Sea (14 and 25 %, respectively). In the case of $a_{ys}(412)$, the MLP is the most performing in the waters of the English Channel and the Baltic Sea (14 and 13%). Instead, the TSM retrieval is the most accurate in the Black Sea and at the Acqua Alta Oceanographic Tower (14 and 19%). To enhance mission specific ocean color resuls, MLP coefficients are also computed applying band-shift corrections to produce R_{RS} spectra at wavelengths matching those of SeaWiFS, MODIS and MERIS. Resulting tables of MLP parameters are reported to permit independent applications of neural networks presented in this analysis.

How to obtain EU publications

Our priced publications are available from EU Bookshop (http://bookshop.europa.eu), where you can place an order with the sales agent of your choice.

The Publications Office has a worldwide network of sales agents. You can obtain their contact details by sending a fax to (352) 29 29-42758.

The mission of the JRC is to provide customer-driven scientific and technical support for the conception, development, implementation and monitoring of EU policies. As a service of the European Commission, the JRC functions as a reference centre of science and technology for the Union. Close to the policy-making process, it serves the common interest of the Member States, while being independent of special interests, whether private or national.

LB-NA-24920-EN-N